

# A Spreading Malaise: Manure Management, Air Pollution, and Health Outcomes in Italy

Jacopo Lunghi<sup>†</sup>

Bocconi University, Milan, Italy

RFF-CMCC European Institute for Economics and the Environment

This version: May 28, 2024

## Abstract

Manure application is a widespread soil fertilization practice in agriculture which may constitute an environmental and public health hazard. Using air quality and hospital discharge data from the Lombardy region in Italy, in this paper I estimate the causal effect of manure spreading on fine particulate matter concentrations, and study how short-term spikes in air pollution affect respiratory and cardiovascular hospitalisations, mortality rate at discharge, and medical treatment costs. To isolate the impact of manure application, I exploit exogenous variation in spreading prohibitions as a repeated event-study design. I estimate an increase of around 27% in  $PM_{2.5}$  concentrations in the five days following a ban lift, paired with an increase in urgent hospitalisations by a factor of 1.04 to 1.145, and higher hospital mortality rate (0.7 to 1 percentage points) during spreading events. Conversely, it is found no significant difference in the cost per hospitalisation. I estimate the financial burden limited to this health threat to range between 30.9 and 67.7 million euros per year. Finally, I simulate the impact of including particulate matter targets in the current regulatory framework and find that, despite reductions in concentrations could be achieved, refined policy may not be sufficient to curb air pollution.

**Keywords:** Air Pollution; Pollution Control; Livestock Farming; Cost Benefit; Environmental Health and Safety

JEL Classification: Q00; Q51; Q53; K32; I18

---

<sup>†</sup>Contact: Jacopo Lunghi, Bocconi University, Via Rontgen 1, 20136 Milano.  
E-mail: [jacopo.lunghi@phd.unibocconi.it](mailto:jacopo.lunghi@phd.unibocconi.it). Web: [jacopolunghi.github.io](https://jacopolunghi.github.io).

Access to the National Hospital Discharges database was authorized by the Ministry of Health, Planning Department, under confidential disclosure agreement. The evidence produced in this paper respects data confidentiality and was formerly approved for disclosure by the Ministry of Health. Any error and inaccuracy are the author's responsibility.

# 1 Introduction

Manure application is a common practice in agriculture to fertilize and condition the soil. Although a potentially valuable source of plant nutrients, the disposal of animal organic waste may pose important environmental concerns, some of which seem notably overlooked. In particular, the contribution of manure application to coarse ( $\text{PM}_{10}$ ) and fine ( $\text{PM}_{2.5}$ ) particulate matter concentrations is still one of the most poorly characterized sources of air pollution and, as such, often poorly addressed in most regulatory frameworks worldwide (Cambra-López et al. 2010). PM emissions from farming activities are primarily the result of secondary inorganic aerosol (SIA) in the atmosphere from its precursors: ammonia ( $\text{NH}_3$ ), nitrogen oxides ( $\text{NO}_x$ ), and sulfur dioxide ( $\text{SO}_2$ ) among the most relevant.  $\text{NO}_x$  and  $\text{SO}_2$  originate mostly from combustion of coal, oil, and fossil fuels, whereas the vast majority of ammonia emissions are produced by agriculture. More specifically,  $\text{NH}_3$  almost entirely originates from soil application and disposal of livestock waste and fertilizers.

Research has shown that the agricultural industry can be a key source of directly emitted PM (*primary emissions*), mostly from storage and handling of agricultural products, agricultural waste burning, land preparation and harvesting (Garg et al. 2023, He et al. 2020, Nian 2023). As such, emissions from agriculture are associated with thousands of annual deaths (Domingo et al. 2021, Lelieveld et al. 2015). Much less is known about the potential harm induced by secondary PM formation and manure management. First, it is often challenging to isolate the contribution of farming activities from other sources of airborne pollution in aggregate settings. Second, even isolating and quantifying PM mass from livestock activities may not fully characterize the hazard posed by animal breeding. Indeed, toxicological studies have questioned the existence of a specific association between SIA particles and risk to health at ambient concentrations, despite the information being still limited (Cassee et al. 2013). Lack of fully conclusive evidence has led the WHO to maintain a cautious stand, assuming equal toxicity of all chemical particles contribution to PM mass, including SIA (WHO 2021).

In this paper, I investigate the environmental and health risks posed by manure spreading activities in the Lombardy region in Italy. I use the unique features of Italy’s regulation in matter of manure spreading prohibitions as a quasi-natural experimental framework to estimate the short-term causal effect of manure spreading on PM concentrations, hospital access, and patient’s conditions for respiratory and cardiovascular acute episodes. To this aim, I collect geolocated patient-level data from hospital discharge forms for the years 2016 through 2019, matched with high-frequency data on pollutants’ concentration and weather conditions at municipal level. To capture the true causal effect of manure spreading, I build a repeated event-study framework, where each event is determined by the conditionally exogenous opening of a “spreading window”, i.e. a period of consecutive days of spreading ban followed by consecutive days of lifted prohibitions. This allows me to estimate the portion of PM mass originating from manure management activities as well as overcome endogeneity concerns that arise from selective exposure of individuals to

air pollution based on unobservable characteristics correlated with individual health. My identifying assumptions rely on the absence of systematic differences between hospitals and patients around the window cutoff, and the absence of endogenous selection of patients on either side of the threshold. I argue that, conditional on observables, the short time interval considered and the limited knowledge of farming regulation of individuals allow to pinpoint causality between spreading of manure, air pollution, and subsequent health externalities. Defining symmetric short-term windows around a spreading event also helps to cope with staggered treatment concerns (De Chaisemartin & d’Haultfoeuille 2020, Sun & Abraham 2021, Callaway & Sant’Anna 2021), as municipalities receive treatment at the same time within each window. To complement my preferred specification, I show the persistence of the results to a difference-in-difference strategy that exploits geographical discrepancies in prohibitions across the region.

I estimate that spreading windows induce a spike in  $PM_{2.5}$  concentrations, roughly 27% increase, peaking at more than 40% at the third consecutive day of lifted prohibitions. The effect is stronger in areas more with higher concentration of farming animals, stressing the key role of husbandry activities as a driver to the observed spike in PM. Municipalities in the highest two deciles of the distribution in terms of farming animal stock experience an increase in  $PM_{2.5}$  7% to 10% higher than those in the three lowest deciles. The results are robust to different combinations of weather controls and fixed effects, and corroborated by both a placebo test using rainfall alone as a discriminant for window opening, and by detecting no comparable trends in pollutants that are not directly caused by livestock emissions, such as Ozone and  $SO_2$ . I then analyse the evolution hospital admissions, mortality at discharge, and treatment costs of inpatients with respiratory and cardiovascular diseases (R&CD) during spreading-induced PM peaks. I find that spreading events are associated with one additional daily urgent admission every 25 patients: this effect is stronger when excluding days close to the cutoff days and peaks around the fourth day of prohibitions lift, up to a maximum of one every 7 patients, suggesting partial lag in the response to PM spikes. Moreover, I find that individuals admitted during a spreading event experience between 0.7% and 1% higher rate of mortality at discharge. Finally, it is found no premium in the cost per hospitalisation during PM peaks: patients do not appear to stay longer in hospital and do not require more expensive procedures compared to the baseline, although the effect could be confounded by limitations in the cost measure available and the endogenous response from medical facilities. I find no effect on the same indicators in inpatients hospitalized for treatment more remotely related to air quality, such as digestive, genitourinary, and musculoskeletal system diseases.

I use these results to estimate the financial burden implied by the observed health externalities associated with spreading activities. I simulate the incremental admissions due to manure application and calculate the monetary equivalent total years of life lost due to the increase in hospital mortality assuming a value of statistical life year (VSLY) of €158,488 (Cots et al. 2011). I obtain a total cost from increased usage of health care facilities between 16.7 and 48.1 million euros, in addition to a total VSLY quantified between 13.8 to 19.5 million euros. These figures likely represent a lower bound to the true

impact of manure application, as they abstracts from potential morbidity and co-morbidity effects, as well as long-term implications to PM exposure.

Finally, I simulate the gains of incorporating targets related to PM concentrations in the region. Hence, I assume a regulator who aims at minimizing the days for which PM levels exceed the threshold considered unhealthy for sensitive groups (set at  $35 \mu\text{g}/\text{m}^{-3}$ ), leaving other restrictions to spreading activities in the current regulation unaltered, and deducing counterfactual PM concentrations considering manure application as an additive increase. I design a constrained finite recursive optimization problem under uncertainty to define a new allocation of spreading days, and benchmark the results with the best allocation achievable under perfect forecasting (i.e. retrospective information on PM levels and weather conditions). The results show the limitations of introducing PM targets in manure management regulation without any complementary policy to sustain such targets. With a potential maximum reduction in days of hazard concentrations around 10% estimated under perfect forecasting, introducing uncertainty cuts the estimated gain to less than 1%, due to low precision in PM and weather predictions.

This paper contributes to the current literature in environmental and health economics that estimates the causal effects of air pollution on human health. There exist many examples of studies that investigate the impact of air quality, many of which focus on one specific health issues such as adult and infant mortality (Chay et al. 2003, Chay & Greenstone 2003, Currie & Neidell 2005, Jayachandran 2009, Currie & Walker 2011, Chen et al. 2013), infant health (Friedman et al. 2001, Neidell 2004, Knittel et al. 2016), mental health (Chen, Oliva & Zhang 2018). Only a subset of them focus specifically on particulate matter, even less so on  $\text{PM}_{2.5}$  (Pope III et al. 1999, Schwartz et al. 2017, Deryugina et al. 2019). Importantly, only few papers are able to quantify healthcare costs and to look in detail at medical procedures and cost per admission, thus separating the effect on the extensive and intensive margin. Schlenker & Walker (2016) estimate hospitalization rates and costs in California, but focus on carbon monoxide exposure. A paper by Deryugina et al. (2019) uses elderly Medicare recipients data to estimate the effect of  $\text{PM}_{2.5}$  exposure on elderly mortality, health care use, and medical costs. However, the authors provide an estimate for overall inpatient spending, without assessing whether the effect may originate from patients requiring more cost-intensive treatment during periods of high PM exposure. There are instead fewer examples of quantification of healthcare costs outside the US setting are found in the literature, given scarce data availability (Xia et al. 2022). In this paper, I look closely at different cost components in a novel setting.

Furthermore, this study is, to the best of the author’s knowledge, the first attempt to estimate the causal impact of manure management in particular on air pollution, health, and healthcare spending. Some studies have tried to impute air-quality related deaths to agricultural activities, including manure management (Jerrett 2015, Lelieveld et al. 2015, Giannakis et al. 2019, Domingo et al. 2021), but they have not yet fully established a direct causal link to pinpoint the share of PM concentrations and the health concerns for which manure management is responsible. I believe this is the first paper that uses winter spreading prohibitions as conditionally exogenous local variation to study the effect of



manure management on air pollution levels and respiratory and cardiovascular diseases. This constitutes a novel approach to directly identify the implications of manure application activities on a large scale. Amid lack of reliable data on PM decomposition and, as such, the impossibility to observe specifically SIA particles, by isolating livestock as primary emission source, the paper indirectly adds to the current knowledge on the hazard to human health posed by different airborne particles (Kelly & Fussell 2016, 2020). Finally, this paper contributes to the regulatory debate around the most suitable policy response to reduce emissions from manure application and increase welfare.

The remainder of this paper is organized as follows. Section 2 provides background information about the current legislation on manure spreading activities in Lombardy, that justifies my strategy. Section 3 presents the empirical strategy employed, and Section 4 describes the data. Section 5 presents main results and assesses their robustness. Section 6 simulates the healthcare spending costs of manure spreading, and Section 7 describes a counterfactual scenario of fully-flexible spreading prohibitions and estimates its benefit in terms of pollution reduction. Finally, Section 8 concludes.

## 2 Background: Spreading Policies in Lombardy and Worldwide

### 2.1 *The environmental concerns of manure application*

Manure application provides nutrients that improve soil quality and increase crop production, but carries consistent environmental risk and, consequently, serious potential harm to human health (Bouwman et al. 2013).

First, manure management and farming activities contribute significantly to emissions of greenhouse gases (GHGs)<sup>1</sup>, which are the main responsible of rising temperature and climate change. The phases of storage, treatment and spreading of manure have all been associated to GHG emissions (Chadwick et al. 2011), and manure management alone is estimated to contribute between 1.6% and 13.6% of total GHGs emissions across Europe<sup>2</sup>. This is particularly true for Lombardy as well, where GHGs concentrations, particularly with regards to N<sub>2</sub>O and CH<sub>4</sub>, spatially correlate with farming intensity (see Figure E.1 in Appendix). While GHGs can potentially pose direct risk to human health, this occurs primarily at very high concentrations and in constrained environments. High concentrations of ambient CO<sub>2</sub> (at 20,000 ppm) have been found to induce physiological responses in blood pressure, hearth and respiratory rate (Maniscalco et al. 2022), while lower atmospheric concentrations (< 5,000 ppm) are thought to represent a direct health risk only through chronic exposure (Jacobson et al. 2019) and long-term modifications of global climate.

Second, the large quantities of nitrogen (N) released into the soil by slurry redepositing can enter groundwater, and later be transported into freshwater, through infiltration and surface runoff (Ongley 1996). This, in turn, poses several environmental concerns

---

<sup>1</sup>Most notably, farming activities are associated to higher concentrations of N<sub>2</sub>O (nitrous oxide), CH<sub>4</sub> (methane), and CO<sub>2</sub> (carbon dioxide).

<sup>2</sup>Source: EEA - Approximated greenhouse gas inventories.

such as eutrophication, algal blooms, loss of biodiversity, and fish stock depletion, in addition to direct threats to human health through the consumption of contaminated water. Evidence of water-linked diseases has been retrieved especially interesting the digestive and endocrine system (Majumdar & Gupta 2000, Azizullah et al. 2011). There is instead no consistent evidence that links exposure to polluted water and respiratory and cardiovascular conditions, which could however be linked to manure application through a different channel. Indeed, organic droppings from livestock are a primary source of ammonia emissions ( $\text{NH}_3$ ), which is a key component for SIA formation of fine particulate matter ( $\text{PM}_{2.5}$ )<sup>3</sup>. Despite the reaction time of precursors forming  $\text{PM}_{2.5}$  is difficult to determine with precision, recent studies suggest that, while part of the reaction may happen locally within few minutes, second stages of the reaction may continue overnight and in the following days after ammonia is released (Kim et al. 2022). In Italy, roughly 95.7% of ammonia emissions between 2008 and 2019 are associated to fertilizers and livestock, which is marginally below the EU average (96.4%)<sup>4</sup>. Exposure to  $\text{PM}_{2.5}$ , in turn, has been largely associated in the literature with serious health concerns. Importantly, even short-term exposure to polluted air (Wong et al. 2008, Larrieu et al. 2007) and high  $\text{PM}_{2.5}$  concentrations (Guaita et al. 2011) have been found to induce respiratory-, natural-, and cardiovascular-cause mortality. If the effects of PM have been largely studied, much less is known about the exact toxicity of particles with different chemical compositions. Finding refined guidelines on the potentially heterogeneous hazard level of airborne particles has been in the agenda for almost 20 years (Council et al. 2004), but the results are still far from conclusive. Toxicological research has found little to no proof of a biological association with ammonium nitrates and sulphates and human health, but strong epidemiological association leaves open the possibility of alternative underlying mechanisms, such as cations associated with these compounds and absorbed components (Schlesinger & Cassee 2003, Reiss et al. 2007, Cassee et al. 2013). Recent lab evidence suggests increased airflow obstruction and respiratory following chronic exposure to SIA in mice (Zhang et al. 2022, 2021). According to the guidelines of the WHO, all chemical particles constituting PM mass are to be considered having equal toxicity (WHO 2021), but it is yet to be determined with precision whether a peak in fine PM concentrations induced by organics waste from livestock should have health consequences on individuals and, if so, to what extent. Scarce empirical evidence on the topic is potentially one of the reasons why PM emissions emerge a second-order concern in the regulation of manure application.

## 2.2 Manure Application Policies in Lombardy

After a first attempt to legislate the utilization of fertilizers in 1984, following the new wave of European legislation on environmental protection, Italy has firstly introduced

---

<sup>3</sup>Secondary PM formation takes place through the chemical reactions between ammonia and gaseous precursors such as sulfates ( $\text{SO}_x$ ) and nitrates ( $\text{NO}_x$ ), forming crystalline solid compounds (ammonium nitrates and ammonium sulphates) that take part in the composition of  $\text{PM}_{2.5}$  (Squizzato et al. 2013).

<sup>4</sup>Source: Eurostat, Air emissions accounts by NACE Rev. 2 activity.

comprehensive regulation about manure management and usage of fertilizers in 2006<sup>5</sup>. The new regulatory framework introduced spatial and temporal prohibitions to the ground application of droppings, in the interest of maintaining proper sanitary conditions of urban and extra-urban areas and, most importantly, preventing pollution of groundwater bodies, which are particularly threatened by nitrates originating from fertilizers (Galloway et al. 2008, Sebilo et al. 2013). Among the restrictions imposed, which vary on the basis of soil composition, average slope, and distance from metropolitan areas, limitations in the timing of sludge application are of particular interest to this paper. Indeed, the law established a minimum ban of 90 days<sup>6</sup> during the winter season, identified as “*typically elapsing between 1st November and 28th February*”. This regulatory action was justified with winter posing the highest risk of frozen ground and, consequently, nitrates runoff and pollution of surface waters during snowmelt (Young & Mutchler 1976). For similar reasons, the law prohibited manure spreading during a rainy day, and the day immediately after. Regional entities were then responsible to introduce further legislation to regulate how exact dates for the constrained period were defined. In Lombardy, these have been regulated by a series of action plans (*Piano d’Azione Nitrati*, henceforth PdA), updated every three years. Starting and ending dates of the ban period have been variable from one year to the other and communicated during spring for the upcoming winter by regional decree.

As manure storage is often a costly activity, especially due to capacity constraints of farmers, to promote cost reduction and prevent overload, in 2016 Italy increased regulation flexibility. While maintaining a 90-days prohibition, the fixed ban period was shortened to 62 days (between 1st December and 31st January), while the remaining 28 out of 58 days were once again set by regional governments. In Lombardy, spreading prohibitions and permits started to be regulated through bulletins (*Bollettini Nitrati*) issued every two to five days throughout the period subjected to the authority’s discretionality. The bulletin reports the manure spreading potential (either “allowed” or “not allowed”) of six different climate zones within the region (*Zone pedoclimatiche*) for the upcoming days. Restrictions are imposed at the climate zone level: discrepancies between zones may occur in case of significantly different weather conditions across the region.<sup>7</sup> Bulletins are easily accessible through a dedicated app as well as regularly posted online in a dedicated webpage<sup>8</sup>. Failure to comply with the restrictions can result in an administrative fee up to 5.000 euros, which is substantial given that the economic size class of more than 70% of farms in Lombardy does not exceed 50.000 euros<sup>9,10</sup>, and even a criminal liability

---

<sup>5</sup>MD 7 Apr 2006. A summary of the most salient regulatory advancements in Italy is reported in Appendix (Section C).

<sup>6</sup>The limitation was extended to 120 days for specific categories of poultry manure.

<sup>7</sup>Climate zone areas are: *Alps* (provinces: SO); *Central plain* (provinces: BG, BS, CR); *West plain* (provinces: LO, MI, PV); *East plain* (provinces: MN); *West Prealps* (provinces: BG, CO, LC, MB); *East Prealps* (provinces: BG, BS). See Figure E.2 in Appendix.

<sup>8</sup>Figure E.4 in Appendix shows the content of the app and online documents available to farmers to gather information about day-to-day restrictions to manure application.

<sup>9</sup>Economic size classes are defined at EU level (Commission Regulation No 1242/2008).

<sup>10</sup>Source: Agricultural Census (ISTAT). See Figure in Appendix.

depending on the degree of environmental damage. Figure 1 summarizes the regulatory framework, which remained in place between 2016 and the beginning of 2021.

From the farmers' perspective, there is a strong incentive to apply manure when winter restrictions are temporarily lifted, given uncertainty about future spreading opportunities. Indeed, initial investment and maintenance of storage containment structures, such as tanks or pits, is a remarkable cost for farmers which, in turn, tend to have limited resources to stock manure during long periods of prohibition and face the risk of storehouse overcapacity. Moreover, while application is not necessarily tied to an individual's farmland (farmers who exhausted storing capacity can rent parts of land from other farms to apply the excess manure), rental fees and high transportation costs lower the incentive to dispose of manure far from the farmstead. Data from 2010 ISTAT Agricultural Census (Figure 2) indicate that more than 50% of farms apply more than 75% of their manure production to their own land. Additionally, considering cattle- and pigs-specialized entities, there exist a negative correlation between farm size and amount of manure disposed outside, meaning that comparatively smaller producers tend to rely on rental farmland, reducing geographical discrepancy between a farm's location and where the manure produced is applied.

Despite the regulatory framework defined a broad set of rules to ensure transparency and control over manure application activities, it did not include any consideration about air pollution in determining spreading prohibitions prior to 2021, which justifies the research design employed in this paper. In fact, only with PdA 2020-2023, a first attempt to bring PM concentrations into the picture was made, in the form of an additional criterion to spreading. Specifically, manure application was forbidden in municipalities where containment measures to reduce air pollution (e.g. traffic stops) are in place.<sup>11</sup>

subsectionOther Examples of Manure Application Regulation Italy and the Lombardy region are not an isolated example of the attempt to cope with the environmental challenges posed by manure management. Other European countries, following the guidelines outlined in the Nitrates Directive (91/676/EEC), have imposed similar restrictions, including prohibitions to manure application during winter months. For example, in Germany spreading is not allowed between 1 November and 31 January on arable land and between 15 November and 31 January on grassland<sup>12</sup>. In the Netherlands, prohibitions span between 1 September to 31 January<sup>13</sup>, while the longest period of restrictions in the UK, depending on soil type and land use, can be as long as 7 months, from 1 August to the end of February<sup>14</sup>. Possibly the regulation closer to the Italian case is observed France,

---

<sup>11</sup>Pollution control measures can be applied in Lombardy between October 1st and March 31st. They are triggered by PM<sub>10</sub> concentrations exceeding  $50\mu/m^3$  for at least four consecutive days, and stay in place until favorable weather conditions to the reduction of airborne pollutants (e.g. rain) or at least two consecutive days below  $50\mu/m^3$  PM<sub>10</sub> concentrations. Temporary measures include restrictions on bonfires, manure application (since 2021), indoor temperatures (i.e. heating systems control), and traffic. They are implemented at province level, with the exception of traffic limitations, which are applied at municipal level and only for municipalities with more than 30,000 inhabitants.

<sup>12</sup>Fertilizer Act; Ordinance on Fertilizer Application (Düngerordnung. Latest amendment 2007)

<sup>13</sup>Decision Using Fertilisers (*Besluit gebruik meststoffen*), 1997.

<sup>14</sup>The Reduction and Prevention of Agricultural Diffuse Pollution (England) Regulations 2018.

where a manure application calendar is in force in winter months. This similarly imposes flexible ban periods depending on soil vulnerability and land use, plus some (less stringent compared to Italy) weather-based restrictions.<sup>15</sup>

Outside Europe, the regulation on manure spreading is relatively laxer: (Liu et al. 2018, (Fig. 2)) provide a summary of existing restrictions. For instance, in countries like Canada, Australia, and the US, where the regulation is applied at sub-national level, with the exception of some Canadian provinces where winter prohibitions are in place, the policy action ranges from application of partial weather restrictions, to submission by farmers of voluntary manure management plans, to even complete absence of guidelines. To the best of the author’s knowledge, there exist no similar regulation in large Asian countries, such as India and China, as well as in developing economies.

The attention, amid considerable heterogeneity, to manure management governance reinforce the relevance of the findings presented in this paper outside of the Italian context, as well as the broad scope of its policy implications. Furthermore, while Lombardy displays high concentration of farming activities, making it potentially more susceptible to the environmental and health threats of manure application (Lombardy is in the 96<sup>th</sup> percentile for animals total headcounts in the EU)<sup>16</sup>, it is not an isolated case. For example, other regions in countries like Spain, France, Germany, and the UK rely heavily on farming industry, displaying comparable figures in terms of livestock presence, as well as similar weather and geographical characteristics.<sup>17</sup>

### 3 Methodology

#### 3.1 Sample definition

To estimate the relationship between manure application, PM concentrations, and health outcomes, I exploit the variation induced by the spreading prohibition framework in Lombardy. To cope with unobservable confounders that may drive the level of pollutants in parallel with manure spreading, I restrict the sample to periods of “spreading windows” ( $W$ ), i.e. consecutive days of spreading ban ( $W^-$ ) followed or preceded by consecutive days in which spreading is allowed ( $W^+$ ). A window is considered closed whenever prohibitions are in place, open otherwise. This implies that windows that are in temporal order either open-closed or closed-open will be considered the same event. The choice of closing and opening intervals lies on two major considerations. First, under the assumption that spreading happens relatively close to the cut-off day<sup>18</sup>, the window should be as such so to allow most of the chemical reaction of gaseous precursors to take place and, in turn, the formation of PM due to the release of ammonia. Second, a window should be short enough

---

<sup>15</sup>Interministerial decree 19 December 2011, 23 October 2013, 11 October 2016.

<sup>16</sup>Source: Eurostat. Animal Production Statistics.

<sup>17</sup>See Figure E.7 in Appendix.

<sup>18</sup>As previously argued, farmers have the incentive to apply manure when a spreading ban is about to be imposed (in order to maximize storing capacity in face of restrictions) and or when this is lifted (to free up storage space).

to ensure as much comparability as possible, conditional on observables, between days before and after the opening/closing cut-off. As such, the choice of the threshold needs to balance the need to let spreading and SIA particles formation occur in the days without prohibitions, as well as to minimize the possibility of confounders, ensuring comparability before and after. I set the windows to be open and close for five consecutive days each, obtaining windows of 10-day duration in total. This number, which serves both goals of particles formation and short time span, is obtained using a data-driven bandwidth selection approach implemented through a regression-discontinuity (RD) design proposed by [Calonico et al. \(2017\)](#). Using data on prohibitions over the entire winter period in my sample years, the RD estimator provides a strategy for bandwidth selection obtained by investigating in the data the persistence of a perturbation induced by a change in treatment status, i.e. relieved spreading prohibitions. Details on the RD estimation and the bandwidth selection method can be found in [Appendix A.1](#).

I consider positive exposure (i.e. open window) as the treatment received by a municipality. Panel [A] in [Figure 3](#) plots the calendar distribution of window days. Spreading windows usually take place around the start (October-November) and the end (February-March) of the regulated winter period. One window exceptionally occurs in December: due to pressure of farmers and impossibility to allocate enough spreading days in the previous months, in 2019 the regulator agreed to a temporary suspension of bans to allow farmers to get rid of accumulated waste<sup>19</sup>. During bulletin-regulated periods, prohibitions may be relieved or imposed heterogeneously across climate zones. For instance, manure application can be delayed in some areas of a few days compared to the rest of the region because of unfavorable weather conditions. As such, in the same 10-day span, some climate zones may exhibit a window with two balanced periods of prohibition and permission, while others may experience longer or shorter periods of window closures (e.g., imagine a climate zone where manure application is restricted for seven consecutive days, and allowed for three ). To avoid imperfect compliance with the treatment status of allowed manure application in my estimates, After identifying the days in which windows take place, in my preferred specification I restrict the sample to climate zones where the window is fully realized ([Figure 3](#), Panel [B]). In most cases (seven out of nine windows), this implies excluding a maximum of two climate zones. The geographical discontinuities in the realization of spreading windows is then used to test the robustness of the results.

After identifying days in which spreading windows took place, using information available through hospital discharge forms, I then select all patients whose hospitalisation occurred on one spreading window day. I focus on patients that have been diagnosed with a respiratory and/or cardiovascular disease. Exposure to high concentrations of particulate matter is associated with additional medical conditions such as skin diseases, psychological disorders, and depression ([Kim et al. 2016](#), [Braithwaite et al. 2019](#)). Yet, R&CDs are the two major and more extensively analyzed effects in the literature, in addition to being comparatively more likely to prompt urgent hospital admissions in case of acute symptoms.

---

<sup>19</sup>Source: *Bollettini Nitrati*, December 2019.



### 3.2 Empirical strategy

My objective is to estimate the effect of short-run exposure to manure spreading events PM concentrations, hospital admissions, hospital mortality, health care use and spending, net of potentially confounding factors. I propose an event-study model summarized by the following equation:

**Model 1:**

$$Y_{ihmt} = \sum_{k \neq -1 \in g} \eta_k \mathbb{1}\{H_{mt} = k\} + X'_{ihmt} \Gamma + \alpha_d + \alpha_{m\tilde{m}} + \alpha_{\tilde{m}y} + \alpha_w + \varepsilon_{ihmt} \quad (1)$$

where  $H_{mt} = t - E_m$  indicates the period relative, to time  $t$ , to the event of manure application being allowed in municipality  $m$  ( $E_m$ ). Periods relative to the spreading event are limited to set  $g = [k : k \in [-T, T - 1]]$ , where  $T = \frac{\text{card}(W)}{2}$  equal to five days.  $\eta_k$  coefficients are estimated pooling together all window events in the sample, with  $k < 0$  characterizing pre-trend coefficients and  $k \geq 0$  capturing treatment at  $k$  days from the window opening.

$Y_{ihmt}$  is the outcome observed in municipality  $m$  at time  $t$ . In the case of healthcare measures, these are also defined at the individual  $i$  and the hospital  $h$  level.  $X$  represent a matrix of of controls, which varies depending on the outcome studied. It always includes six weather controls: temperature, rainfall, humidity, radiance, wind direction (16 indicators), wind speed, average boundary layer height, measured up to the third lag, and interacted amongst each other in current and lagged periods. For health outcomes, when the variable is identified at the individual level (e.g. mortality at discharge, cost of admission), I control for a patient's age class, gender, citizenship, and type of disease (respiratory or cardiovascular) and admission (surgical or medical).  $\alpha_d, \alpha_{m\tilde{m}}, \alpha_{\tilde{m}y}, \alpha_w$ , respectively identify day-level controls (day-of-the-week and holiday fixed effects), province-by-month, month-by-year, and window fixed effects.

Restricting the sample to climate zones that fully experience a spreading window implies that my framework does not include never-treated unit. Thus, the causal identification of the impact of manure application relies crucially on the full comparability of patients, municipalities and hospitals to the left and to the right of the spreading window. In other words short time intervals around spreading windows entails that a municipality's counterfactual is given by the municipality itself few days before. This is true under the assumption of existence of parallel trends in the baseline outcome, conditionally on observables<sup>20</sup>. The assumption rests on multiple considerations. First, spreading limitations are independent from air quality in the regulatory framework, since no PM control objective

---

<sup>20</sup>Formally, let  $Y_{m,t}^\infty$  be the potential outcome of municipality  $m$  which never receives the treatment. Parallel trends require that:

$$\mathbb{E} [Y_{m,t}^\infty - Y_{m,s}^\infty | E_m = k, X_{mt}, \alpha] = \bar{\nu}, \quad \forall s \neq t \text{ and } \forall k \in \text{supp}(E_m)$$

, where in my framework the absence of never-treated unit is represented by  $\infty \notin \text{supp}(E_m)$



exist in the regulator’s agenda. Even more so, manure application is independent from the level and severity of hospital admissions in the region in the eyes of the policymaker. Second, windows are driven by the combination of exogenous events, such as the structure of temporal winter prohibitions (exogenous cut-off days, 90-day fixed prohibition period) and weather conditions (i.e. temperature, rainfall) in the region. Restricting the attention to a short time-span around the cut-off also reduces importantly the probability of capturing underlying trends induced by events correlated with manure application.

Moreover, causal identification of the impact of manure spreading implies no pre-treatment anticipatory behaviour able to affect outcome in absence of treatment<sup>21</sup>. For what concerns PM concentrations, once again the assumption is reinforced by the nature of the spreading control policy implemented in the region, seemingly unrelated to air pollution. Furthermore, manure spreading prohibitions are quite far from the knowledge of the general public and health management structures, and receive minimal news coverage. Yet, being correlated with spikes in airborne pollutants, individuals may have knowledge of high levels of PM in the region potentially induced by manure spreading even without knowing its exact source. In turn, they may take preventive action to avoid exposure: other studies have found that individuals can exhibit shielding behaviour when air quality decreases (Zivin & Neidell 2009, Moretti & Neidell 2011, Neidell 2009). Even under this assumption, however, observing a negative impact on the health of individuals would imply that the real effect of manure management activities could be even higher in absence of prevention from citizens.<sup>22</sup>

Using closed spreading windows as suitable counterfactual is my preferred choice to capture the true impact of manure application. However, the existence of discrepancies in spreading restrictions across climate zones may lead to consider municipalities where spreading is still prohibited compared to the rest of the region as effectively non-treated units, representing a more robust counterfactual and allowing for a difference-in-difference (DiD) kind of estimator. There are two major limitations to this alternative strategy. First, manure application is a source of secondary PM<sub>2.5</sub> generating through the reaction of gaseous precursors. Due to air transportation of pollutants, spillovers, in the form of SIA particles reaching areas where spreading is still restricted, are to be expected and quite complex to quantify. As such, a DiD estimator would likely be biased downward. Second, discrepancies between climate zones are often short-lived: given the 30-day prohibitions lift period universally applying to all climate zones, the regulator has incentive to avoid differences in terms of cumulative restriction days imposed growing large across the region.

---

<sup>21</sup>Formally, this entails:

$$\mathbb{E} \left[ Y_{m,k+l}^k - Y_{m,k+l}^\infty | E_m = k, X_{mt}, \alpha \right] = 0 \quad \forall k \in \text{supp}(E_m) \text{ and } l < 0$$

<sup>22</sup>It is important to notice that the treatment such defined does not suffer from staggered adoption the canonical sense (De Chaisemartin & d’Haultfoeuille 2020, Sun & Abraham 2021, Callaway & Sant’Anna 2021). Indeed, within each window, units enter and exit the window period at the same time, while receiving treatment homogeneously in the same time period. Demeaning by a window identifier allows to cope with window-specific differences in the effect of spreading.

As such, municipalities stay untreated for rather short time, which makes it cumbersome to isolate the effect of manure application. In addition, my main strategy allows to capture causality while preserving a larger number of data points, implying higher statistical power to estimate an impact of manure application rather small in magnitude, as it is expected in particular for health outcomes. These constraints drive the choice to adopt Model ?? as preferred specification. Using a refined sample definition, I still investigate the robustness of the results to a DiD strategy that considers municipalities where prohibitions are still to be relieved as control group. I detail the empirical model in Appendix, Section A.2.

In the spirit of [Borusyak & Jaravel \(2017\)](#), I refer to Equation 1 as *semi-dynamic*. In addition, I estimate the same model in *static* form, i.e.:

**Model 2:**

$$Y_{ihmt} = \eta_0 D_{mt} + X'_{ihmt} \Gamma + \alpha_d + \alpha_{m\tilde{m}} + \alpha_{\tilde{m}y} + \alpha_w + \varepsilon_{ihmt} \quad (2)$$

where  $D_{mt} = \mathbb{1}\{t \geq E_m\}$ . I use the static model to explore spatial treatment heterogeneity based on livestock concentration. I interact  $D_{mt}$  with a set of indicators obtained by binning the number of livestock units at municipal level:

**Model 2b:**

$$Y_{ihmt} = \eta_0 D_{mt} + \sum_{b=1}^9 \gamma_{0b} L_{b0mt} + \sum_{b=1}^9 \rho_b [E_{mt} \times L_{bmt}] + \quad (3)$$

$$+ X'_{ihmt} \Gamma + \alpha_d + \alpha_{m\tilde{m}} + \alpha_{\tilde{m}y} + \alpha_w + \varepsilon_{ihmt}$$

Finally, when my dependent variable has a count nature, such as for daily hospital admissions, I account for non-negative and discrete nature of hospital admissions data with possibly many zeros through a pseudo-Poisson regression model with high dimensional fixed effects ([Correia et al. 2020](#)):

**Model 3:**

$$\mathbb{E}[Y_{ihmt} | D_{mt}, X_{ihmt}, \alpha] = \alpha \exp[\eta_0 D_{mt} + X'_{ihmt} \Gamma] \quad (4)$$

The model thus specified allows the coefficient to differ all across the dimensions accounted by the fixed effects.

## 4 Data Description

### 4.1 Air Quality and Weather

I access high frequency data on major air pollutants between 2016 and early 2020 from ARPA Lombardia.<sup>23</sup> Hourly concentrations of four pollutants, PM<sub>2.5</sub>, PM<sub>10</sub>, ozone, and sulphur dioxide (SO<sub>2</sub>), are recorded through a grid of monitoring stations (Figure E.5, Panel [A]). Data on NO<sub>2</sub> are also collected, but not employed in the analysis. ARPA also provides daily estimates of corresponding municipality-level values are calculated by model interpolation<sup>24</sup>, and they are used to compute daily average concentrations. ARPA is also responsible for collecting data on principal weather variables: humidity, radiance, rainfall, temperature, wind direction and speed. These measures, all potentially correlated with PM levels<sup>25</sup>, are provided uniquely at station level: to match the dimension of air quality measures, municipality-level daily conditions (average temperature, wind direction and speed, humidity, radiance, total rain) are derived taking the value registered at the closest station, as the grid of weather stations provides extensive coverage over the region (Figure E.5, Panel [B]). Alongside weather data, I collect information on Planetary Boundary Layer Height (PBLH) through the ERA5 Reanalysis provided by ECMWF. PBLH is the height above the surface of the ground of the lowest part of the atmosphere, and it is important in affecting weather patterns and the rate of exchange of particulate matter (PM) between the boundary layer and the free atmosphere above it, thus influencing concentrations at ground level (Seidel et al. 2010). The measure is computed on a  $0.25^\circ \times 0.25^\circ$  grid, hence its value derived at municipal level is imputed using the corresponding value at higher geospatial level. Each of these variables directly impacts airborne pollutants concentrations.

The initial sample of winter days (November to March) comprises 2046920 day- municipality observations. Subsequent restriction to windows of spreading discontinuity reduces the sample size 111050 data points. Table 1 describes the dataset, including summary statistics for the full sample, winter months and spreading windows days only. Looking at levels of pollutants (Panel [A]), they all exhibit consistent variation both across municipalities and across time. Focusing on levels of particulate matter, as predictable given colder

---

<sup>23</sup>Regional Agency for Environmental Protection.

<sup>24</sup>Data on concentration of air pollutants are calculated by a private ARPA contractor (AriaNet) using a specific Chemical Transport Model (CTM) called Eulerian FARM-type (Flexible Air Quality Regional Model) (Silibello et al. 2008). FARM-type models account for the transport, chemical conversion and deposition of atmospheric pollutants. Detailed information about this modelling approach is described in Calori et al. (2008). AriaNet also provides an extensive description of the model. See Arianet R2016.12 - FARM (Flexible Air quality Regional Model) formulation and user’s Manual (Version 4.11).

<sup>25</sup>Warmer temperatures are usually associated with lower concentrations, given higher thermal dispersion. Positively correlated with temperature, PBLH constitutes an even more cogent measure for vertical dispersion: higher PBL implies increased dispersion capacity and is associated with lower pollutants concentrations. Similarly, increased level of rainfall reduces PM concentrations through “wet deposition”. As previously noted, wind speed and direction can affect the presence of pollutants in an area by dispersing pollution plums. With increased humidity, moisture particles grow in size to the point of “dry deposition”, reducing PM10 concentrations. Finally, radiance can impact PM levels especially through photochemical reactions.

temperatures and thermal inversion taking place at much lower height, winter months and spreading windows days display consistently higher levels of both  $PM_{10}$  and  $PM_{2.5}$ . Interestingly, the table highlights the extremely poor air quality of Lombardy which, in turn, is matched by a more tolerant policy about warning levels and concentration targets. Indeed, Italy sets the targets for annual average levels for  $PM_{10}$  and  $PM_{2.5}$  at  $40 \mu/m^3$  and  $25 \mu/m^3$  respectively<sup>26</sup>, while the WHO recommendations for the same parameters are respectively  $15 \mu/m^3$  and  $5 \mu/m^3$  (Organization & for Environment 2021). Despite more permissive limitations, warning levels are exceeded frequently, especially during the winter season. Between November and February, the probability of exceeding annual averages is 57% for  $PM_{10}$  and 48% for  $PM_{2.5}$ . Moreover surpassing of control levels happens with similar probability in days when spreading is prohibited against days when it is allowed<sup>27</sup>. Looking at other pollutants, it is important to underline the relatively higher presence of precursors (here only limited to  $SO_2$  and  $NO_2$ ) to secondary aerosol formation.

Turning to weather variables (Panel [B]), the table shows comparable climate conditions between winter months and window days (temperature, radiance, humidity, wind speed and direction tend to display similar averages and standard deviations). Rainfall levels differ instead between winter and spreading windows, with the latter taking place during relatively drier periods. Assessing the correlation between rainfall and spreading window days by regressing rainfall level on a set of dummies for each  $t \in W$ , controlling for fixed effects and other weather conditions (Figure E.8 in Appendix), I notice that there is indeed negative correlation when  $t \in W^+$ , (per regulation, barring spillovers and unexpected weather conditions, spreading is prohibited during rainy days). Yet, the same is true for days right before the opening threshold, and with the size of the coefficients being particularly low, manure application does not strike as a simple proxy for absence of rainfall.

#### 4.2 Livestock concentration and land use

Data on livestock concentrations are accessed through the national zootechnics registry (*Anagrafe Nazionale Zootecnica*) database. The database contains information about number of livestock units and farms for four main breeding animals (chicken, cattle, sheep and goats, swine), calculated at municipal level through a census repeated twice a year (June and December). Summary statistics are reported in Table 2. The table highlights chicken and pig rearing tends to be more concentrated in the region, with a much higher number of animals per farm compared to cow and beef rearing, which is instead more dispersed. The same is true for sheep and goat husbandry, which is however generally carried out in smaller numbers.

Figure 4 shows the presence of farming animals in the region, with the South-West end of the Po Valley emerging as the area with the highest concentrations. As stocks of farming animals are rather stable through time, the number of livestock units is used as a

---

<sup>26</sup>Legislative Decree 155/2010

<sup>27</sup>Figure E.6 shows the cumulative distribution of daily average concentrations of PM under presence and absence of manure application prohibitions.

cross-sectional proxy for intensity of farming activities in a municipality. I apply two main transformations to the data. First, the livestock units in a municipality are recomputed as the average number of livestock within a 5km-radius buffer. This is motivated as census data may account for large farms by assigning all animals to a single municipality. Yet, in this case animals will not be accounted for in neighbouring municipalities which, however, would be similarly exposed to livestock presence due to geographic proximity. Figure E.9 in Appendix show the result of the buffering process.<sup>28</sup> Secondly, to account for differences among farming animals in terms of organic waste impact, the number of units is recalculated using weights given by relative manure daily production, obtained from Hillel & Hatfield (2005). Weights used are reported in Table 2. Weighting does not induce dramatic changes in the computation of animal stocks, thus it affects only marginally the results and does not influence the main conclusions of the analysis. All additional data on the farming industry in the region, i.e. economic class size of firms in the farming industry, disposal outside of farm territory, are computed as time-invariant measures and provided by the 2010 ISTAT Agricultural Census.

#### 4.3 Hospital admissions and treatment outcomes

Data on hospital admission, prognosis, and discharge are obtained from the National Hospital Discharges database. Access to the full dataset is protected, and was authorized by the Ministry of Health, Planning Department. Data is available between 2016 and the end of 2019. The dataset contains main patient-level characteristics, including gender, age, nationality, marital status. Each record also contains detailed information about the urgency of the hospital admission (i.e. either scheduled or unscheduled), date of admission and discharge, municipality of residence and hospital location. For the purpose of this study, I focus on patients resident and hospitalised in Lombardy. A patient is assigned a principal diagnosis and up to five secondary diagnoses that identify co-existing medical conditions. Similarly, the treatment received by each individual is divided into main procedure and up to five secondary procedures performed during the stay. Moreover, it is included the patient's condition at discharge (death, transfer to another structure, regular discharge).

The dataset does not include a cost measure of the hospitalisation. Medical costs of hospital admissions are usually obtained through billing data, but often patients who benefit from NHS coverage do not sustain the true cost of the treatment received thanks to subsidized healthcare provided by the mostly publicly financed NHS. Indeed, the Italian NHS is a decentralized potential payment system (PPS), where regions developed a regional DRG fee-schedule to classify admissions and to identify DRG tariffs, which are designed to cover most of hospital costs (Fattore & Torbica 2006). The Lombardy region provides a detailed tariff scheme that lists monetary values of different DRG points, with further distinction among multiple categories of hospital services (e.g. ordinary admissions, long-term hospital care etc.). I compensate for the lack of a direct cost measure

---

<sup>28</sup>Results are comparable using 2km and 10km buffering radius. See the replication material.

using regional tariffs as a proxy for the actual cost of the hospital stay of an individual. The cost calculation depends on the length of the hospital stay and the treatment received by the individual. A detailed explanation of how the measure is computed using information available is included in Section B. Fee-schedule tariffs are likely less sensitive at the margin, as hospitalisations are assigned a fixed reimbursement whenever the duration of the stay does not exceed the DRG-specific threshold, after which the reimbursement is quantified daily. That is, as long as patients are not hospitalised for longer than the threshold assigned to their diagnosis group, hospitalisations of different duration will be compensated with the same amount, which may not reflect precisely the marginal cost faced by the health facility. Yet, the measure still proxies for the true financial burden of the admission on the public system.

I use the information available to define the following variables. First, I compute an aggregate measure at municipality level which contains the number of hospital admissions of patients from the given municipality on each day. Second, I define a set of admission-specific variables. I include an indicator for the hospitalisation terminating with a patient’s demise versus regular discharge, and calculate the length of a hospital stay in days. I also compute the cost of hospitalisation using DRG tariffs according to Equation A2, and calculate the ratio between admission cost and number of medical procedures executed on a patient. Procedures count alone importantly abstracts from the complexity of treatment received and is not fully representative of the burden sustained by the healthcare facility. Conversely, the ratio defined aims to capture a monetary form of complexity associated with the hospitalisation: patients exhibiting higher cost per procedure are assumed to require more cost-intensive treatment. For brevity, I refer to this measure as “cost-to-procedure”. Finally, I use another proxy for severity derived from a measure provided by the SDO database to gauge the complexity of the hospitalisation. This measure is expressed by a relative weight assigned to DRG codes, relating the average costs of treating patients within one DRG to the average costs of treating all patients included in the DRG system in Italy (Cots et al. 2011).<sup>29</sup> The variable takes value one when the score exactly coincides with the national average. Relative weights of 2 and above are considered serious instances.

To study the impact of manure application through secondary PM emissions, I focus on patients hospitalized for respiratory and cardiovascular medical conditions. The SDO database is organized according to the International Classification of Diseases, Ninth Revision, Clinical Modification (ICD-9-CM) 2007. I select all patients which display as either primary or secondary diagnosis a disease of the respiratory system (ICD 460-519), a disease of the circulatory system (ICD 390-459), or a malignant neoplasm of respiratory and intrathoracic organs (ICD 160-165). This includes 173,405 patients between 2016 and 2019, 83,675 of which are hospitalised during spreading windows. I differentiate between urgent and non-urgent (regular) patients. Despite regular admissions being scheduled in advance, usually in accordance with patient’s and practitioner’s needs, the health facility maintains the right to reschedule an hospitalisation in order to prevent overcrowding. As

---

<sup>29</sup>The relative score assigned to DRG categories in Italy is listed in the Ministerial Decree 18/12/2008.

such, fluctuations in the number of urgent admissions required could reflect in variability of regular hospitalisations, and vice-versa.

Table 3 summarizes the main characteristics of the healthcare data. R&CD admissions during spreading windows constitute slightly more than 10% of the total in winter months, and around 3.7% of all admissions in the years considered. Spreading window days show negligible aggregate differences in terms of patients average age, sex, and hospital mortality rate. Also financial variables show little difference between the selected sample and the overall population of patients. An average weight of 1.3 shows how the average cost of R&CDs, calculated between 16.5 and 17 thousands euros, is generally higher than the average over all DRG codes. Figure 5 shows instead the distribution of hospitalisations across healthcare facilities in the region. Each bubble pinpoints a facility, with size being proportional to the number of patients admitted for R&CD, and blue shade indicating generally larger hospitals in terms of treated patients. With few exceptions, the map shows possibly unsurprising positive correlation between overall capacity of the facility and hospitalisations for respiratory and cardiovascular conditions. Furthermore, while the largest number of admissions is once again registered in the Milan area, several large facilities also exist in the area with higher livestock concentration.

## 5 Results

### 5.1 Manure Spreading on Air Quality

Panel [A] of Figure 7 reports the estimated pre- and post-treatment coefficients from Equation 1, with the natural logarithm of  $PM_{2.5}$  concentrations as outcome of interest. Coefficients for days before the window opening period are reported to visually inspect the absence of clear pre-trends. Even after conditioning for weather conditions and their interaction up to the third lag, a clear jump in  $PM_{2.5}$  levels emerges when spreading windows are opened. Pre-trend coefficients are considerably lower in magnitude, and lose significance when standard errors are clustered at station level. I perform an F-test in the spirit of [Borusyak & Jaravel \(2017\)](#), who suggest to drop any two pre-trend terms (usually, the omitted categories as far apart as possible, in my case four and one day before the event) and perform an F-test on the remaining ones. The p-value for the test (reported in Panel [A]) barely rejects absence overall significance at 5% level, and fails to reject at 1% level. Conversely, coefficients for the first 3 days remain strongly significant even after conservative clustering and the addition of municipality monthly trends.

The magnitude of the effect of manure application in days of relaxed prohibitions is estimated under the assumption of absence of pre-trends, setting the coefficients for days prior to the opening window day to zero. I report the estimates of static (Columns 1 to 3) and semi-dynamic models (Columns 4 to 6) in Table 4. Static model estimates show an increase between roughly 26.9% and 27.4% in  $PM_{2.5}$  concentrations, extremely stable across specifications. This correspond to around 7.24 to 7.30  $\mu g/m^3$ .<sup>30</sup> Semi-dynamic

---

<sup>30</sup>Results for the same models estimated without log transformation of  $PM_{2.5}$  concentrations are reported



estimates highlight a monotonic increase in the impact of manure application on PM up to the third day after a window opens, with a peak at more than 40% after three consecutive spreading days. The impact also appears to fade out quickly, decreasing to roughly a 8.2% increase on day five, with once again relative stability across specifications.

Panel [B] in Figure 7 reports the estimates for the interaction terms in Model 2b. The estimated coefficients follow an increasing path, with the the effect of a manure application expected to be larger for municipalities where livestock is more concentrated. When a spreading window is open, a municipality in the highest decile of the distribution of livestock units, PM<sub>2.5</sub> concentrations is expected to experience an increase between 7% and almost 10% higher than a municipality in the lowest decile. The effect is also substantially stable to weighting livestock units by animal-specific manure production.

The results of estimating the same models using log concentrations of pollutants other than PM<sub>2.5</sub> as outcome are listed in Appendix. PM<sub>10</sub> exhibits a similar trend (Figure E.10), possibly unsurprising thinking that this measure also includes PM<sub>2.5</sub> particles. Pre-trend coefficients tend to oscillate more, but this could be due by the concurrence of a higher number of sources in the formation of PM<sub>10</sub> compared to fine particulate matter. Conversely, it is found no impact of spreading windows on the levels of pollutants likely unrelated to farming activities, such as ozone and sulphur dioxide (Figure E.12). The coefficients of interest follow no specific patterns, with scattered significance: positive peaks both to the right and to the left of the opening window period. The increasing pattern of the interactions with livestock concentration indicators also disappears.

As the correlation with rainy events and temperatures implied by the regulatory framework on manure application, despite extensive controls, may pose some concerns regarding the presence of omitted confounders, I further assess the robustness of the results using a placebo test which looks at rain events disregarding manure spreading prohibitions. The regulation imposes no spreading during rainy days, and the day immediately after. Assuming that rainfall is the primary driver of the effect on PM concentrations, one may expect to observe a similar increment every time rainfall follows the same pattern underlying the presence of spreading windows. Hence, I restrict the sample to what I define as “rain windows”, rainy days followed by seven days without precipitations. These, per regulation, are viable over which a spreading window as defined in my sample may take place. To make sure that rain windows are not perfectly overlapping with spreading windows, which would nullify the scope of this exercise, I focus on the months not regulated by bulletins (October, December, January and March), where spreading windows are less likely to occur. I then newly estimate Equation 1, where the discontinuity is now set two days away from the rainy event. The results reported in Appendix (Figure E.11) show no similar pattern to the one observed for spreading windows, as coefficients appear not significant, fluctuating in magnitude.

---

in Table D.2 in Appendix. Log transformation does not impact significantly the magnitude and sign of the estimates.

## 5.2 Manure Spreading on Health Outcomes

I explore three sets of results that highlight how of spreading-induced air pollution spikes constitute an active threat to individuals. Table 5 reports the estimated coefficients of the static model, where the outcome investigated is now the number of urgent hospital admissions. The estimation comes with the challenge of municipalities (i.e. patients resident in a municipality) recording zero admissions in several periods, with the fitting zero-inflated models through linear regression often results in unreasonable fit (Greene 1994). To overcome this concern, I first estimate a linear model using day-municipality observations with strictly positive hospital admissions (Columns 1 to 3). Second, I compare these results to the same coefficients estimated on the overall sample through the Poisson model in Equation 4 (Columns 5 to 8). The Poisson model requires minimal assumptions on the data distribution, and can account for the many zeros entries in the number of hospitalisations at day-municipality level. Controls and fixed effects are the unchanged from previous regressions. Columns 1 and 2 show how daily admissions during positive PM spikes are expected to be higher by roughly 0.04 units, around 2% increase with respect to the average number of daily admissions. Since PM concentrations are found to peak around the third consecutive day of manure application, the effect of the spike may be stronger towards the end of opening period. To explore this possibility, in Columns 3 and 4 I restrict the sample to observations that are at least two days apart from the cutoff date.<sup>31</sup> The effect of manure application is even stronger comparing days further apart, since daily admissions now increase by around 0.1 units, with the coefficient significant. The existence of a partial lag in the response of R&CD admissions is also confirmed by estimating the semi-dynamic model (Figure 8). Despite reduced statistical power induced by adding more indicators to the regression, the highest impact is observed on the fourth days into a spreading event, with the coefficient peaking at around 1.08 (Panel A). The same trend is not observed for non-urgent hospitalisations, which are not expected to react to the spike, with coefficients oscillating around zero, never meeting significance at 5% level (Panel B). The pseudo-Poisson estimates show comparable results: lifted prohibitions are associated with an increase in daily urgent hospitalisations by a factor of around 1.046 for the entire sample, and between 1.132 and 1.145 then restricting to days away from the cutoff.

Table 6 illustrates the second set of results concerning mortality at discharge. Model 2 is estimated using the probability of hospital mortality as outcome measure. To enhance interpretability of the coefficients, I use a linear probability model, which also allows to control for a more comprehensive set of fixed effects more easily<sup>32</sup>. Columns 1 to 3 show a 0.7% to 1% increase in the probability of hospital mortality for patients admitted

---

<sup>31</sup>The reason for excluding days close to the threshold symmetrically must be traced in the definition of spreading window. By considering a spreading event as the five days preceding or following the start of a prohibition period, a lag in the impact of PM spike could confound the effect both in days preceding and following the observed cutoff.

<sup>32</sup>The estimated effect is comparable in magnitude to the one obtained at the mean of all continuous controls in a fixed-effects logit model employing the estimation routine on the pseudo demeaning algorithm developed by [Stammann et al. \(2016\)](#).

during spreading events. This could be the result of the increased number of urgent patients hospitalised as spreading windows open, that is a change in the composition of hospitalisations toward patients in more severe conditions. Still, focusing on urgent patients only in Columns 4 to 6 leads to comparable coefficients, with slightly reduced statistical significance due to losing roughly half of the observations. Hence, even urgent hospitalisations appear more likely to result in a patient’s demise when the individual is admitted during a PM spike.

Third, Table 7 shows the estimated impact of manure application on treatment costs and severity. I again separate between the entire sample of patients (Panel A) and urgent admissions only (Panel B)<sup>33</sup>. First, I investigate the effect on the duration of hospital stay in days (Columns 1 and 2). While the negative sign may arise from the highlighted increased mortality rate during hospitalisation, the coefficient for the threshold indicator is never significant and rapidly decreases in magnitude when a more extensive structure of fixed effects is imposed. A comparable patterns is observed for urgent patients. Looking at the "cost-to-procedure" indicator in Columns 3 and 4, there seem to be no significant difference in the average pricing per procedure between patients hospitalised before and after spreading events, although the effect estimated for urgent patients is now stronger in magnitude. Similar considerations apply for the total cost of hospitalisation: the coefficients, while mostly positive and higher for urgent patients, are never significant at 5% level (Column 5 and 6). Lastly, in line with the previous results, the relative financial weight calculated displays positive but non-significant coefficients (Column 7 and 8). The absence of evidence for differential estimated treatment costs per patient during spreading events may have multiple explanations. Firstly, the use of tariffs as an approximation of the cost faced by the healthcare facility may not capture relatively small fluctuations at the margin. Indeed, in a scenario in which the impact of spikes in PM concentrations following manure spreading is not substantial enough to increase the duration of hospital admissions over the DRG-specific threshold, heterogeneous resource utilization spurring from difference in health conditions of inpatients will not result in an increased compensation for the hospital. Moreover, again under the assumptions that higher concentrations of airborne pollutants may not induce severe complications in the majority of patients, healthcare facilities may discharge patients in non-critical conditions also on the basis of budgetary decisions, and the data at hand would not capture general health status at discharge. Being specific to a DRG code and not a single patients, even relative weights may fail to capture any effect on healthcare expenditure per patient, especially under the assumption that increasing PM concentrations will not shift hospital admissions towards diseases with more expensive estimated cost of treatment. While not able to dispel any doubt, these results point towards the existence of no detectable difference in the cost per hospital admissions between outside and during spreading events.

To further ensure my strategy is not capturing underlying trends in hospital activity potentially correlated with winter spreading activities, I propose a placebo test that repeats

---

<sup>33</sup>The results are mostly unchanged when excluding hospitalisations terminated with the patient’s de-  
cease.

the same estimation using diseases that are not directly associated with fine particulate matter. I include digestive system diseases (ICD 520-579), genitourinary diseases (ICD 580-629), and musculoskeletal diseases (ICD 710-740). Whereas these pathologies could still be tangentially correlated to fine PM concentrations,<sup>34</sup> their sensitivity is expected to be much lower, and a comparable effect would rather indicate the presence of underlying omitted factors. The results are condensed in Table D.1. Most of the coefficients are not significant and tend to oscillate between positive and negative. The only recognizable pattern is an observed decrease in hospital admissions, which is however considerably lower in magnitude compared to the effect estimated for R&CD. This may be due to the endogenous response of medical facilities, which may choose to delay or relocate admissions in other departments due to resource constraints (e.g. medical staff, operating rooms, etc.) and limited capacity, although this result is not robust. No upward trend in admissions, as well as no increased mortality from patients in other departments is detected, which reinforces the belief that PM spikes are indeed responsible for the deterioration in R&CD patients' conditions.

## 6 Medical Costs Associated with Manure Application

The results have shown the role of manure application in indirectly influencing the hospital activity and patients' wellbeing through PM emissions. This, in turn, implies a cost for the Italian NHS. I propose a simple back-of-the-envelope calculation to quantify the monetary implications short-term impact of winter spreading activities. This analysis does not encompass the entire cost of manure application borne by Lombardy's population, as it does not account for the potential long-term impact of PM exposure, as well as the presence of symptoms and morbidity not captured by my data as not severe enough to require hospital assistance. As such, this is to be considered an attempt to identify a lower bound to the overall economic cost of manure application in the region. Further research may expand this result with additional evidence on the health concerns of livestock-related emissions other than hospitalisation.

I proceed in two steps. First, the estimates obtained suggest that daily urgent R&CD hospital admissions at the municipal level increase by a factor of 1.04 to 1.145 in response to spreading events. In the 4-year period considered, Lombardy has recorded 355,611 urgent admissions during winter months. Given that spreading activities are allowed 30 out of 120 days, i.e. 25% of winter days, I estimate the average yearly R&CD hospitalisations induced by manure spreading through a simple linear calculation. I find that spreading is responsible for 977.4 to 2814.6 yearly R&CD hospitalisations. This approach rests on the assumption that the effect obtained using a 5-day cutoff is unchanged for windows of different temporal durations. Under the hypothesis that PM may have a more severe and non-linear impact on individuals as exposure to high concentrations is prolonged through time, the impact may vary depending on how prolonged and/or isolated

---

<sup>34</sup>It is argued in the literature that PM could have an immunosuppression function and create systemic inflammation (Marín-Palma et al. 2023).

manure application opportunities are. Yet, given the tendency of the regulator to lift spreading prohibitions for consecutive days, taking advantage of favorable weather conditions observed in the data, this assumption is deemed suitable for the purpose of my cost analysis. As my estimates show no sign of systematic cost differences of hospitalisations during spreading events, I calculate the additional healthcare expenditure resulting from increased hospital activity using the average cost per urgent R&CD admission, set at 17.1 thousand euros. This leads to a 16.7 to 48.1 million euros expenditure increase per year.

Second, I provide a monetary value to the increase in hospital mortality induced by spreading activities. Given the impossibility of following patients after their discharge in the data, pinpointing with precision the average life expectancy of an individual previously hospitalized for a R&CD disease requires some assumptions. Indeed, I rely on life expectancy at birth, set at 78.9 years for men and 83.9 years for women<sup>35</sup>, as a counterfactual to estimate the total of years of life lost in my sample due to spreading activities. Between 2016 and 2019, a total of 20,096 male and 17,633 female casualties upon R&CD hospitalisation took place in winter months, averaging respectively 5024 and 4408 per year. Using the estimated effect in Table 6 and assuming a mortality rate increase by 0.7% to 1% for 30 out of 120 days per year, I calculate a total of 8.8 to 12.6 male and 7.7 to 11 female yearly casualties imputable to manure application. These numbers alone, however, cannot inform on the actual loss in terms of years of life. To derive a total of years of life lost (YLL), I use the gender-specific probability of death upon R&CD hospitalisation for one-year population age groups, computed as the ratio between casualties per age group over total hospital mortality in winter months<sup>36</sup>. I then calculate years of life lost according to the following expression:

$$YLL_g = \frac{1}{4} \sum_{k=0}^{90} \min [\text{Exp}_g - k, 0] \cdot \overline{\text{Dth}}_g \cdot \frac{\text{Dth}_{g,k}}{\sum_{k=0}^{90} \text{Dth}_{g,k}} \quad (5)$$

where  $\text{Dth}_{g,k}$  is the number of casualties in age group  $k$  of patients of gender  $g$  and  $\overline{\text{Dth}}_g$  the average yearly casualties in R&CD departments. The number of inferred casualties in each age group is multiplied by the corresponding expected life span, given life expectancy at birth ( $\text{Exp}_g$ ).<sup>37</sup>

The calculation of years of life lost leads to a yearly total between 86.3 and 123.3. I multiply this number by the value of a statistical life year (VSLY). Conventionally assumed in the literature at 100,000 US dollars (Cutler 2005), a more recent review of European

<sup>35</sup>Source: ISTAT, Statistical survey of "Deaths of resident population" (Istat/P.5)

<sup>36</sup>The weights distribution can be found in Figure 9.

<sup>37</sup>Using life expectancy at birth of the general population may overestimate the years of life lost imputed to young cohorts, under the assumption that history of R&CD hospitalisation may shorten the life expectancy of individuals. Conversely, this strategy necessarily underestimates the years of life lost of cohorts older than the life expectancy threshold, as these individuals will be mechanically imputed a loss of zero. In the absence of any post-discharge information, and given the heterogeneous set of diseases considered, this calculation can still constitute a reasonable approximation, also considering that the inverted U-shaped relationship with age exhibited by the value of statistical life (VSL) in the literature (Aldy & Viscusi 2008).

studies by [Schlander et al. \(2017\)](#) sets this number at 158,448 euros for continental Europe. I thus obtain an estimated cost of 13.8 to 19.5 million.

Altogether, the back-of-the-envelope calculation performed in this section shows an immediate burden on Lombardy's healthcare system spurring from short-term exposure to high PM concentrations, ranging between 30.9 and 67.7 million euros, which sets around 0.8% to 1.8% of the yearly gross value added by the agriculture industry in the region.<sup>38</sup>

## 7 Counterfactual Simulation: Air Pollution with PM targets

### 7.1 Theoretical Framework

The evidence presented in this paper highlights the importance of combining water quality preservation with curbing the impact particulate of matter emissions generated by manure management activities. In 2021, the regional regulator partially acknowledged this concern by adding manure spreading among the prohibited economic activities when temporary measures of air pollution control are in place. As argued throughout the paper, while recognizing spreading as an additional source of air pollution, this policy does not elevate PM concentrations as a driver of manure management activities, but rather as an additional and hardly stringent constraint. However, it is not obvious if, and how, different air pollution targets for farmers should be introduced and what could be the potential gains of bringing PM concentrations into the picture without neither limiting farming activities or improving the current technology for livestock waste disposal.

In this Section, I propose and test the performance of an alternative prohibition scheme that combines the objectives of water- and air-quality preservation, aiming to improve the externalities of management of manure spreading without limiting farmers' activity. The objective of this simple exercise is to minimize the number of days exceeding levels of PM<sub>2.5</sub> unhealthy for sensitive groups, set at  $35 \mu\text{g}/\text{m}^3$ .<sup>39</sup> The key idea behind this procedure is that a more flexible and comprehensive decision rule of spreading prohibitions could optimally target days of foreseen higher PM concentrations, relieving restrictions when pollutants' levels are expected to be low, conditional on suitable weather conditions. As such, the problem entails a decision rule under constraints, amid imperfect predictability of PM levels in future weather conditions. To this aim, the winter prohibition scheme implemented in the Lombardy region, and in other countries in a similar fashion, appears unnecessarily rigid. The long two-month prohibition interval between December and January reduces flexibility and limits the ability of authorities to allocate spreading windows according to multiple types of goals. I abstract from this constraint in my simulated exercise.

I approach the problem in two steps. First, I evaluate the reduction in days character-

---

<sup>38</sup>Total value added calculated at chain linked prices (reference year 2015). Source: ISTAT - National Accounts regional main aggregates

<sup>39</sup>This value is defined according to the standards for the Air Quality Index (AQI) set by the US Environmental Protection Agency (EPA). The threshold was adopted after the revision of the Clean Air Act in 2006. See 71 FR 61144 Oct 17, 2006.

ized by hazardous levels of PM (henceforth, HL days) using a decision rule under perfect forecasting. That is, I use data on pollutant concentration, rainfall, and temperature over my sample period under retrospective allocation of prohibitions days by the regulator. This exercise is an abstraction from the true decision-making process of the regulator, which inevitably can only have a reasonable guess on what will be weather conditions and PM levels in the future. Yet, the strategy is useful to define the maximum reduction achievable through redistribution: the optimum achieved under imperfect forecasting can only approach (but likely never reach) the optimum determined under perfect forecasting. In turn, this helps determine the gains to be expected as precision in forecasting increases. The allocation problem can be solved through a standard linear programming allocation algorithm, regulated by the following set of equations:

$$\min_D \sum_i^T f(D_i) = \sum_i^T (L1_i + L2_i \cdot D_i) \quad (6a)$$

$$\text{s.t.} \quad \sum_i D_i = \frac{T}{4} = W, \quad (6b)$$

$$D_i \leq (1 - \mathbb{1}(R_i > 0)) - \varepsilon, \quad (6c)$$

$$D_i \leq (1 - \mathbb{1}(R_{i-1} > 0)) + \varepsilon, \quad (6d)$$

$$D_i \leq \mathbb{1}(T_i > 0) \cdot \varepsilon + 1 \quad (6e)$$

where  $D_i$  is our decision binary variable taking value one when spreading is allowed, zero otherwise.  $L1_i$  is an indicator taking value one whenever PM levels exceed hazardous levels in the absence of spreading. This entails calculating counterfactual concentrations in days when spreading is observed in the sample. Formally,  $L1_i$  on day  $i$  is calculated as follows:

$$L1_i = \mathbb{1} \left\{ PM_i - \hat{\eta}_0 PM_i \cdot D_i > \bar{\kappa} \right\}$$

Conversely,  $L2_i$  is an indicator taking value one whenever spreading induces PM concentrations to exceed HL under our counterfactual scenario. Formally:

$$L2_i = \mathbb{1} \left\{ PM_i + \hat{\eta}_0 PM_i \cdot D_i > \bar{\kappa} > PM_i - \hat{\eta}_0 PM_i \cdot D_i \right\}$$

$\mathbb{1}(R_i > 0)$  and  $\mathbb{1}(T_i > 0)$  are two indicators taking value one when respectively positive rainfall and average daily temperature below  $0^\circ\text{C}$  are observed on day  $i$ . Given  $\varepsilon \in \mathbb{R}_0^+$  such that  $\varepsilon \rightarrow 0$ , conditions 6c to 6e ensure that spreading cannot be allocated in rainy days and the day immediately after, and in days when the air temperature entails the risk of frozen ground. Condition 6b are integrates in the problem the 90-days winter prohibition period already imposed by the regulator. Finally,  $\hat{\beta}$  represents the counterfactual average effect of spreading activities on PM levels, which is retrieved through the estimation of Equation 2, at  $7.8 \mu\text{g}/\text{m}^3$ .<sup>40</sup>

---

<sup>40</sup>The estimated  $\hat{\eta}_0$  value is reported in Table D.2 in Appendix.



In the day-to-day reality of spreading management, counterfactual PM concentrations cannot be possibly measured retrospectively. A more realistic representation of the decision-making process faced by the regulator implies introducing uncertainty in the model. Specifically, to represent the allocation problem of a forward-looking policymaker, the model needs to incorporate forecasts about future levels of PM. There exist multiple examples of predictive models for PM levels in the literature, each presenting a series of advantages and drawbacks (Gianquintieri et al. 2024). In this paper, I employ a class of Bayesian spatio-temporal models, which exploit the geographically referenced and temporally correlated nature of pollution data, allowing for a minimal set of context-specific assumptions in terms of regional geography (Banerjee et al. 2003, Sahu 2022). Bayesian modeling assumes PM concentrations in site  $s_i$  and time  $t$  to depend linearly on a set of regressors, accommodating for time-varying coefficients, as well as a random process ( $\omega(s_i, t)$ ) and a pure error term ( $\epsilon(s_i, t)$ ) independent across time and space.

$$\text{PM}(s_i, t) = \mathbf{X}'(s_i, t)\beta(s_i, t) + \omega(s_i, t) + \epsilon(s_i, t), \quad i = 1, \dots, n \quad t = 1, \dots, T \quad (7)$$

Given a moderately large number of locations (i.e. municipalities) in my data, model fitting involves large dimensional matrices. As such, I estimate the model using a Gaussian Predictive Process (GPP) proposed by Sahu & Bakar (2012), which defines an autoregressive structure of the random effects at a smaller number of locations (knots), and then predicts those random effects at the data and prediction locations via interpolation (Kriging method). Methodological details on the GPP model choice and the forecasting methodology can be found in Appendix (Section D.1).

As observable regressors, the model employs the same set of weather covariates used in other specifications. To forecast PM levels, it is assumed that expectations of weather conditions coincide with their true value up to three days in the future. This assumption simplifies the reality of weather forecasting, which is usually estimated with partial error<sup>41</sup>. Yet, given the absence of systematic bias in weather forecasts, the prediction error on weather variables is considered a zero-mean random variable, i.e.

$$\begin{aligned} \tilde{T}_{i+1} &= T_{i+1} + u_{i+1} \\ \mathbb{E}[\tilde{T}_{i+1}] &= \mathbb{E}[T_{i+1} + u_{i+1}] \\ &= T_{i+1} + \mathbb{E}[u_{i+1}] = T_{i+1} \end{aligned} \quad (8)$$

This assumption allows to importantly simplify the algorithm by taking the observed future values of weather regressors as a proxy for forecast values. On the other hand, it necessarily abstracts from inaccuracies in weather forecasts, with implications that will be discussed in the next paragraph.

---

<sup>41</sup>The Italian Air Force Meteorological Service estimates that temperatures are normally predictable through weather forecasts within a confidence interval of 4 degrees Celsius up to 72 hours in the future. Wind speed and the probability of rainfall are estimated respectively with a 5 m/s confidence interval and an accuracy of 90%. See <https://www.meteoam.it/it/rmsc---general-information>.

The forecasting of PM levels comes with considerable error. This is related to the idiosyncratic shocks affecting air quality that are not captured by simple weather conditions. As such, my spatio-temporal model does not possess enough precision to simply apply the static algorithm in Equations 6a to 6e substituting actual with predicted values. Instead, I propose a refined dynamic optimization algorithm that compares the predicted daily levels of PM with a reasonable benchmark, identified with the monthly average of the previous year. The rationale behind this approach is to recognize days in which weather conditions are more favorable to limit emissions from spreading and prioritize allocation to those days. Formally, let a location  $s_0$ , and let the forecast level of PM at time  $i+k$  given by

$$\widehat{\text{PM}}_{i+k} = \Phi(\mathbf{X}'_{i+k}(s_{j \neq i}), \omega_{i+k}(s_{j \neq i})) \quad (9)$$

In addition, let  $\overline{\text{PM}}_i$  be the corresponding monthly average PM concentrations at time  $i$  in the previous year. Allocation is determined by solving the following dynamic optimization problem:

$$\min_D \quad V(D_i) = \sum_i^T g(D_i) = \sum_i^T (D_i + w_i) \exp[\overline{\text{PM}}_i - \widehat{\text{PM}}_i] \quad (10a)$$

$$\text{s.t.} \quad \sum_i^T D_i = \frac{T}{4} = W, \quad (10b)$$

$$D_i \leq (1 - \mathbb{1}(\mathbb{E}[\tilde{R}_i] > 0)) - \varepsilon, \quad (10c)$$

$$D_i \leq (1 - \mathbb{1}(\mathbb{E}[\tilde{R}_{i-1}] > 0)) + \varepsilon, \quad (10d)$$

$$D_i \leq \mathbb{1}(\mathbb{E}[\tilde{T}_i] > 0) \cdot \varepsilon + 1 \quad (10e)$$

where  $w_i$  is a time-varying penalty score that depends on the number of days allocated up to period  $i$ , i.e.:

$$w_i = \begin{cases} -1 & \text{if } T - i \leq W - \sum_i D_i \\ 1 - \frac{T/W(\sum_i W - D_i)}{T+1-i-(\sum_i W - D_i)} & \text{if } T - i > W - \sum_i D_i \end{cases} \quad (11)$$

Despite adding complexity to the problem, this formulation of  $w_i$  ensures that the payoff of allowing a spreading day increases when the number of days still to be allocated increases relative to the days remaining till the end of the period, up to the point of forcing allocation regardless of predicted levels of PM when the end period is approaching and constraint 10b has yet to be met<sup>42</sup>.

The algorithm is solved via dynamic programming. The three-day assumption on forecast precision of weather covariates conveniently mimics the frequency of bulletins issued by the authority (between 3 and 4 days). As such, the problem is solved iteratively in intervals of three days. After solving the algorithm, I then compare the number of HL

---

<sup>42</sup>Penalty weights are plotted in Section D.

days obtained under the optimized allocation with the actual number between 2016 and 2020.

## 7.2 Simulation Results

The results of the allocation algorithms under perfect forecasting and prediction uncertainty are summarized in Table 8. Supplemental material and additional results of the simulations are detailed in Appendix (Section D). The exercise is repeated separately for each winter excluding 2019-20, year in which the number of actual prohibition days was reduced since spreading was exceptionally allowed in December as an emergency response to farmers exceeding storage capacity. In turn, this complicates the comparison with the simulation algorithm. The Table reports the number of days exceeding hazard levels (*HL*) and days allocated to spreading (*Spread*) by climate zone under the current scenario and compares them to the new allocation under perfect and imperfect forecasting. The number of days allocated using the algorithm is higher in both simulations. In the case of perfect information, the discrepancy originates from imperfect compliance with actual regulation in the sample, i.e. prohibitions being extended over 90 days. With imperfect information, this is also due to the tendency of the algorithm to overshoot by one to two days, which is related to the discrete nature of recurring intervals over which optimization is achieved, and the strong penalty assigned to missing out on the allocation of at least 30 days.<sup>43</sup> In those instances where the algorithm allows more spreading days, I reconcile the number of HL days to be expected with fewer prohibitions involved by using the average yearly probability of a spreading day exceeding hazard levels. For the current allocation, the table also reports violations (Column 4), that is days where the weather constraints are not met (either rainfall during the current day or the day before or temperature below the zero mark), but manure application was allowed. I exclude from the calculation municipalities where PM levels never exceed hazard levels throughout the year. Moreover, I exclude municipalities where weather conditions are such that the restrictions imposed on temperature and rainfall impose more than 90 days of prohibitions regardless of air pollution levels.

First, looking at the results for the allocation under perfect forecasting (Columns 4 to 7), it emerges how targeting PM concentrations alongside other regulatory objectives could potentially reduce HL days in the region by around 10.1 to 14.1 percentage points every year. This only represents an upper bound to the maximum abatement achievable and does not inform on how a prohibitions redistribution scheme may perform without the luxury of knowing PM concentrations in advance. In fact, the results under imperfect forecasting (Columns 8 to 11) are far less stunning in terms of HL days reduction. The percentage variation after accounting for partial overshooting (Column 11) oscillates between positive and negative across climate zones. A modest net gain (i.e. a reduction in HL days) is achieved in winter 2016 and 2018 (around 0.8% in both years), whereas in the winter

---

<sup>43</sup>For instance, if the number of days allocated by the last 3-days forecast window is still 29, the algorithm will consider all possible remaining days as suitable for spreading, allowing up to 32 days. See Appendix for more details.

season of 2017 the algorithm even induces an increase in the HL days, although this is partially justified by that winter having significantly more violations, induced by a wetter and colder season.

Overall, it seems that the refined spreading scheme is not particularly more suitable for keeping PM concentrations within safe levels through simple redistribution, despite the theoretical existence of at least some more room for reduction demonstrated by the static minimization results. This, in turn, gives rise to two considerations. First, the discrepancy between perfect forecasting and allocation of prohibitions under uncertainty implies some room for further improvement in the design of environmental policies regulating manure application. To bridge the gap between the two algorithms, more sophisticated models could be considered to predict PM levels with increased precision. Second, there is only so much that including PM targets can do without any complementary policy action in the farming industry. A perfectly informed management of spreading prohibitions could reduce HL days by around 10%, and even in this scenario, one out of four days would still exceed the danger threshold set for PM concentrations. Alternative measures exist for policymakers to address the concern of secondary emission from manure application, including subsidizing the adoption of best available technologies (e.g. manure injector units) and other mitigation practices (e.g. feeding formulation adjustment) that encompass not only the application phase, but also production and storage (Yan et al. 2024).

## 8 Discussion and Conclusion

Understanding the implications of manure management activities for air quality is essential for crafting adequate environmental conservation policies and protecting the population from unsafe exposure to pollutants. Yet, it is difficult to perform a residual analysis able to isolate the impact of animal waste disposal, given the presence of multiple confounders and simultaneous sources of airborne pollution. Moreover, uncertainty surrounding the toxicity of different PM chemical species makes it even more cumbersome to infer the hazard imposed by organic fertilizers on human health.

My study exploits the unique regulatory framework of the Lombardy region in Italy to isolate the causal effect of manure spreading on PM concentrations. I find a substantial effect on PM levels, stronger in areas where farming animals are densely concentrated. I also find spreading activities negatively affect health, increasing by a small yet relevant amount of urgent respiratory- and cardiovascular-disease-related hospitalisations and on the mortality rate of patients at discharge. I calculate this effect to account for an immediate financial burden on health care facilities and individual of as much as 37.14 million euros per year. This effect does not take into account the economic cost of long-term repeated exposure to PM spikes, in addition to potentially submerged costs from individual morbidity and sickness not resulting in hospital admission. In this regard, the findings in this paper are in line with the evidence of epidemiological studies showing association between inorganic aerosol particles, respiratory and cardiovascular diseases and mortality (Dockery & Pope 1994, Lippmann & Thurston 1996, Chen, Xu, He, Wang, Du, Du, Qian,

Ji & Li 2018, Joshi et al. 2022).

I conclude my analysis by investigating the potential gains of a more flexible spreading scheme, which incorporates the minimization of winter days with  $\text{PM}_{2.5}$  concentration exceeding the hazard levels into the utility function of a recursively optimizing regulator. Under the assumption of perfect forecasting, the algorithm achieves an average reduction in hazardous days by around 10%. However, using value function iteration by forecasting future weather conditions and PM levels, the new spreading scheme achieves only negligible reductions in days when PM is in dangerous concentrations.

The paper highlights an important, yet rather specific type of externality implied by manure management. Future research should focus on quantifying other aspects of airborne pollution from farming, such as milder forms of individual sickness. Simulating the impact of a more flexible regulation including PM targets in the objective function of the policymaker calls for more research expanding the results and improving formulas to regulate spreading and reduce environmental concerns. Finally, the paper did not consider how different policies may influence farmers' perception and productivity. Hence, understanding the shape and determinants of the demand curve for environmental regulation in the farming sector constitutes a possible avenue for future research.

## References

- Aldy, J. E. & Viscusi, W. K. (2008), ‘Adjusting the value of a statistical life for age and cohort effects’, *The Review of Economics and Statistics* **90**(3), 573–581.
- Azizullah, A., Khattak, M. N. K., Richter, P. & Häder, D.-P. (2011), ‘Water pollution in pakistan and its impact on public health—a review’, *Environment international* **37**(2), 479–497.
- Banerjee, S., Carlin, B. P. & Gelfand, A. E. (2003), *Hierarchical modeling and analysis for spatial data*, Chapman and Hall/CRC.
- Borusyak, K. & Jaravel, X. (2017), ‘Revisiting event study designs’, *Available at SSRN 2826228*.
- Bouwman, L., Goldewijk, K. K., Van Der Hoek, K. W., Beusen, A. H., Van Vuuren, D. P., Willems, J., Rufino, M. C. & Stehfest, E. (2013), ‘Exploring global changes in nitrogen and phosphorus cycles in agriculture induced by livestock production over the 1900–2050 period’, *Proceedings of the National Academy of Sciences* **110**(52), 20882–20887.
- Braithwaite, I., Zhang, S., Kirkbride, J. B., Osborn, D. P. & Hayes, J. F. (2019), ‘Air pollution (particulate matter) exposure and associations with depression, anxiety, bipolar, psychosis and suicide risk: a systematic review and meta-analysis’, *Environmental health perspectives* **127**(12), 126002.
- Callaway, B. & Sant’Anna, P. H. (2021), ‘Difference-in-differences with multiple time periods’, *Journal of Econometrics* **225**(2), 200–230.
- Calonico, S., Cattaneo, M. D., Farrell, M. H. & Titiunik, R. (2017), ‘rdrobust: Software for regression-discontinuity designs’, *The Stata Journal* **17**(2), 372–404.
- Calori, G., Finardi, S., Nanni, A., Radice, P., Riccardo, S., Bertello, A. & Pavone, F. (2008), ‘Long-term air quality assessment: modeling sources contribution and scenarios in ivrea and torino areas’, *Environmental Modeling & Assessment* **13**(3), 329–335.
- Cambra-López, M., Aarnink, A. J., Zhao, Y., Calvet, S. & Torres, A. G. (2010), ‘Airborne particulate matter from livestock production systems: A review of an air pollution problem’, *Environmental pollution* **158**(1), 1–17.
- Cassee, F. R., Héroux, M.-E., Gerlofs-Nijland, M. E. & Kelly, F. J. (2013), ‘Particulate matter beyond mass: recent health evidence on the role of fractions, chemical constituents and sources of emission’, *Inhalation toxicology* **25**(14), 802–812.
- Chadwick, D., Sommer, S., Thorman, R., Fanguero, D., Cardenas, L., Amon, B. & Misselbrook, T. (2011), ‘Manure management: Implications for greenhouse gas emissions’, *Animal Feed Science and Technology* **166**, 514–531.
- Chay, K., Dobkin, C. & Greenstone, M. (2003), ‘The clean air act of 1970 and adult mortality’, *Journal of risk and uncertainty* **27**(3), 279–300.
- Chay, K. Y. & Greenstone, M. (2003), ‘The impact of air pollution on infant mortality: evidence from geographic variation in pollution shocks induced by a recession’, *The quarterly journal of economics* **118**(3), 1121–1167.
- Chen, C., Xu, D., He, M. Z., Wang, Y., Du, Z., Du, Y., Qian, Y., Ji, D. & Li, T.

- (2018), ‘Fine particle constituents and mortality: a time-series study in beijing, china’, *Environmental science & technology* **52**(19), 11378–11386.
- Chen, S., Oliva, P. & Zhang, P. (2018), Air pollution and mental health: evidence from china, Technical report, National Bureau of Economic Research.
- Chen, Y., Ebenstein, A., Greenstone, M. & Li, H. (2013), ‘Evidence on the impact of sustained exposure to air pollution on life expectancy from china’s huai river policy’, *Proceedings of the National Academy of Sciences* **110**(32), 12936–12941.
- Correia, S., Guimarães, P. & Zylkin, T. (2020), ‘Fast poisson estimation with high-dimensional fixed effects’, *The Stata Journal* **20**(1), 95–115.
- Cots, F., Chiarello, P., Salvador, X., Castells, X. & Quentin, W. (2011), ‘Drg-based hospital payment: Intended and unintended consequences’, *Diagnosis-Related Groups in Europe: Moving towards transparency, efficiency and quality in hospitals* pp. 75–92.
- Council, N. R. et al. (2004), ‘Research priorities for airborne particulate matter: Iv. continuing research progress’.
- Currie, J. & Neidell, M. (2005), ‘Air pollution and infant health: what can we learn from california’s recent experience?’, *The Quarterly Journal of Economics* **120**(3), 1003–1030.
- Currie, J. & Walker, R. (2011), ‘Traffic congestion and infant health: Evidence from e-zpass’, *American Economic Journal: Applied Economics* **3**(1), 65–90.
- Cutler, D. M. (2005), *Your money or your life: Strong medicine for America’s health care system*, Oxford University Press.
- De Chaisemartin, C. & d’Haultfoeuille, X. (2020), ‘Two-way fixed effects estimators with heterogeneous treatment effects’, *American Economic Review* **110**(9), 2964–96.
- Deryugina, T., Heutel, G., Miller, N. H., Molitor, D. & Reif, J. (2019), ‘The mortality and medical costs of air pollution: Evidence from changes in wind direction’, *American Economic Review* **109**(12), 4178–4219.
- Dockery, D. W. & Pope, C. A. (1994), ‘Acute respiratory effects of particulate air pollution’, *Annual review of public health* **15**(1), 107–132.
- Domingo, N. G., Balasubramanian, S., Thakrar, S. K., Clark, M. A., Adams, P. J., Marshall, J. D., Muller, N. Z., Pandis, S. N., Polasky, S., Robinson, A. L. et al. (2021), ‘Air quality-related health damages of food’, *Proceedings of the National Academy of Sciences* **118**(20).
- Fattore, G. & Torbica, A. (2006), ‘Inpatient reimbursement system in italy: how do tariffs relate to costs?’, *Health care management science* **9**(3), 251–258.
- Friedman, M. S., Powell, K. E., Hutwagner, L., Graham, L. M. & Teague, W. G. (2001), ‘Impact of changes in transportation and commuting behaviors during the 1996 summer olympic games in atlanta on air quality and childhood asthma’, *Jama* **285**(7), 897–905.
- Galloway, J. N., Townsend, A. R., Erisman, J. W., Bekunda, M., Cai, Z., Freney, J. R., Martinelli, L. A., Seitzinger, S. P. & Sutton, M. A. (2008), ‘Transformation of the nitrogen cycle: recent trends, questions, and potential solutions’, *Science* **320**(5878), 889–892.
- Garg, T., Jagnani, M. & Pullabhotla, H. K. (2023), ‘Rural roads, farm labor exits, and



- crop fires', *American Economic Journal: Economic Policy* .
- Giannakis, E., Kushta, J., Giannadaki, D., Georgiou, G. K., Brüggeman, A. & Lelieveld, J. (2019), 'Exploring the economy-wide effects of agriculture on air quality and health: Evidence from Europe', *Science of The Total Environment* **663**, 889–900.
- Gianquintieri, L., Oxoli, D., Caiani, E. G. & Brovelli, M. A. (2024), 'State-of-art in modelling particulate matter (pm) concentration: a scoping review of aims and methods', *Environment, Development and Sustainability* pp. 1–23.
- Greene, W. H. (1994), 'Accounting for excess zeros and sample selection in poisson and negative binomial regression models'.
- Guaita, R., Pichiule, M., Maté, T., Linares, C. & Díaz, J. (2011), 'Short-term impact of particulate matter (pm<sub>2.5</sub>) on respiratory mortality in Madrid', *International Journal of Environmental Health Research* **21**(4), 260–274. PMID: 21644129.  
**URL:** <https://doi.org/10.1080/09603123.2010.544033>
- Hausman, C. & Rapson, D. S. (2018), 'Regression discontinuity in time: Considerations for empirical applications', *Annual Review of Resource Economics* **10**, 533–552.
- He, G., Liu, T. & Zhou, M. (2020), 'Straw burning, pm<sub>2.5</sub>, and death: Evidence from China', *Journal of Development Economics* **145**, 102468.  
**URL:** <https://www.sciencedirect.com/science/article/pii/S0304387820300432>
- Hillel, D. & Hatfield, J. L. (2005), *Encyclopedia of Soils in the Environment*, Vol. 3, Elsevier Amsterdam.
- Imbens, G. & Kalyanaraman, K. (2011), 'Optimal Bandwidth Choice for the Regression Discontinuity Estimator', *The Review of Economic Studies* **79**(3), 933–959.  
**URL:** <https://doi.org/10.1093/restud/rdr043>
- Jacobson, T. A., Kler, J. S., Hernke, M. T., Braun, R. K., Meyer, K. C. & Funk, W. E. (2019), 'Direct human health risks of increased atmospheric carbon dioxide', *Nature Sustainability* **2**(8), 691–701.
- Jayachandran, S. (2009), 'Air quality and early-life mortality evidence from Indonesia's wildfires', *Journal of Human Resources* **44**(4), 916–954.
- Jerrett, M. (2015), 'The death toll from air-pollution sources', *Nature* **525**(7569), 330–331.
- Joshi, P., Dey, S., Ghosh, S., Jain, S. & Sharma, S. K. (2022), 'Association between acute exposure to pm<sub>2.5</sub> chemical species and mortality in megacity Delhi, India', *Environmental Science & Technology* **56**(11), 7275–7287.
- Kelly, F. J. & Fussell, J. C. (2016), 'Health effects of airborne particles in relation to composition, size and source', *Airborne Particulate Matter: Sources, atmospheric processes and health*. London: Royal Society of Chemistry pp. 344–82.
- Kelly, F. J. & Fussell, J. C. (2020), 'Toxicity of airborne particles—established evidence, knowledge gaps and emerging areas of importance', *Philosophical Transactions of the Royal Society A* **378**(2183), 20190322.
- Kim, D.-y., de Foy, B. & Kim, H. (2022), 'The investigations on organic sources and inorganic formation processes and their implications on haze during late winter in Seoul, Korea', *Environmental Research* **212**, 113174.

- Kim, K. E., Cho, D. & Park, H. J. (2016), ‘Air pollution and skin diseases: Adverse effects of airborne particulate matter on various skin diseases’, *Life sciences* **152**, 126–134.
- Knittel, C. R., Miller, D. L. & Sanders, N. J. (2016), ‘Caution, drivers! children present: Traffic, pollution, and infant health’, *Review of Economics and Statistics* **98**(2), 350–366.
- Larrieu, S., Jusot, J.-F., Blanchard, M., Prouvost, H., Declercq, C., Fabre, P., Pascal, L., Le Tertre, A., Wagner, V., Rivière, S. et al. (2007), ‘Short term effects of air pollution on hospitalizations for cardiovascular diseases in eight french cities: the psas program’, *Science of the Total Environment* **387**(1-3), 105–112.
- Lelieveld, J., Evans, J. S., Fnais, M., Giannadaki, D. & Pozzer, A. (2015), ‘The contribution of outdoor air pollution sources to premature mortality on a global scale’, *Nature* **525**(7569), 367–371.
- Lippmann, M. & Thurston, G. D. (1996), ‘Sulfate concentrations as an indicator of ambient particulate matter air pollution for health risk evaluations.’, *Journal of exposure analysis and environmental epidemiology* **6**(2), 123–146.
- Liu, J., Kleinman, P. J., Aronsson, H., Flaten, D., McDowell, R. W., Bechmann, M., Beegle, D. B., Robinson, T. P., Bryant, R. B., Liu, H. et al. (2018), ‘A review of regulations and guidelines related to winter manure application’, *Ambio* **47**(6), 657–670.
- Majumdar, D. & Gupta, N. (2000), ‘Nitrate pollution of groundwater and associated human health disorders’, *Indian journal of environmental health* **42**(1), 28–39.
- Maniscalco, J., Hoffmeyer, F., Monsé, C., Jettkant, B., Marek, E., Brüning, T., Bünger, J. & Sucker, K. (2022), ‘Physiological responses, self-reported health effects, and cognitive performance during exposure to carbon dioxide at 20 000 ppm’, *Indoor air* **32**(1), e12939.
- Marín-Palma, D., Fernandez, G. J., Ruiz-Saenz, J., Taborda, N. A., Rugeles, M. T. & Hernandez, J. C. (2023), ‘Particulate matter impairs immune system function by up-regulating inflammatory pathways and decreasing pathogen response gene expression’, *Scientific Reports* **13**(1), 12773.
- Moretti, E. & Neidell, M. (2011), ‘Pollution, health, and avoidance behavior evidence from the ports of los angeles’, *Journal of human Resources* **46**(1), 154–175.
- Neidell, M. (2009), ‘Information, avoidance behavior, and health the effect of ozone on asthma hospitalizations’, *Journal of Human resources* **44**(2), 450–478.
- Neidell, M. J. (2004), ‘Air pollution, health, and socio-economic status: the effect of outdoor air quality on childhood asthma’, *Journal of health economics* **23**(6), 1209–1236.
- Nian, Y. (2023), ‘Incentives, penalties, and rural air pollution: Evidence from satellite data’, *Journal of Development Economics* **161**, 103049.
- Ongley, E. D. (1996), *Control of water pollution from agriculture*, Vol. 55, Food & Agriculture Org.
- Organization, W. H. & for Environment, E. C. (2021), *WHO global air quality guidelines: particulate matter (PM<sub>2.5</sub> and PM<sub>10</sub>), ozone, nitrogen dioxide, sulfur dioxide and*

- carbon monoxide*, World Health Organization.
- Pope III, C. A., Verrier, R. L., Lovett, E. G., Larson, A. C., Raizenne, M. E., Kanner, R. E., Schwartz, J., Villegas, G. M., Gold, D. R. & Dockery, D. W. (1999), ‘Heart rate variability associated with particulate air pollution’, *American heart journal* **138**(5), 890–899.
- Reiss, R., Anderson, E. L., Cross, C. E., Hidy, G., Hoel, D., McClellan, R. & Moolgavkar, S. (2007), ‘Evidence of health impacts of sulfate-and nitrate-containing particles in ambient air’, *Inhalation toxicology* **19**(5), 419–449.
- Sahu, S. (2022), *Bayesian modeling of spatio-temporal data with R*, CRC Press.
- Sahu, S. K. & Bakar, K. S. (2012), ‘Hierarchical bayesian autoregressive models for large space–time data with applications to ozone concentration modelling’, *Applied Stochastic Models in Business and Industry* **28**(5), 395–415.
- Schlender, M., Schaefer, R. & Schwarz, O. (2017), ‘Empirical studies on the economic value of a statistical life year (vsly) in europe: what do they tell us?’, *Value in Health* **20**(9), A666.
- Schlenker, W. & Walker, W. R. (2016), ‘Airports, air pollution, and contemporaneous health’, *The Review of Economic Studies* **83**(2), 768–809.
- Schlesinger, R. B. & Cassee, F. (2003), ‘Atmospheric secondary inorganic particulate matter: the toxicological perspective as a basis for health effects risk assessment’, *Inhalation toxicology* **15**(3), 197–235.
- Schwartz, J., Bind, M.-A. & Koutrakis, P. (2017), ‘Estimating causal effects of local air pollution on daily deaths: effect of low levels’, *Environmental health perspectives* **125**(1), 23–29.
- Sebilo, M., Mayer, B., Nicolardot, B., Pinay, G. & Mariotti, A. (2013), ‘Long-term fate of nitrate fertilizer in agricultural soils’, *Proceedings of the National Academy of Sciences* **110**(45), 18185–18189.
- Seidel, D. J., Ao, C. O. & Li, K. (2010), ‘Estimating climatological planetary boundary layer heights from radiosonde observations: Comparison of methods and uncertainty analysis’, *Journal of Geophysical Research: Atmospheres* **115**(D16).
- Silibello, C., Calori, G., Brusasca, G., Giudici, A., Angelino, E., Fossati, G., Peroni, E. & Buganza, E. (2008), ‘Modelling of pm10 concentrations over milano urban area using two aerosol modules’, *Environmental Modelling & Software* **23**(3), 333–343.
- Squizzato, S., Masiol, M., Brunelli, A., Pistollato, S., Tarabotti, E., Rampazzo, G. & Pavoni, B. (2013), ‘Factors determining the formation of secondary inorganic aerosol: a case study in the po valley (italy)’, *Atmospheric chemistry and physics* **13**(4), 1927–1939.
- Stammann, A., Heiss, F. & McFadden, D. (2016), ‘Estimating fixed effects logit models with large panel data’.
- Sun, L. & Abraham, S. (2021), ‘Estimating dynamic treatment effects in event studies with heterogeneous treatment effects’, *Journal of Econometrics* **225**(2), 175–199.
- WHO (2021), *WHO global air quality guidelines: particulate matter (PM<sub>2.5</sub> and PM<sub>10</sub>), ozone, nitrogen dioxide, sulfur dioxide and carbon monoxide*, World Health Organization.

tion.

- Wong, C.-M., Vichit-Vadakan, N., Kan, H. & Qian, Z. (2008), ‘Public health and air pollution in asia (papa): a multicity study of short-term effects of air pollution on mortality’, *Environmental health perspectives* **116**(9), 1195–1202.
- Xia, F., Xing, J., Xu, J. & Pan, X. (2022), ‘The short-term impact of air pollution on medical expenditures: Evidence from beijing’, *Journal of Environmental Economics and Management* **114**, 102680.  
**URL:** <https://www.sciencedirect.com/science/article/pii/S0095069622000523>
- Yan, X., Ying, Y., Li, K., Zhang, Q. & Wang, K. (2024), ‘A review of mitigation technologies and management strategies for greenhouse gas and air pollutant emissions in livestock production’, *Journal of Environmental Management* **352**, 120028.  
**URL:** <https://www.sciencedirect.com/science/article/pii/S0301479724000148>
- Young, R. & Mutchler, C. (1976), Pollution potential of manure spread on frozen ground, Technical report, Wiley Online Library.
- Zhang, J., Cheng, H., Di Narzo, A., Zhu, Y., Shan, M., Zhang, Z., Shao, X., Chen, J., Wang, C. & Hao, K. (2022), ‘Within- and cross-tissue gene regulations were disrupted by pm2.5 nitrate exposure and associated with respiratory functions’, *Science of The Total Environment* **850**, 157977.  
**URL:** <https://www.sciencedirect.com/science/article/pii/S0048969722050768>
- Zhang, J., Cheng, H., Wang, D., Zhu, Y., Yang, C., Shen, Y., Yu, J., Li, Y., Xu, S., Zhang, S. et al. (2021), ‘Chronic exposure to pm2. 5 nitrate, sulfate, and ammonium causes respiratory system impairments in mice’, *Environmental Science & Technology* **55**(5), 3081–3090.
- Zivin, J. G. & Neidell, M. (2009), ‘Days of haze: Environmental information disclosure and intertemporal avoidance behavior’, *Journal of Environmental Economics and Management* **58**(2), 119–128.

# Tables

Table 1: Summary statistics - Pollutants and Weather Measures

	Full year			November - March			Spreading windows		
	Overall	Within	Between	Overall	Within	Between	Overall	Within	Between
<i>Panel A - Pollutants</i>									
PM <sub>10</sub> ( $\mu\text{g}/\text{m}^3$ )	22.61 (16.10) [0.2; 205.8]	(14.57) [-9.3; 200.1]	(6.85) [4.7; 36.1]	30.49 (18.89) [0.2; 201.3]	(16.10) [-16.2; 187.6]	(9.88) [3.7; 53.5]	34.02 (21.70) [0.7; 198.0]	(19.19) [-11.2; 187.8]	(10.27) [4.9; 54.7]
PM <sub>2.5</sub> ( $\mu\text{g}/\text{m}^3$ )	18.41 (13.34) [0.2; 167.3]	(12.42) [-8.9; 161.9]	(4.87) [4.2; 30.3]	25.75 (15.50) [0.2; 167.3]	(13.40) [-16.9; 158.8]	(7.79) [3.3; 50.4]	24.34 (14.75) [0.4; 137.9]	(13.27) [-9.5; 134.7]	(6.61) [3.9; 45.1]
NO <sub>2</sub> ( $\mu\text{g}/\text{m}^3$ )	23.21 (16.59) [0.0; 174.5]	(13.30) [-19.5; 157.7]	(9.92) [1.1; 56.4]	33.06 (17.19) [0.0; 148.3]	(11.98) [-16.9; 119.6]	(12.34) [1.8; 68.8]	40.11 (21.71) [0.0; 157.6]	(17.54) [-14.5; 139.7]	(12.95) [7.3; 76.7]
Ozone ( $\mu\text{g}/\text{m}^3$ )	98.38 (43.87) [1.9; 370.8]	(43.56) [-3.0; 376.0]	(5.21) [79.2; 112.8]	61.08 (28.84) [1.9; 359.5]	(27.11) [-6.2; 359.2]	(9.84) [38.7; 90.5]	57.57 (18.92) [6. ; 263.3]	(16.22) [3.2; 252.1]	(9.80) [34.9; 86.8]
SO <sub>2</sub> * ( $\mu\text{g}/\text{m}^3$ )	2.51 (2.34) [0.0; 204.5]	(2.10) [-3.0; 201.7]	(1.03) [1.4; 5.6]	2.90 (2.54) [0.0; 204.5]	(2.33) [-2.8; 201.8]	(1.01) [1.8; 5.7]	2.86 (2.45) [0.0; 64.3]	(2.17) [-3.2; 61.1]	(1.14) [1.4; 6.0]
<i>Panel B - Weather</i>									
Temperature (° C)	13.15 (8.32) [-18.7; 37.3]	(8.04) [-13.3; 42.0]	(2.16) [0.5; 15.9]	5.35 (4.25) [-18.7; 21.3]	(3.90) [-14.6; 20.9]	(1.70) [-6.2; 8.3]	7.13 (4.05) [-16.5; 23.3]	(3.77) [-6.7; 23.0]	(1.53) [-3.3; 9.8]
Rainfall (mm)	0.15 (11.29) [0.0; 3250.8]	(11.28) [-2.1; 3248.7]	(0.27) [0.0; 2.3]	0.12 (11.00) [0.0; 2812.8]	(10.99) [-4.5; 2808.3]	(0.43) [0.0; 4.7]	0.05 (0.74) [0.0; 255.5]	(0.74) [-2.5; 253.1]	(0.08) [0.0; 2.5]
Wind Speed (m/s)	2.25 (1.34) [0.0; 26.3]	(1.12) [-3.7; 26.7]	(0.73) [1.0; 6.5]	2.13 (1.51) [0.0; 26.3]	(1.28) [-4.5; 26.5]	(0.80) [0.8; 7.1]	1.96 (1.43) [0.0; 20.5]	(1.26) [-2.8; 19.2]	(0.68) [0.7; 6.2]
Wind Direction (Degree (°))	178.87 (108.81) [0.0; 360.0]	(103.42) [-86.5; 484.9]	(33.95) [53.9; 266.4]	189.17 (110.65) [0.0; 360.0]	(102.94) [-101.5; 506.7]	(40.63) [42.2; 292.6]	187.97 (110.89) [0.0; 360.0]	(105.63) [-96.4; 473.1]	(33.80) [73.3; 298.0]
Radiance (W/m <sup>2</sup> )	158.96 (103.09) [0.0; 1156.7]	(102.74) [-22.8; 1147.4]	(8.39) [115.4; 181.7]	80.63 (59.85) [0.0; 545.9]	(59.54) [-19.3; 544.6]	(6.09) [40.3; 102.4]	71.90 (44.90) [0.0; 321.8]	(44.46) [-22.4; 317.3]	(6.33) [32.9; 94.5]
Humidity (%)	73.90 (16.62) [0; 100]	(16.00) [-8; 111]	(4.50) [63; 82]	80.47 (18.60) [0; 100]	(16.79) [-12; 123]	(8.02) [56; 93]	81.90 (16.43) [0; 100]	(15.20) [-6; 122]	(6.28) [57; 91]
PBLH (km)	1.65 (1.44) [0.0; 5.7]	(1.44) [-0.2; 5.8]	(0.11) [1.3; 1.8]	0.38 (0.35) [0.0; 3.1]	(0.34) [-0.1; 3.2]	(0.07) [0.2; 0.5]	0.41 (0.38) [0.0; 3.1]	(0.37) [-0.1; 3.0]	(0.09) [0.2; 0.6]

*Notes:* summary statistics report mean values, standard deviation (in parentheses), minimum and maximum value (in brackets). Statistics are reporting including all municipality-day observations from 2016 to 2019 (2046920 obs.), months from November till March (848808 obs.), and only spreading window days (111050 obs.).

\* Data on SO<sub>2</sub> are only provided by ARPA at station level. Municipality-level estimates have been computed through interpolation, i.e. distance-weighted average of 4 closest stations.

Table 2: Summary statistics - Livestock

Animal	Livestock Units	Farms	Weight
Chicken	45,985.8 (116,685.7) [0;3,616,334]	1.6 (2.5) [0;21]	0.34
Cow and Beef	1,040.2 (2,402.3) [0;31,517]	13.4 (16.4) [0;225]	74.77
Sheep and Goat	134.3 (347.0) [0;6,267]	10.3 (13.8) [0;192]	40
Pigs	2,916.5 (8,953.3) [0;94,935]	1.9 (3.9) [0;46]	76.73

*Notes:* summary statistics report mean values, standard deviation (in parentheses), minimum and maximum value (in brackets). Column 3 reports statistics for the number of farms per municipality .

\* Weights are computed using relative manure daily production in kg, obtained from [Hillel & Hatfield \(2005\)](#).

Table 3: Summary statistics - Hospital Admissions

	Full year (2016-19)		Nov - Feb (2016-19)		Spreading windows (2016-19)	
	R&CD	Urgent R&CD	R&CD	Urgent R&CD	R&CD	Urgent R&CD
N. admissions	1,831,792	968,667	641,880	355,611	67,979	37,315
Admissions by hospital*	2,026.00 (1,507.95)	1,294.67 (821.63)	714.35 (519.27)	478.85 (292.73)	77.90 (57.83)	54.07 (36.14)
Admissions by municipality*	3,302.49 (7,457.50)	1,918.51 (4,184.33)	1,143.87 (2,588.08)	682.68 (1,498.93)	116.91 (257.81)	62.63 (137.29)
Age	66.08 (24.68)	68.64 (23.72)	65.37 (27.16)	67.07 (25.91)	65.87 (25.15)	68.15 (24.71)
Female (%)	0.43	0.45	0.43	0.46	0.43	0.45
Italian (%)	0.96	0.95	0.95	0.95	0.96	0.95
Mortality rate**						
0-10	3.56	3.63	2.96	2.71	2.83	3.34
10-20	5.72	12.28	5.90	11.68	2.58	6.79
20-30	7.10	22.14	7.52	22.73	9.51	32.93
30-40	10.54	28.43	10.74	28.19	9.49	21.85
40-50	16.51	37.20	16.91	38.75	16.18	37.88
50-60	24.43	49.65	25.20	49.82	25.88	52.96
60-70	32.26	62.90	34.87	64.68	34.10	64.17
70-80	48.78	83.59	54.11	90.02	47.86	81.27
80+	105.31	137.59	115.35	147.27	105.66	136.73
Total					54.84	89.54
Length (days)	10.82 (13.26)	10.86 (10.39)	10.77 (13.19)	10.77 (10.17)	10.50 (12.16)	10.78 (9.80)
N. Procedures	3.35 (1.72)	3.55 (1.65)	3.34 (1.72)	3.52 (1.65)	3.32 (1.72)	3.54 (1.64)
Cost (thousands euros)	17.12 (122.82)	17.29 (139.46)	16.81 (121.25)	16.85 (137.15)	16.55 (108.48)	17.13 (125.98)
Cost-to-procedure (thousands euros)	1.35 (2.20)	0.99 (2.09)	1.32 (2.18)	0.97 (2.07)	1.38 (2.95)	1.08 (2.12)
Severity (weight)	1.36 (1.30)	1.38 (1.30)	1.35 (1.29)	1.35 (1.29)	1.33 (1.21)	1.37 (1.24)

*Notes:* summary statistics report mean values, standard deviation (in parentheses), minimum and maximum value (in brackets) for all four years (2016-19), winter months and days of spreading windows only, including respiratory and cardiovascular diseases (R&CD).

\* Admissions per million of inhabitants.

\*\* Number of casualties per 1000 admissions.



Table 4: Effect of spreading windows on PM<sub>2.5</sub>

log(PM <sub>2.5</sub> )	Static Model			Semi-dynamic model		
	(1)	(2)	(3)	(4)	(5)	(6)
Window	0.269*** (0.004)	0.274*** (0.004)	0.274*** (0.014)			
Day 1				0.221*** (0.006)	0.225*** (0.006)	0.225*** (0.020)
Day 2				0.352*** (0.004)	0.358*** (0.004)	0.358*** (0.014)
Day 3				0.399*** (0.003)	0.406*** (0.003)	0.406*** (0.015)
Day 4				0.137*** (0.002)	0.134*** (0.002)	0.134*** (0.008)
Day 5				0.079*** (0.003)	0.057*** (0.003)	0.057*** (0.017)
Obs	112213	112207	112207	112213	112207	112207
Adj. $R^2$	0.768216	0.802428	0.799565	0.774324	0.809452	0.806691
Weather (extended)	✓	✓	✓	✓	✓	✓
Municipality FE	✓	✓	✓	✓	✓	✓
Municipality-by-month FE		✓	✓		✓	✓
Month-by-year FE	✓	✓	✓	✓	✓	✓
DoW & Holiday FE		✓	✓		✓	✓
Standard errors	Rob	Rob	Clust	Rob	Rob	Clust

*Notes:* the table reports the estimated  $\eta_0$  from Equation 2 (Columns 1 to 3) and the estimated  $\eta_k$  coefficients from Equation 1, where pre-trend coefficients are set to zero. Weather controls include temperature, wind direction, wind speed, rainfall, radiance, humidity, and average planetary boundary layer height, interacted with each other up to three lags. Robust (Columns 1-2 and 4-5) and clustered at sensor level (Columns 3 and 6) standard errors, are reported in parentheses. \*\*\*  $p < 0.01$ , \*\*  $p < 0.05$ , \*  $p < 0.1$ .

Table 5: Effect of spreading windows on hospital admissions

	Linear model				Poisson			
	(1)	(2)	(3)	(4)	(5)	(6)	(7)	(8)
Window	0.040** (0.020)	0.041* (0.021)			0.046** (0.021)	0.048** (0.021)		
Window <sup>†</sup>			0.104** (0.051)	0.102** (0.052)			0.132*** (0.041)	0.145*** (0.041)
Obs	19,689	19,689	11,587	11,587	80225	80225	46210	46210
Adj. $R^2$	0.94	0.94	0.94	0.95				
Dep. Var mean					0.42	0.42	0.42	0.42
Dep. Var mean (>0)	1.81	1.81	1.81	1.81				
Weather Contr.	✓	✓	✓	✓	✓	✓	✓	✓
Distant Days			✓	✓			✓	✓
Month-by-year FE	✓	✓	✓	✓	✓	✓	✓	✓
Municipality FE	✓	✓	✓	✓	✓	✓	✓	✓
DoW & Holiday FE	✓	✓	✓	✓	✓	✓	✓	✓
Month-by-prov FE		✓		✓		✓		✓
Window FE		✓		✓		✓		✓

*Notes:* the table reports the estimated impact of a spreading window on daily urgent R&CD hospital admissions registered in the five days before and five days after an opening event. Weather controls include temperature, wind direction, wind speed, rainfall, radiance and humidity, interacted with each other at up to the third lag. Columns 1 to 4 include only strictly positive observations for hospital admissions, and are estimated through a linear model. Columns 5 and 8 include observations with no admissions, and are estimated through pseudo-Poisson ML fixed effects model.

†: only days at least two days away from the cutoff date are considered to account for potential lag in the effect of PM spikes.

Standard errors, clustered at municipal level, are reported in parentheses. \*\*\*  $p < 0.01$ , \*\*  $p < 0.05$ , \*  $p < 0.1$ .

Table 6: Effect of spreading windows on hospital mortality

	All patients			Urgent patients		
	(1)	(2)	(3)	(4)	(5)	(6)
Window	0.010*** (0.003)	0.008*** (0.003)	0.007*** (0.003)	0.009** (0.004)	0.011** (0.004)	0.011** (0.004)
Dep. Var mean	0.063	0.063	0.063	0.108	0.108	0.108
Obs	57902	57900	57844	30090	30090	30038
Adj. $R^2$	0.002	0.063	0.069	0.002	0.057	0.060
Weather contr.	✓	✓	✓	✓	✓	✓
Indiv. contr.		✓	✓		✓	✓
Municipality FE	✓	✓	✓	✓	✓	✓
Month-by-year FE	✓	✓	✓	✓	✓	✓
Month-by-prov FE			✓			✓
Hospital FE			✓			✓
Window FE			✓			✓

*Notes:* The table reports the estimated impact of a spreading window on hospital mortality. Weather controls include temperature, wind direction, wind speed, rainfall, radiance, humidity, and average planetary boundary layer height, interacted with each other at time  $t$ . Individual controls include sex, age class, disease. Standard errors, clustered at municipal level, are reported in parentheses. \*\*\*  $p < 0.01$ , \*\*  $p < 0.05$ , \*  $p < 0.1$ .

Table 7: Effect of spreading windows on length and complexity of stays

	Length		Cost-to-procedure		Total cost		Severity (weight)	
	(1)	(2)	(3)	(4)	(5)	(6)	(7)	(8)
<i>All patients</i>								
Window	-0.148 (0.113)	-0.040 (0.105)	0.011 (0.288)	0.022 (0.276)	-0.417 (1.022)	0.123 (0.991)	0.018 (0.013)	0.006 (0.011)
Dep. Var mean	10.061	10.061	4.255	4.255	13.989	13.989	1.335	1.335
Obs	66,771	66,706	55,955	55,900	66,684	66,619	66,772	66,707
$R^2$	0.03	0.23	0.02	0.04	0.01	0.03	0.02	0.28
<i>Urgent patients</i>								
Window	-0.141 (0.125)	-0.088 (0.143)	0.371 (0.547)	0.513 (0.580)	0.673 (1.764)	1.426 (1.907)	0.015 (0.017)	0.020 (0.015)
Dep. Var mean	10.458	10.458	4.482	4.482	14.084	14.084	1.356	1.356
Obs	36,175	36,117	30,058	30,007	36,167	36,109	36,175	36,117
$R^2$	0.05	0.14	0.04	0.07	0.03	0.06	0.04	0.39
Weather contr.	✓	✓	✓	✓	✓	✓	✓	✓
Indiv. contr.		✓		✓		✓		✓
Municipality FE	✓	✓	✓	✓	✓	✓	✓	✓
Month-by-year FE	✓	✓	✓	✓	✓	✓	✓	✓
Month-by-prov FE		✓		✓		✓		✓
Hospital FE		✓		✓		✓		✓
Window FE		✓		✓		✓		✓
DoW & Holiday FE		✓		✓		✓		✓

*Notes:* The table estimates the impact of a spreading window on indicators of healthcare utilization and expenditure. Weather controls include temperature, wind direction, wind speed, rainfall, radiance, humidity, and average planetary boundary layer height, interacted with each other at time  $t$ . Individual controls include sex, age class, disease. Cost-to-procedure and total cost of hospitalisation are derived from average pricing and reimbursement tables determined at regional level.

Table 8: Optimized spreading scheme - summary

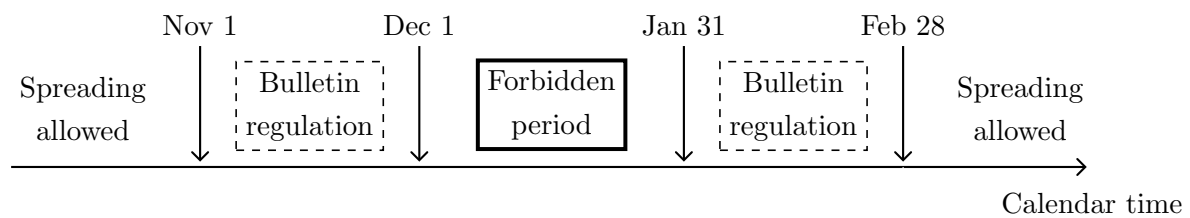
Climate zone	Current allocation			Perfect information				Imperfect information			
	(1) HL	(2) Spread	(3) Violations	(4) HL	(5) HL*	(6) Spread	(7) % change	(8) HL	(9) HL*	(10) Spread	(11) % change
<i>2016-2017</i>											
Alps	972	1050	10	854	854	1050	-12.14	1016	1002	1072	3.09
Central plain	16704	8250	0	15129	15129	8250	-9.43	16722	16630	8396	-0.44
West plain	17134	9780	4	15039	15039	9780	-12.23	16955	16833	9974	-1.76
East plain	2672	1410	0	2450	2450	1410	-8.31	2750	2732	1439	2.25
West Prealps	17693	9750	8	16197	16197	9750	-8.46	17708	17616	9897	-0.44
East Prealps	9297	5880	4	8226	8226	5880	-11.52	9197	9130	5986	-1.8
Total	64472	36120	26	57895	57895	36120	-10.2	64348	63943	36764	-0.82
<i>2017-2018</i>											
Alps	818	1440	23	778	778	1440	-4.89	931	927	1449	13.33
Central plain	9914	6168	76	8974	8247	7674	-16.81	10651	9831	7868	-0.84
West plain	10314	10260	16	9119	9119	10260	-11.59	11022	10952	10406	6.19
East plain	2085	1296	0	1911	1758	1614	-15.68	2284	2133	1609	2.3
West Prealps	13111	9750	273	11719	11719	9750	-10.62	13124	13058	9886	-0.4
East Prealps	6168	5886	449	5647	5481	6231	-11.14	6430	6067	6639	-1.64
Total	42410	34800	837	38148	37102	36969	-12.52	44442	42967	37857	1.31
<i>2018-2019</i>											
Alps	303	630	8	302	302	630	-0.33	411	406	640	26.28
Central plain	10899	8400	0	9670	9670	8400	-11.28	10448	10414	8468	-4.32
West plain	13428	11280	0	12220	12220	11280	-9	13263	13193	11417	-1.24
East plain	1902	1530	0	1729	1729	1530	-9.1	1848	1834	1560	-2.92
West Prealps	7691	9850	19	6925	6925	9850	-9.96	7932	7797	10116	3.04
East Prealps	4154	5310	9	3790	3790	5310	-8.76	4148	4099	5414	-0.14
Total	38377	37000	36	34636	34636	37000	-9.75	38050	37742	37615	-0.86

*Notes:* The table shows the variation in days exceeding hazard levels of PM by climate zone, together with the number of spreading days allocated. The penalty scheme induces the algorithm to prioritize allocating more rather than less days than the imposed target of 30. Winter 2019-20 is excluded due to imperfect compliance with the fixed prohibition period by the regulator (spreading allowed in mid-December), which makes comparison more cumbersome.

\* Days exceeding hazard levels are recalculated accounting for fewer prohibitions than what imposed by the algorithm, using the average yearly probability of a spreading day exceeding hazard levels.

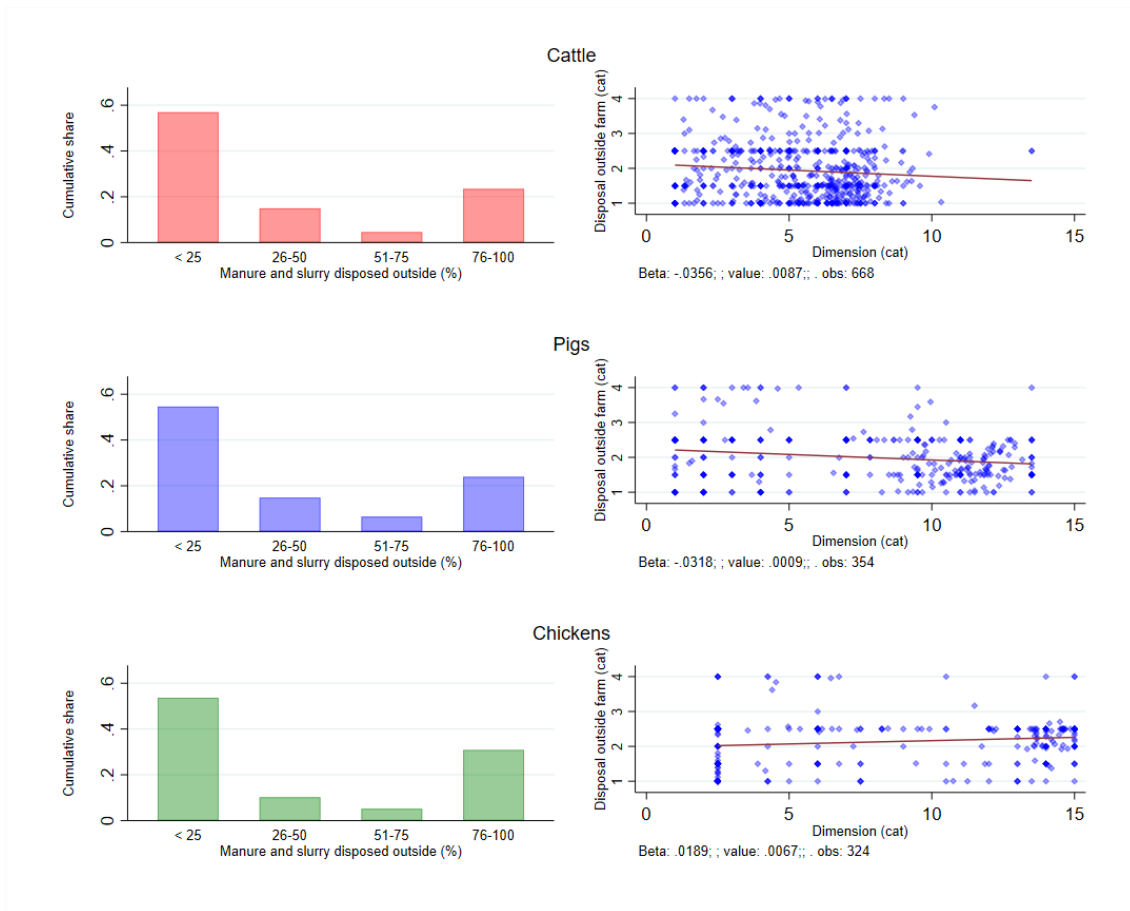
## Figures

Figure 1: Prohibition periods structure in Lombardy



*Notes:* the figure summarizes the periods in which spreading is conditionally or entirely forbidden. This prohibition scheme has been in force in Lombardy between 2016 and 2021.

Figure 2: Frequency of manure disposal outside farm and firm size

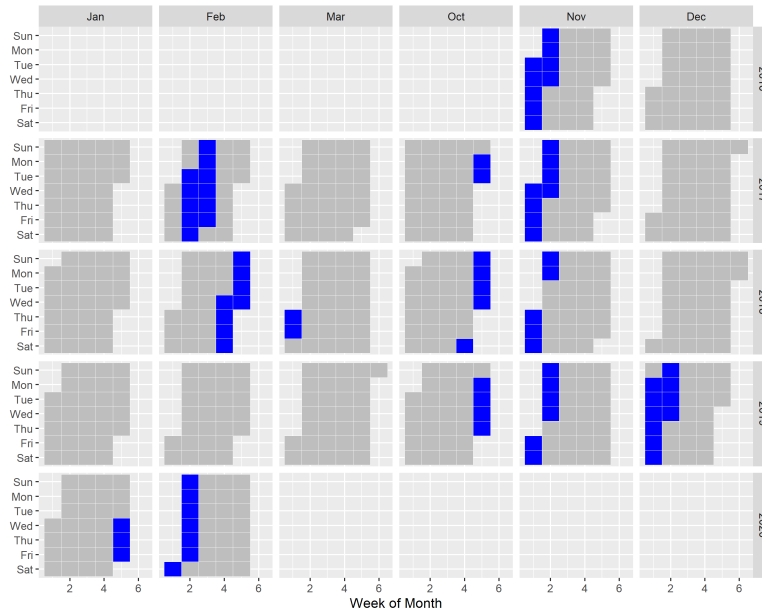


*Notes:* to the left, the figure shows the average cumulative share at municipal level of manure and slurry disposed outside of the farm, divided in 4 categories. To the right, the figure plots the relationship between disposal outside the farm and average farm dimension at municipality level. The variable on the Y-axis is calculated at municipal level as the mean of outside disposal categories 1 (<25) to 4 (76-100) of each farm within the municipality weighted by the relative concentration of animals of the farm. The same weights are applied to the X-axis variables, which is calculated at municipal level as the weighted mean of dimension categories 1 (1-2) to 15 (50000 +) of each farm within the municipality. Coefficient, robust p-values and number of observations of the fitted regression line are reported. Data is not available for goats and sheeps. Source: 2010 Agricultural Census, ISTAT.

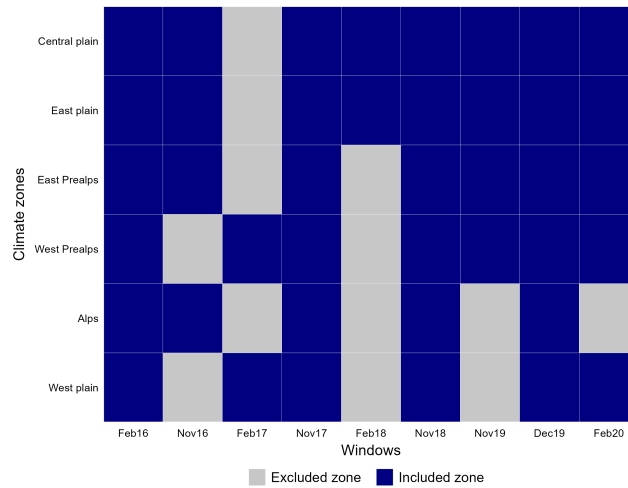


Figure 3: Window days calendar distribution and included climate zones

[A] Window days distribution



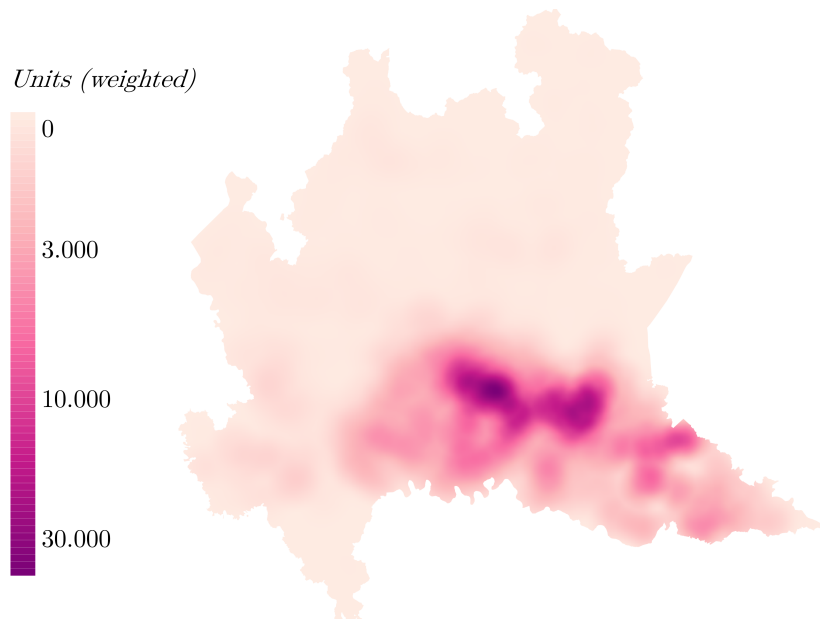
[B] Treated municipalities



Notes: Panel [A] shows the calendar distribution of window days since 2016. One window is located during the yearly fixed prohibition period (December 2019) due to the result of extraordinary amend to regulation (Source: *Bollettini Nitrati*).

Panel [B] presents the climate zones included in the sample for each window. Municipalities are aggregated according to six climate zones, as per current regulation on spreading bans, see Figure E.2. Four out of nine windows set equal restrictions for all climate zones, with seven windows set equal restrictions for more than 50% of the sample municipalities.

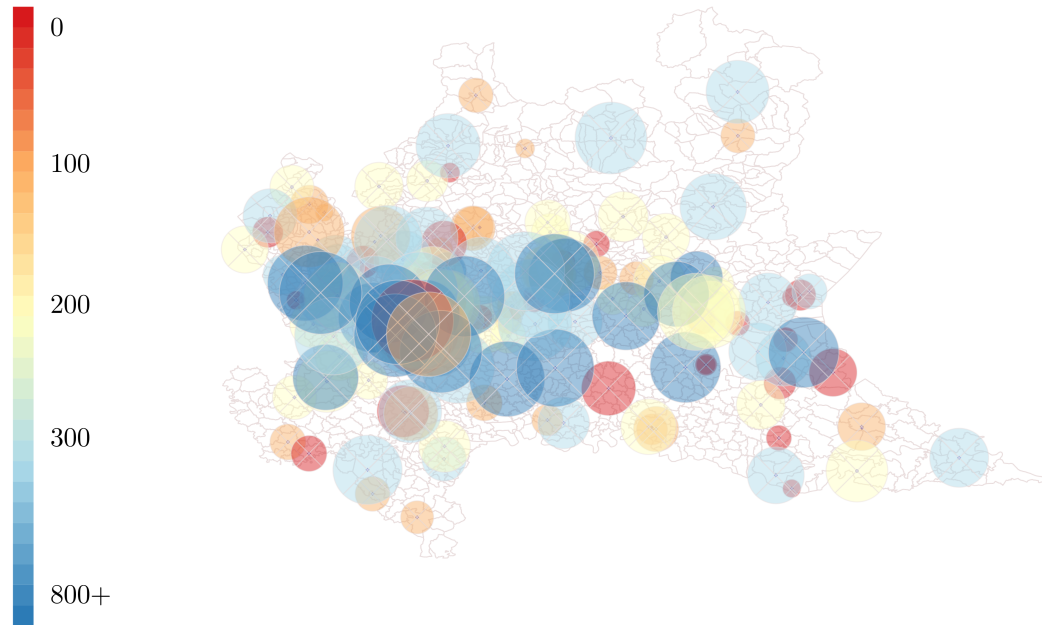
Figure 4: Livestock concentration in the Lombardy region



*Notes:* the figure shows the concentration of farming animals (chicken, cow and beef, sheep and goat, pigs) in the Lombardy region. In computing the total headcount, each animal is weighted by their expected daily production of manure. Weights are obtained from [Hillel & Hatfield \(2005\)](#) and are reported in Table 2.

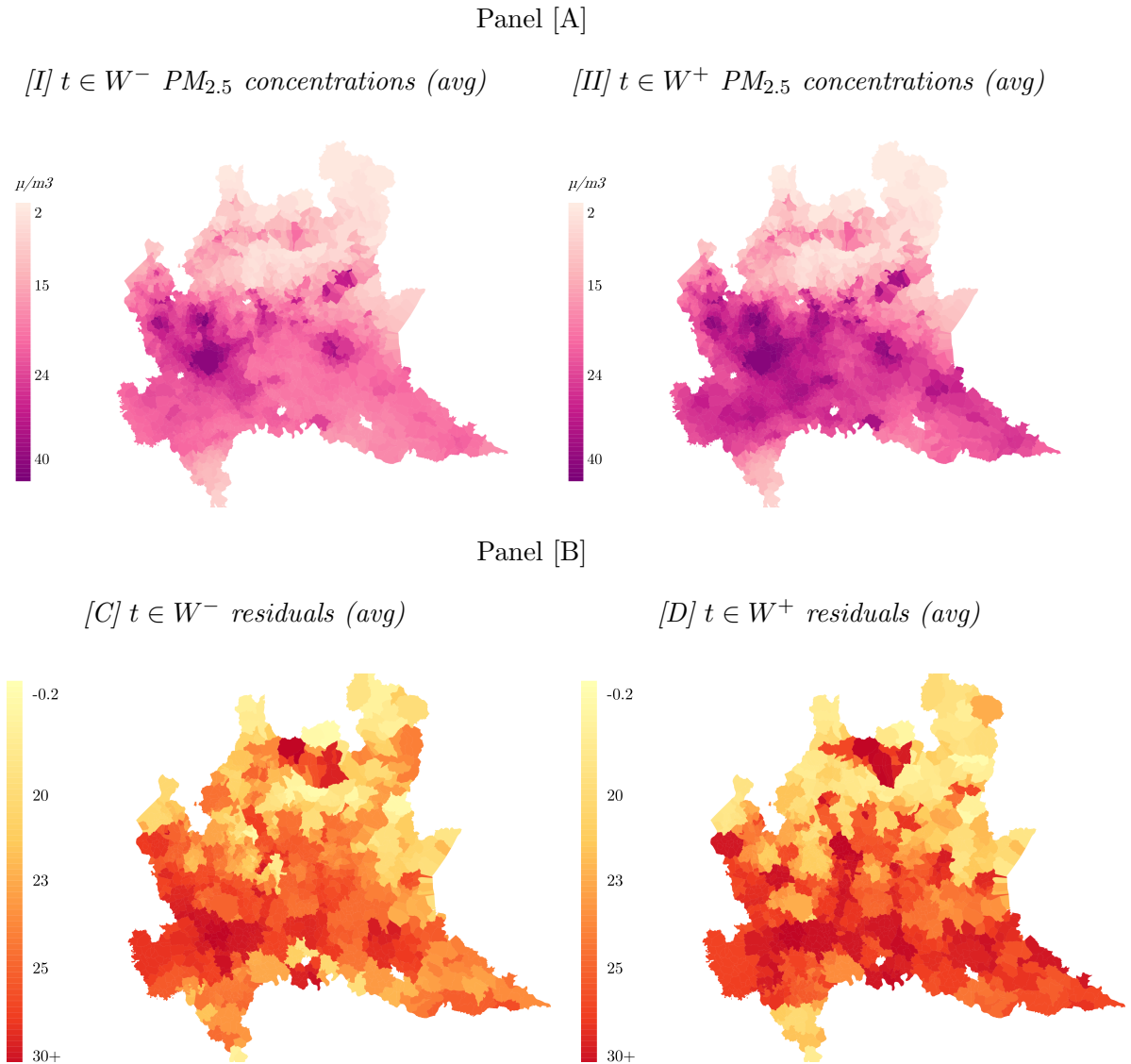
Figure 5: Admissions by Hospital

Admissions R&CD  
(yearly avg.)



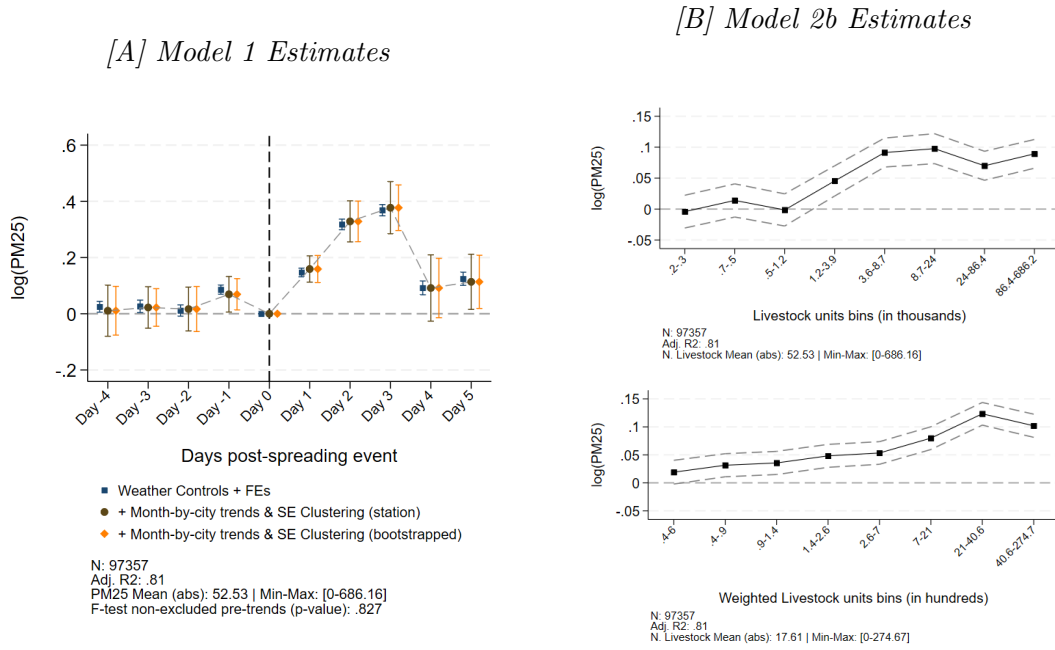
*Notes:* each buffered geopoint represents a hospital. The buffer radius is proportional to the yearly average number of daily hospital admissions across all departments: geopoints of similar size indicate hospitals of comparable overall capacity. The color heatmap represents the yearly average number of daily hospital admissions limited to R&CD: geopoints of similar color indicate hospitals with comparable reception capacity of R&CD patients.

Figure 6:  $PM_{2.5}$  concentrations around spreading windows



*Notes:* the figure depicts air quality conditions around spreading windows ( $W$ ). In Panel [A], average  $PM_{2.5}$  concentrations for days before ( $t \in W^-$ ) and after ( $t \in W^+$ ) the window allowing spreading opening are plotted at municipality level. When spreading is allowed, systematically higher levels of  $PM_{2.5}$  appear in the Po Valley area, where the majority of farming activities is concentrated. In Panel [B],  $PM_{2.5}$  levels in days before and after the window opening are regressed on a set of environmental covariates: humidity, radiance, rainfall, temperature, wind speed, wind direction, included singularly and interacted with each up to the third lag. Predicted residuals are then plotted at municipality level. When spreading is allowed, systematically higher residual variation appears in the Po Valley.

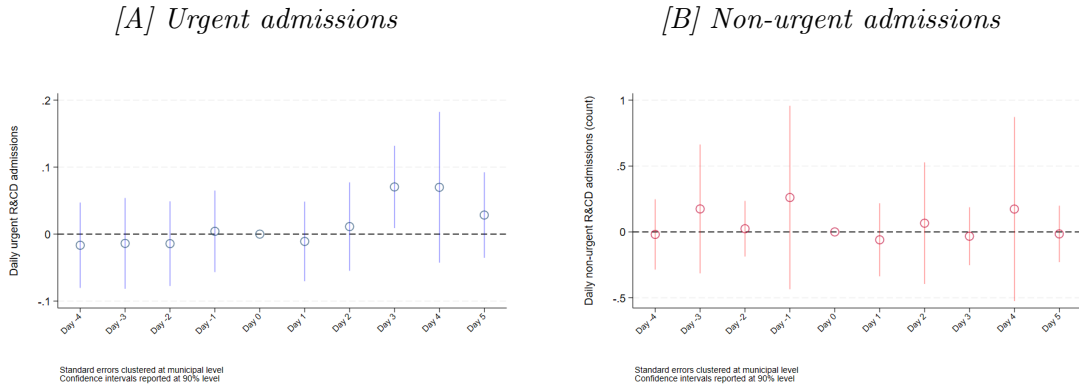
Figure 7: Effect of manure spreading on PM<sub>2.5</sub> concentrations (baseline)



*Notes:* Panel [A] plots the effect of manure spreading windows opening on log PM<sub>2.5</sub> concentrations, depicting the estimates for  $\eta_k$  coefficients in Equation 1. Controls include weather conditions up to the third lag and interacted in each period, and FEs include municipality, month-by-year, day of the week, holiday. Bootstrapped standard errors are sampled with 100 iterations. Coefficients on last prohibition day (day 0) are set to zero. Confidence intervals are plotted at 95% level.

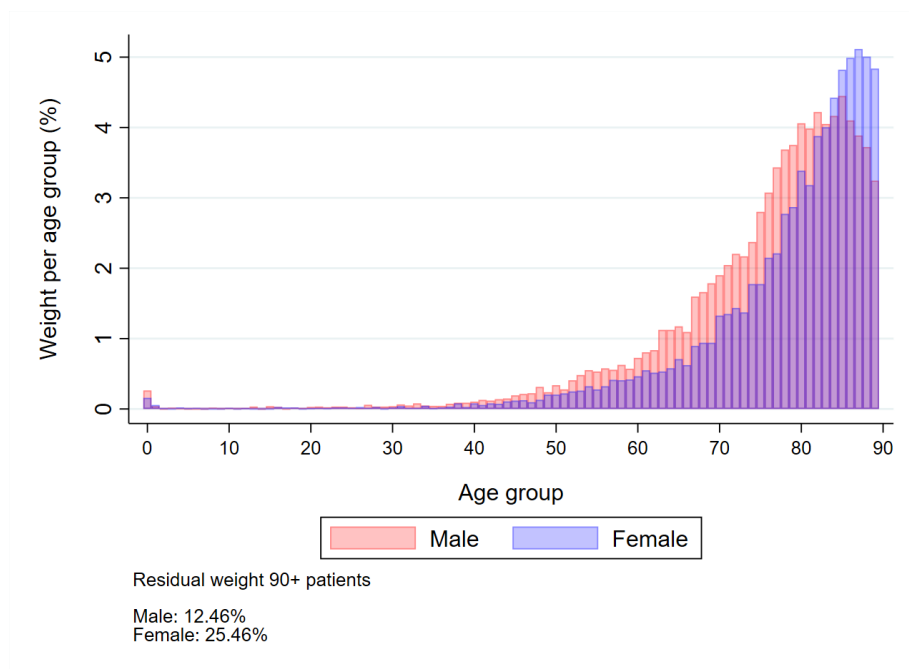
Panel [B] provides the estimates of the  $\rho_b$  coefficients in the static model 2b. Weighted livestock units at municipality level are computed using the weights in Table 2.

Figure 8: Effect of manure spreading on PM<sub>2.5</sub> concentrations (baseline)



*Notes:* the figure shows the effect of manure spreading windows opening on hospital admissions, plotting the estimates for  $\eta_k$  coefficients in Equation 1, where  $k$  is restricted to observations at least two days apart from the window opening cutoff. Controls include weather conditions up to the third lag and interacted in each period, and FEs include municipality, month-by-year, day of the week, holiday, month-by-province and window. Standard errors are plotted at municipal level. Confidence intervals plotted at 95% level. Coefficients in Panel [A] and [B] refer to urgent and non-urgent R&CD hospital admissions respectively.

Figure 9: Computing total VSLY lost to manure spreading - Age group weights distribution



*Notes:* the figure reports the distribution of weights assigned to one-year age groups in the computation of total VSLY lost in response to manure spreading activities. The weights are calculated as the share of deaths at discharge per age group over the total during the sample period. Weights are employed to redistribute the estimated number total casualties across age groups, and derive a counterfactual simulation of years of life lost by individuals in Lombardy.

## Online Appendix

### A Supplementary Models

#### A.1 Regression-Discontinuity Design

In a typical RD design, it is observed an outcome  $Y_i = Y_i(0) \times (1 - T_i) + Y_i(1) \times T_i$ , where  $Y_i(0)$ ,  $Y_i(1)$  represent the outcome in the absence and in the presence of treatment respectively, and  $T_i$  is a determinant of treatment status. Treatment is determined by a running variable  $X_i$  influencing the treatment status whenever  $X_i$  exceeds a cutoff  $c$ , such that  $T_i = \mathbf{1}(X_i \geq \bar{x})$ . My setting can be considered a regression discontinuity in time (Hausman & Rapson 2018), so the unit is considered treated (spreading allowed) past the date of prohibition lift ( $t_i > c$ ). The parameter of interest is identified at the cutoff as:

$$\tau = \tau(c) = \mathbb{E}[Y_i(1) - Y_i(0)|t_i = c, \mathbf{Z}_i]$$

where  $\mathbf{Z}_i$  is a set of covariates. For the derivation of the RD estimator  $\tilde{\tau}$ , I refer to Calonico et al. (2017).

In this framework, estimating the effect of manure spreading using an RD design could pose several challenges, given the volatile and repeated nature of prohibitions, which give rise to multiple discontinuities within a short time span. Yet, the process of neighbor selection implied in the RD estimation can provide a useful benchmark to capture the persistence of the effect of a spreading event through time. For bandwidth selection, it is employed a mean squared error (MSE) optimal criterion, obtained by fitting a curve over a sub-portion of the support of the data, subsequently minimizing errors (Imbens & Kalyanaraman 2011). Let  $h$  be the bandwidth such that  $\tilde{\tau}$  is estimated within the interval  $t_i \in [c - h, c + h]$ , it can be shown that the typical asymptotic MSE expansion is such that:

$$\text{MSE}(\tilde{\tau}(h)) \approx h^{2p+2}B + \frac{1}{nh}V$$

where  $B$  and  $V$  denote the squared bias and the variance of  $\tilde{\tau}$ , and  $p$  is the polynomial order of fit. As such, optimal bandwidth choice can be derived as

$$h_{mse} = \left\{ \frac{\hat{V}_j/n}{2(1+p)\hat{B}_j} \right\}^{\frac{1}{3+2p}}$$

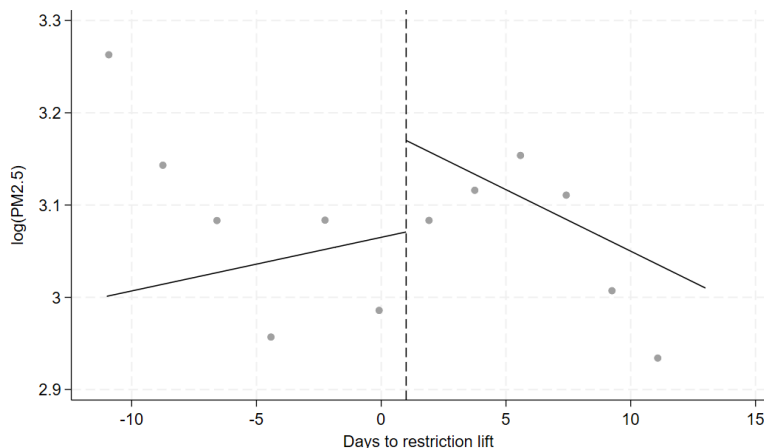
an alternative version of this estimate allows for the bandwidth to vary at the right ( $h_{mse,r}$ ) and at the left ( $h_{mse,l}$ ) of the cutoff, allowing for side-specific  $\hat{B}$  and  $\hat{V}$  estimated parameters.

By defining a running variable as a time counter resetting every time a window is opened (or closed), bandwidth selection can be employed to investigate in the data the persistency of a perturbation induced by a prolonged policy change, in the form of lifted (or reintroduced) spreading prohibitions. I estimate the quantities  $h_{mse,r}$  and  $h_{mse,l}$  using the package `rdrobust` in Stata version 18.0. I consider a first-order polynomial ( $p = 1$ )



and control for the same structure of fixed effects explained in Section 3.2, as well as weather covariates. I focus only on observations between November and March, to align with the period of spreading restrictions.

Figure A.1: Spreading-induced discontinuity in PM levels



*Notes:* the figure plots binned sample means for outcome variable  $\log(PM_{2.5})$  conditional on a running variable computed as relative distance to the day of spreading restrictions being lifted (set to 1), weather controls and fixed effects. Bins including two days around the threshold. The domain is limited to 12 days around the cutoff for visualization convenience. Solid lines represent the conditional mean functions computed with a polynomial of degree 1.

Table A.1: Estimated RD treatment effect and bandwidth span

	(1)	(2)	(3)	(4)
	$\log(PM_{2.5})$	$\log(PM_{2.5})$	$\log(PM_{2.5})$	$\log(PM_{2.5})$
RD Estimate	0.0779*** (0.0146)	0.0580*** (0.0183)	0.0836*** (0.0179)	0.0538*** (0.0144)
Observations	1,225,279	1,156,051	1,084,346	1,002,643
Weather controls	N	N	Y	Y
Fixed effects	Y	Y	Y	Y
Bandwidth (L)	5.174	4.262	5.132	4.173
Bandwidth (R)	5.174	4.643	5.132	4.9879
BW bias (L)	12.19	12.23	12.02	12.56
BW bias (R)	12.19	12.86	12.02	12.99
BW selector	One	Two	One	Two

*Notes:* the table reports the estimated RD coefficient  $\tilde{\tau}$ , together with left- and right-side bandwidth, and bias estimator. In Columns (1) and (3), one common MSE-optimal bandwidth selector for the RD treatment effect estimator is allowed, whereas two separate selectors are specified in Column (2) and (4). Weather controls include temperature, wind direction, wind speed, rainfall, radiance, humidity, and average planetary boundary layer height, up to three lags. Fixed effects include municipality, month-by-year, day of the week, and holiday. Standard errors clustered at PM sensor level in parentheses. \*\*\*  $p < 0.01$ , \*\*  $p < 0.05$ , \*  $p < 0.1$

As previously noted, the RD estimator implies a lower effect of spreading on PM<sub>2.5</sub> concentrations at the cutoff (roughly 25% of the effect estimated through Equation 2). This is explained by considering that in this framework, it is relaxed the requirement of windows exhibiting consecutive days of prohibitions alternated to consecutive days of ban lift. This, in turn, casts part of the effect on either side of the threshold, resulting in a much lower point estimate. Importantly, the estimated bandwidth for discontinuity around the cutoff oscillates between a value of 5.17 and 4.26, which drives my choice of adopting  $T = \frac{\text{card}(W)}{2} = 5$  in Equation 1.

## A.2 Difference-in-Difference Estimator

I propose here an alternative specification that exploits short-lived discrepancies in spreading prohibitions across climate zones. Differently from Models 1 and 2, the goal is to maintain a set of never-treated observations to construct a more classic double-difference estimator. To obtain a reasonable counterfactual to PM concentrations in the absence of spreading, I focus again on short time windows, this time of five days in total. Compared with my preferred strategy, the reduced length is mostly forced by data availability. Instances where spreading is allowed in only part of the region are relatively rare and often involve only a few days of fragmented prohibitions. I consider as a control group municipalities where spreading is not allowed throughout all five days. I then define three levels of spreading-induced treatment, depending on whether spreading is allowed on the fifth day only (level one), on the fourth and fifth day (level two), or starting from the third day onward (level three).<sup>†</sup> Table A.2 lists the days suitable for this strategy and identifies the treated climate zones.

Table A.2: Inclusion of climate zones in DiD strategy

	Day-municipality observations									
	Level three		Level two				Level one			
	Control	Treat	Control	Treat	Control	Treat	Control	Treat	Control	Treat
Alps	385	0	0	385	0	385	0	385	0	385
Central plain	1485	0	0	1485	1485	0	1485	0	1485	0
West plain	0	1900	1900	0	0	1900	0	0	0	1900
East plain	320	0	0	0	320	0	320	0	320	0
West Prealps	0	2135	2135	0	0	2135	0	0	0	2135
East Prealps	1315	0	0	1315	1315	0	0	1315	1315	0
Start date	5-Nov-16		8-Feb-17		31-Jan-18		6-Nov-16		30-Jan-18	

*Notes:* the table reports the number of day-municipality observations identified as treatment and control sample in each event, by climate zone. It is reported start date of the five-day period over which the DiD model is estimated.

I then estimate the following difference-in-difference (DiD) model:

<sup>†</sup>Differently from my main specification, I do not allow a window to be defined backward in time. This prevents confusion in the definition of pre-treatment periods and allows for an easier interpretation of time relative to the relaxation of prohibitions.

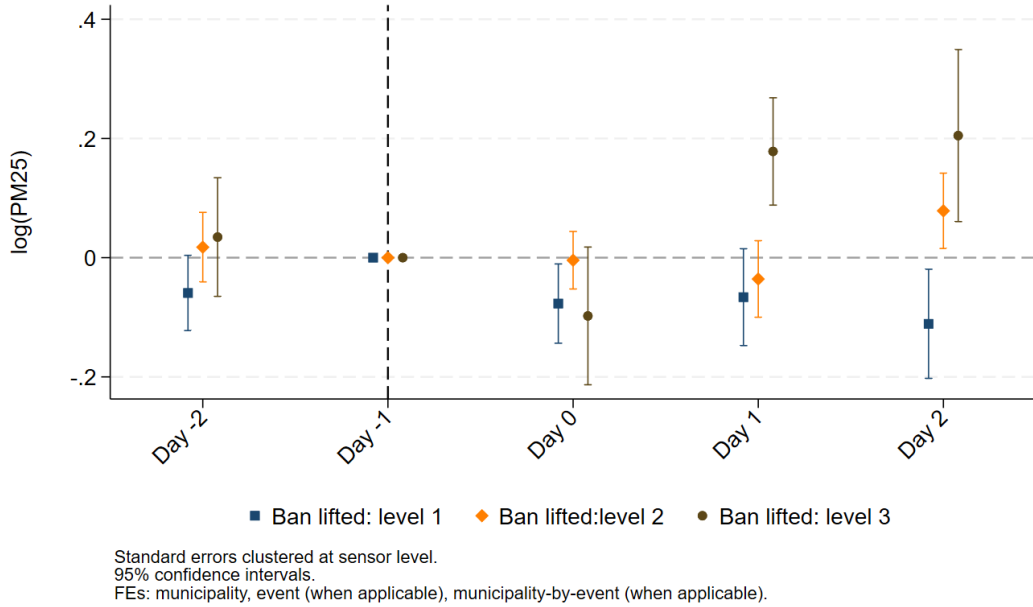
**Model 1b:**

$$\begin{aligned}
 Y_{mt} = & \lambda_0 Treat_m + \sum_{k=-2, k \neq -1}^{k=3} \lambda_{1k} \mathbb{1}\{H_{mt} = k\} + \sum_{k=-2, k \neq -1}^{k=3} \lambda_{2k} \mathbb{1}\{H_{mt} = k\} \times Treat_m + \\
 & + X'_{mt} \Gamma + \alpha_m + \alpha_w + \alpha_{wm} + \varepsilon_{mt}
 \end{aligned}
 \tag{A1}$$

where indices  $i$  and  $h$  are omitted for conciseness as the model is used uniquely to study concentrations of pollutants. The variable  $Treat$  indicates whether spreading is either partially or fully allowed in the municipality starting from the third day. Other variables are defined as in Models 1 and 2, with the exception of fixed effects, for which the reduced number of days considered imposes a different structure to avoid perfect separation. I include municipality, window (when more than one event is present), and municipality-by-window. The DiD coefficients of interest  $\lambda_{2k}$  capture the difference in PM concentrations in climate zones where spreading is allowed compared to the rest of the region. Importantly, one must notice the possibility of treatment spillover induced by the transportation of pollutants. Especially in municipalities bordering climate zones, the effect of spreading in a neighboring area is expected to impact the concentrations of airborne pollutants, albeit to a reduced extent. As such, looking only at DiD coefficients is likely underestimating the true impact of spreading on air quality. Yet, by re-introducing never-treated units in the framework, this strategy reinforces the conclusions presented in the paper.

In the sample I construct, for some municipalities, it is possible to define multiple levels of treatment, depending on whether the start of the observation period is set on a day or the day immediately after. To avoid overlapping definitions of the treatment, I estimate separately Equation A1 for each level of treatment. I then combine the estimated values for  $\lambda_{2k}$  into the same graph (Figure A.2).

Figure A.2: Effect of manure application on PM<sub>2.5</sub> concentrations - DiD estimation



*Notes:* the figure plots the estimated for  $\lambda_{2k}$  coefficients in Equation A1. Controls include weather conditions up to the third lag and interacted in each period, and FEs include municipality, event (when applicable), municipality-by-event (when applicable). Standard errors are clustered at sensor level. Coefficients on last prohibition day (day -1) are set to zero. Confidence intervals are plotted at 95% level. It is reported for each day the coefficient of three levels of treatment: restrictions lifted on day five (level one), restrictions lifted on day four (level two), restrictions fully lifted (level three).

The results exhibit dynamics similar to what already obtained through the main specification in Section 5. Focusing first on level three treatment, it is estimated a sizeable increase in PM<sub>2.5</sub> concentrations in municipalities with early lift in spreading prohibitions starting from the second day. The maximum is observed on day three, with estimated PM concentrations around 20% higher in treated municipalities. As previously argued, the effect is lower than the one reported in Figure 7, likely due to the presence of spillover in the form of circulation of pollutants emitted in treated climate zones being air transported to control zones. The results for municipalities with other degrees of treatment point toward a similar scenario. For treatment of level two, the effect of spreading emerges, even though with a smaller magnitude, on the last day of the selected time window, when spreading prohibitions have been lifted for two consecutive days in treated municipalities. Since the spike in PM concentrations is expected to emerge with a one-day lag, for treatment of level one it is estimated no increase in treated municipalities, with even a slight decrease on the last day of the window. By considering a different combination of days and municipalities compared to the sample included in the estimation of Model 1, these results, paired with the rest of the evidence presented in this paper, strongly support the presence of a true effect of spreading on PM<sub>2.5</sub> pollution.

## B Variables Description

### B.1 Procedure Reimbursement and Cost of Hospitalisation

Similarly to other countries, the Italian National Healthcare System is a prospective payment system (PPSs). Reimbursement for each hospitalisation is based on predetermined, fixed amounts, based on Diagnosis Related Group (DRG) Codes. Being the Italian system subject to considerable decentralisation, tariff lists are determined at regional level. In the case of Lombardy, these were lastly updated in 2015. The table exemplifies the nature of tariff lists.

DRG	MDC	Description	OrdTariff	DHTariff	Threshold	OverTariff
078	04	Pulmonary Embolism	4,466	214	33	155

where columns left to right report DRG code and description, Major Diagnostic Category (MDC), the corresponding daily tariffs for respectively an ordinary hospitalisation lasting more than one day, and a day-hospital regime. In addition, it is set a threshold value for each hospitalisation, after which a second tariff regime (usually with reduced amounts) is applied. In addition to threshold value specific to each DRG, an hospital admission is considered long-term care after 60 days, to which it is applied a fixed reimbursement of 154 euros per day.

As my dataset allows to retrieve the length of the hospital stay and the DRG codes of all procedures undergone by a patient, my measure of cost of hospital stay is calculated according to the following formula:

$$\begin{aligned}
 Cost = & \mathbb{1}\{t = 1\} \times DHTariff + \mathbb{1}\{t \in (1, \text{Threshold}]\} \times OrdTariff + \\
 & \mathbb{1}\{t \in (\text{Threshold}, 60]\} \times (t - \text{Threshold}) \times OverTariff + \\
 & \mathbb{1}\{t > 60\} \times (t - 60) \times 154
 \end{aligned} \tag{A2}$$

## C Manure Spreading Regulation in Italy

Following the Council Directive 91/676/EEC of 1991 concerning the protection of waters against pollution caused by nitrates from agricultural sources, Italy has started regulating the application and storage of manure and slurry. In 2006, the regulatory authority was decentralized from the central to the regional governments (Ministerial Decree 7 April 2006), *de facto* initiating the stream of reforms in the governance of pollutants from farming activities. The table below summarizes the evolution of the regulatory framework in Lombardy since then.

Period	Length prohibitions	Start	End	Scheme	Bulletin	PM attention
2007-2011	90 days	1st Dec (fixed)	28th Feb	Continuous	No	No
2012-2015	90 days to 120*	1st Nov (variable)	28th Feb	Continuous	No	No
<b>2016-2020</b>	<b>90 days (62 continuous)</b>	<b>1st Nov (1st Dec)</b>	<b>28th Feb (31st Jan)</b>	<b>Mixed</b>	<b>Yes</b>	<b>No</b>
2021-Present	90 days (32 continuous)	1st Nov (15th Dec)	28th Feb (15th Jan)	Mixed	Yes	Yes**

\* Restrictions varied depending on the animal source (e.g. poultry) and nature of animal waste (e.g. liquid slurry).

\*\* Attention to PM is limited to additional restrictions at municipal level, imposed when PM control measures (e.g traffic restrictions) are implemented by a municipality.

## D Flexible Spreading Scheme Simulation: Dynamic Optimization

I hereby present in detail the underlying theory and the most salient results of the intermediate steps involved in the dynamic optimization process.

### D.1 Spatio-temporal models of PM concentrations

Spatio-temporal models have been systematically employed in environmental studies related to airborne pollutants, given the geographically referenced and temporally correlated nature of pollution data. In this paper, I focus on the class known as Bayesian spatio-temporal models<sup>†</sup>. Bayesian modeling firstly assumes the independent variable to be described as

$$Y(s_i, t) = \mu(s_i, t) + e(s_i, t), \quad i = 1, \dots, n \quad t = 1, \dots, T$$

where  $s_i$  and  $t$  identify site and time,  $\mu(s_i, t)$  is a space-time process modelled as a regression model of the form

$$\mu(s_i, t) = \mathbf{X}'(s_i, t)\beta(s_i, t)$$

and  $e(s_i, t)$  is a zero-mean space-time process. The model is flexible in accommodating spatio-temporally varying regression coefficients ( $\beta(s_i, t)$ ). It is common to model this overall error term as the some of two independent zero-mean process, a random process  $\omega(s_i, t)$  and a pure error term  $\epsilon(s_i, t)$ , assumed to be independent for all spatial locations at all time points, i.e.

$$Y(s_i, t) = \mathbf{X}'(s_i, t)\beta(s_i, t) + \omega(s_i, t) + \epsilon(s_i, t), \quad i = 1, \dots, n \quad t = 1, \dots, T$$

Starting from this general formulation, I test the performance of multiple model specifications. Firstly, I consider a model which assumes a temporally independent GP for  $\omega(s_i, t)$  and time independent and spatially varying regression coefficients such that

$$\mathbf{X}'(s_i, t)\beta(s_i, t) = \sum_{j=1}^p x_j(s_i, t)\beta_j(s_i, t) \quad (\text{Dynamic GP})$$

and

$$\beta_j(s_i, t) = \beta_{j0} + \beta_j(s_i)$$

where each  $\beta_j(s)$  is assumed to follow an independent GP.

Secondly, I consider an autoregressive model (AR) that reintroduces times series dependence. The model specifies autoregression on a centered random effect  $O_t$  instead of

---

<sup>†</sup>Banerjee et al. (2003) and Sahu (2022) explain thoroughly the nature and properties of this class of models.

directly on the data, and limits autoregression to a single period. The model can be formulated as

$$\begin{aligned} Y(s_i, t) &= O(s_i, t) + \epsilon(s_i, t) \\ O(s_i, t) &= \rho O(s_i, t-1) + \mathbf{X}'(s_i, t)\beta + \omega(s_i, t) \end{aligned} \tag{AR}$$

Part of the reason for imposing independence of one process is the dimensionality implied in fitting the model, especially when the number of locations increases. As a third model, I implement a model of Gaussian Predictive Process (GPP) proposed by [Sahu & Bakar \(2012\)](#), which defines random effects at a smaller number of locations (knots), and assumes an AR model only for the random effects at the knot locations. The model is specified as follows:

$$\begin{aligned} \mathbf{Y}_t &= \mathbf{X}_t\beta + A\mathbf{O}_t + \epsilon_t \\ \mathbf{O}_t &= \rho\mathbf{O}_{t-1} + \mathbf{w}_t \end{aligned} \tag{GPP}$$

where

$$A = CS_{\omega^*}^{-1}$$

with  $C$  the cross-correlation matrix between random effects at locations  $(s_1, \dots, s_n)$  and knots  $(s_1^*, \dots, s_m^*)$  and  $S_{\omega^*}$  the correlation matrix of the random effects  $\mathbf{o}_t$ , depending on the distance between sites.

I fit the models separately for each province and use them to forecast PM levels at municipal level and winter months between 2016 and the beginning of 2020. I use as covariates all weather conditions available (temperature, rainfall, radiance, humidity, wind direction and wind speed). All models are implemented `spTimer` in R. I report here the results for the Lodi province as an example. Results for other provinces and values of PM predicted concentrations can be found in the replication code of this paper. To compare the models, I look in [Table A.3](#) primarily the Posterior Predictive Model Choice Criteria (PMCC), which is the sum of a model's goodness-of-fit (GOF) and penalty terms. According to PMCC, the best model must balance goodness-of-fit and predictive penalty, minimizing the sum of the two. I compare all models with a simple linear alternative as benchmark. In this case, AR strikes as the most suitable model, but all three performs much better than the linear model. Secondly, I compare statistics of model validation through out of sampling predictions. This is done by randomly selecting three municipalities and using half of the observations as a training set to predict the remaining half through the estimated parameters of the models. The results are illustrated in [Figure A.3](#). Visually, all models display very high predictive power. To confirm this intuition, I report commonly used validation criteria, which indeed show little discrepancy between the three models. Given that models score comparatively in validation tests, I opt for the GPP which also minimizes computational burden having to operate with large matrices.

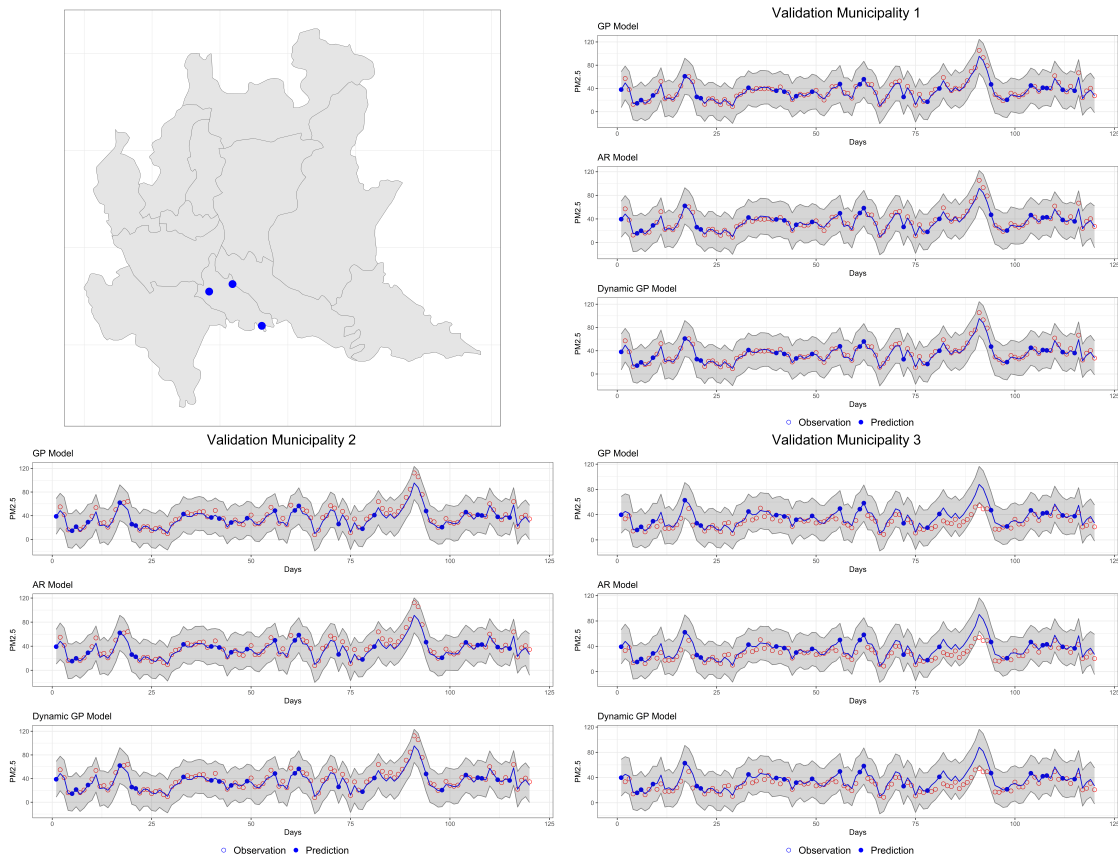


Table A.3: Selection criteria and validations statistics for PM spatio-temporal models

Model	GOF	Penalty	PMCC	RMSE	MAE	CRPS	CVG
Linear	1445979	1453800	2899779	14.7435	11.0604	7.862227	94.44
GPP	1930.16	19820.52	21750.68	7.090132	5.315292	18.50795	100
AR	1928.81	7396.39	9325.2	7.067555	5.200269	7.903886	100
Dyn GP	1727.86	8506.37	10234.23	7.299482	5.519052	8.722338	100

The table reports model selection and validation criteria for three different spatio-temporal models (Gaussian Predictive Process, Autoregressive, Dynamic Gaussian Process) compared to a simple linear alternative. For selection, it is reported the Posterior Predictive Model Choice Criteria (PMCC), obtained as the sum between goodness-of-fit (GOF) and penalty. For validation, Root Mean Square Error (RMSE), Mean Absolute Error (MAE), Continuous Ranked Probability Score (CRPS), and coverage (CVG) are reported. Best-fitting models are expected to minimize all selection and validation criteria while maximizing coverage.

Figure A.3: Validation of spatio-temporal models at three random locations



The figure plots observation predictions and 95% intervals for three municipalities (top-left corner) and three spatio-temporal models (GPP, AR, Dynamic GP). Fitted values are plotted with a solid line. The (true) observations in the training set are plotted as open circles and the (true) observations set aside for validation are plotted as filled circles.

Note that Figure A.3 does not inform on the ability of spatio-temporal models to

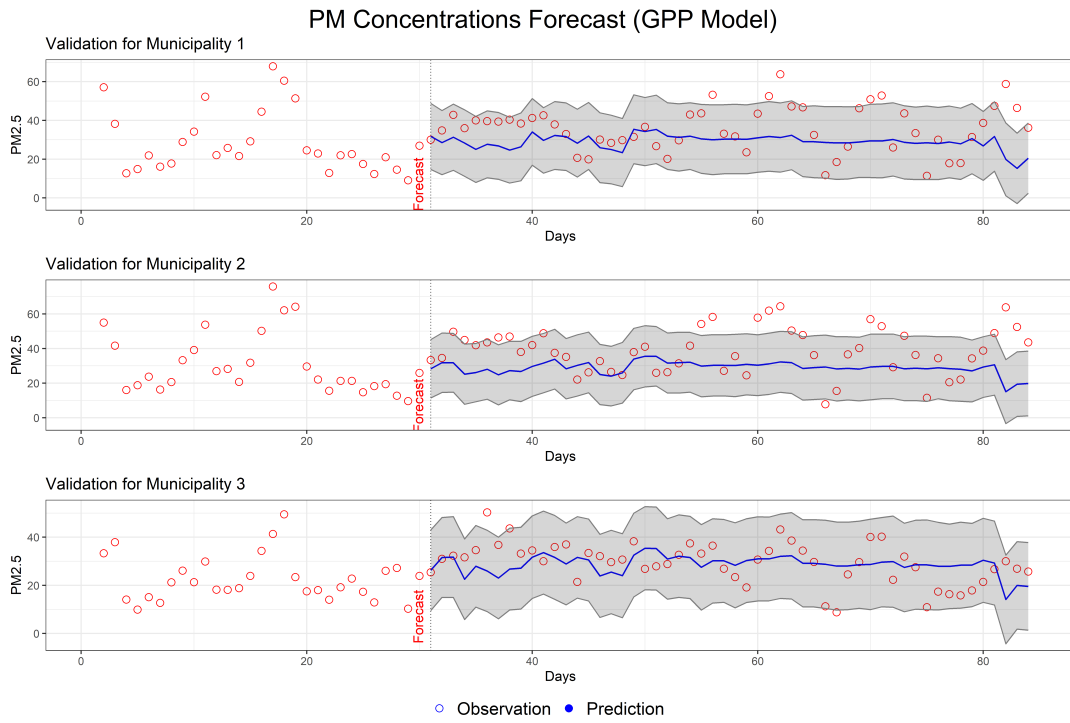
forecast PM concentrations, which constitutes a far more demanding task. This validation technique considers concentrations in neighbouring municipalities as known quantities, and thus exploits tight geospatial correlation in PM distribution to achieve close-to-perfect fit. However, this does not reflect the decision-making process of a regulator who needs to lift spreading prohibitions using incomplete information about future PM levels. Hence, I use the GPP model to forecast PM concentrations three days into the future.

Forecasting implies estimating random effects for each location into the future. Let an unobserved location  $s_0$ . The  $k$ -steps ahead forecasting at such location is performed by assuming independently normally distributed errors ( $\omega_t \sim N(\mathbf{0}, \sigma_\omega S_{\omega*})$ ) and random effects ( $\mathbf{O}_0 \sim N(\mathbf{0}, \sigma_w^2 S_0)$ ) where  $S_0$  is a correlation matrix obtained via the exponential correlation function with a decay parameter  $\phi_0$ . The predictive distribution of  $Y(s_0, T+k)$  is obtained by simply advancing the top-level model equation by  $k$  periods:

$$Y(s_0, T+k) = \mathbf{x}'(s_0, T+k) \beta + \mathbf{a}'_0 S_{\omega*}^{-1} \mathbf{O}_{T+k} + \epsilon(s_0, T+k)$$

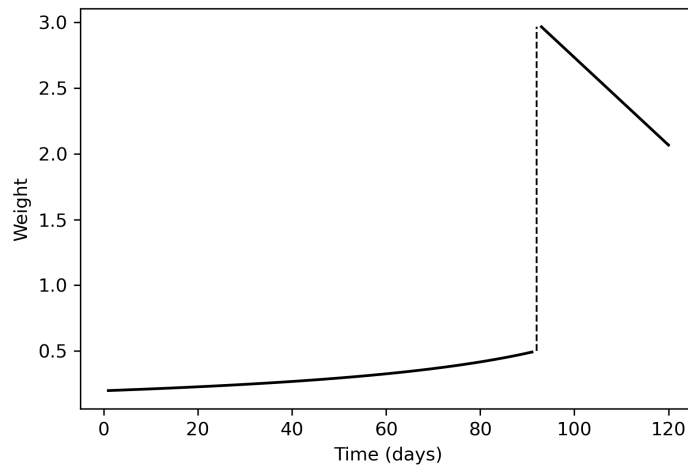
where  $\mathbf{a}'_0$  is a vector of covariance functions that depend on the distance between  $s_0$  and site  $s_j$ . The forecast value for  $Y(s_0, T+k)$  is iteratively drawn from the obtained distribution via Markov chain Monte Carlo sampling. The approach can be then generalized for each  $s_n$ . The forecasting is performed iteratively: the model is estimated using the 30 days prior to the starting date of forecasting. Then, PM levels are observed and the true values are added to the training set before the model is estimated again and forecasts are computed for the following three days. The results for the same three validation municipalities are reported in Figure [A.4](#).

Figure A.4: Forecast PM levels at three random locations



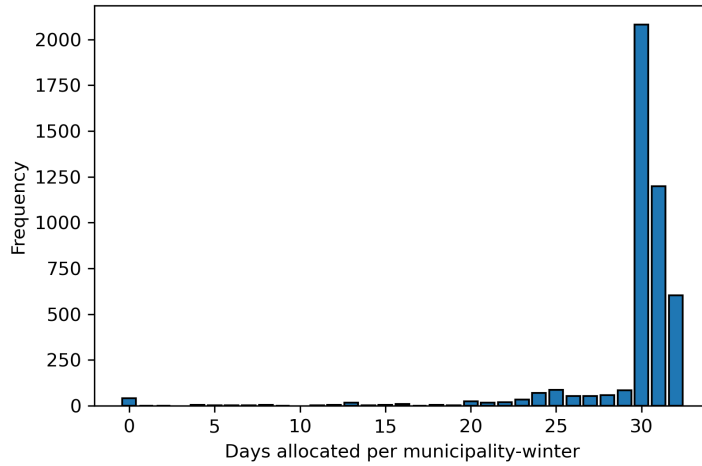
*D.2 Dynamic Optimization Simulation: Additional Results*

Figure A.5: Dynamic optimization algorithm - weighting



*Notes:* the figure plots the weighting function  $\omega$  under the assumption of having still to allocate 30 days over the entire length  $T$ . The discontinuity is set such that, as the algorithm reaches 30 days left till the end of  $T$  with still 30 days to allocate, a strong penalty is imposed for not selecting the following days. In turn, this forces the algorithm to allocate all the following days to spreading as long as weather constraints are met.

Figure A.6: Dynamic optimization algorithm - distribution of allocated days



*Notes:* the figure plots the distribution of spreading days allocated by the dynamic algorithm for each municipality-season combination.

## D Appendix Tables

Table D.1: Placebo test - Effect of spreading prohibitions on other diseases

	Pooled		Digestive		Genitourinary		Musculoskeletal	
	All patients	Urgent	All patients	Urgent	All patients	Urgent	All patients	Urgent
Admission (linear)	0.184 (0.461)	-0.187 (0.140)	0.178 (0.531)	-0.180* (0.105)	-0.280 (0.236)	-0.162 (0.159)	-0.391 (0.259)	-0.280 (0.190)
Obs	69982	47144	29115	20699	25278	18917	21081	11723
R <sup>2</sup>	0.93	0.97	0.92	0.97	0.92	0.97	0.94	0.97
Admissions (Poisson)	-0.012 (0.009)	-0.016** (0.008)	-0.009 (0.009)	-0.012 (0.007)	-0.011 (0.012)	-0.017** (0.008)	-0.016* (0.009)	-0.024* (0.013)
Obs	69982	69733	29115	28859	25278	25131	21081	19686
R <sup>2</sup>								
Mortality	-0.001 (0.003)	0.000 (0.009)	0.002 (0.006)	0.010 (0.018)	0.007 (0.005)	0.019 (0.011)	0.001 (0.003)	0.088 (0.120)
Obs	25928	8298	10835	3816	9975	4646	6770	339
R <sup>2</sup>	0.12	0.20	0.20	0.32	0.18	0.27	0.28	0.96
Length	-0.151 (0.123)	0.137 (0.295)	0.087 (0.232)	0.883* (0.479)	-0.111 (0.251)	0.167 (0.437)	0.059 (0.199)	-2.777 (1.758)
Obs	28239	8787	11303	4121	10204	4779	8619	506
R <sup>2</sup>	0.33	0.27	0.40	0.39	0.30	0.34	0.58	0.87
Cost-to-procedure	-284.311* (168.007)	225.257 (584.765)	120.116 (369.545)	1,759.920 (1,392.755)	-621.581** (289.127)	-458.110 (623.723)	-198.179 (154.683)	763.017 (1,526.433)
Obs	25820	7472	10183	3417	9276	4107	7840	374
R <sup>2</sup>	0.08	0.22	0.15	0.32	0.19	0.32	0.26	0.93
Total cost	-605.278 (784.199)	1,668.843 (2,751.575)	707.800 (1,852.196)	6,653.459 (6,658.251)	-1,634.978 (1,076.116)	206.293 (2,145.908)	-333.029 (448.733)	-3,412.881 (5,401.949)
Obs	28193	8782	11264	4119	10189	4779	8591	503
R <sup>2</sup>	0.07	0.17	0.14	0.29	0.18	0.30	0.33	0.85
Severity (weight)	-0.011 (0.014)	0.018 (0.036)	0.014 (0.020)	0.113*** (0.043)	-0.040 (0.029)	-0.029 (0.054)	0.012 (0.020)	-0.144 (0.155)
Obs	28242	8787	11305	4121	10205	4779	8619	506
R <sup>2</sup>	0.19	0.34	0.26	0.47	0.23	0.39	0.47	0.89

*Notes:* the table reports the estimated impact of a spreading window on daily urgent admissions, mortality, length of stay, cost-to-procedure, total cost of stay, and relative severity weight in three class of diseases (digestive, genitourinary, musculoskeletal) observed in the five days before and after an opening event. Weather controls include temperature, wind direction, wind speed, rainfall, radiance and humidity, interacted with each other at up to the third lag. When estimated through a linear model, only strictly positive observations for hospital admissions are included. Observations with no admissions when the model is estimated through fixed-effects pseudo-Poisson ML. Standard errors, clustered at municipal level, are reported in parentheses. \*\*\*  $p < 0.01$ , \*\*  $p < 0.05$ , \*  $p < 0.1$ .

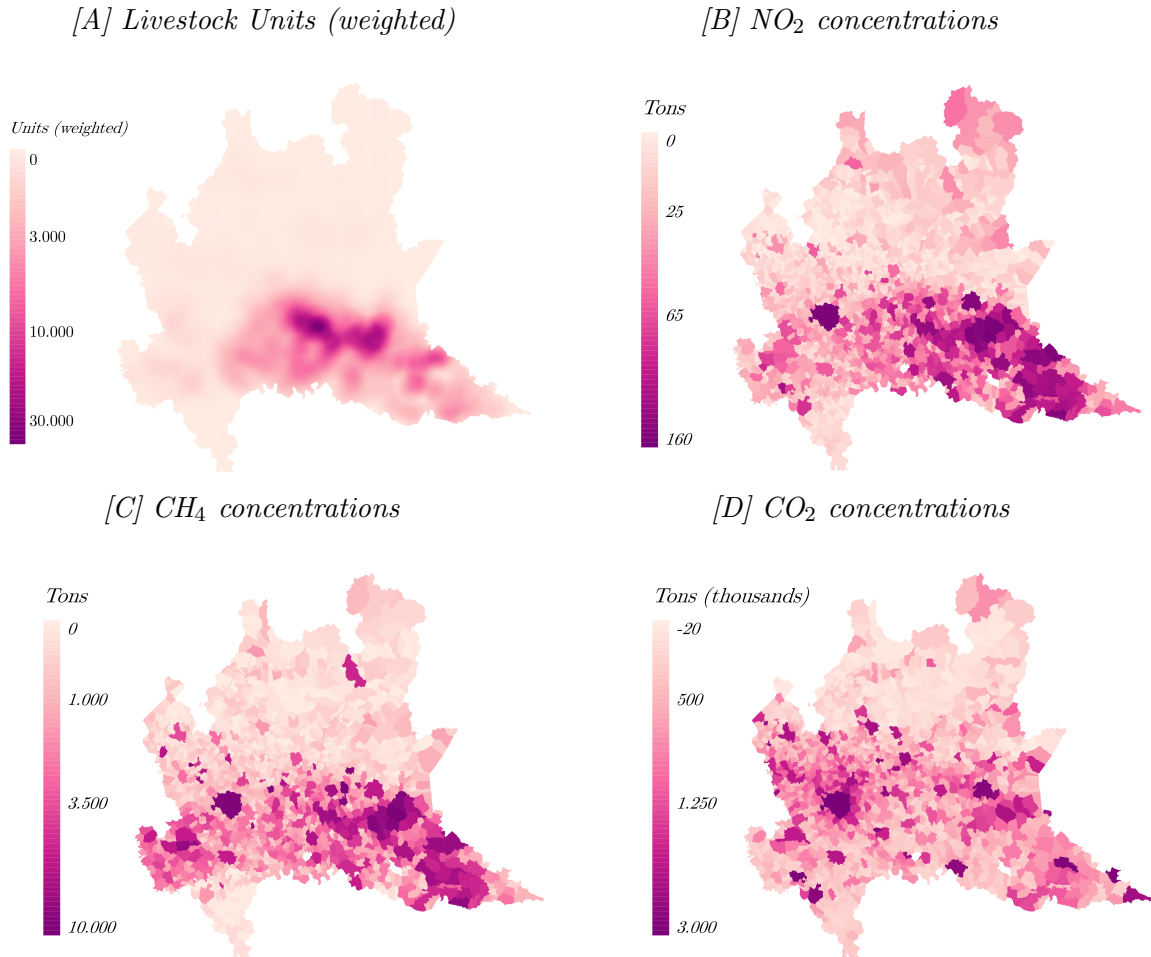
Table D.2: Effect of spreading windows on PM<sub>2.5</sub> concentrations (untransformed)

PM <sub>2.5</sub>	Static Model			Semi-dynamic model		
	(1)	(2)	(3)	(6)	(7)	(8)
Window	7.297*** (0.095)	7.299*** (0.091)	7.243*** (0.416)			
Day 1				6.422*** (0.131)	6.411*** (0.122)	6.417*** (0.436)
Day 2				10.030*** (0.078)	10.088*** (0.075)	10.013*** (0.421)
Day 3				10.487*** (0.063)	10.378*** (0.061)	10.264*** (0.372)
Day 4				3.898*** (0.042)	3.589*** (0.040)	3.473*** (0.314)
Day 5				0.865*** (0.062)	0.205*** (0.057)	0.137 (0.084)
Obs	112213	112207	105932	112213	112207	105932
Adj. R <sup>2</sup>	0.739401289	0.778952049	0.775829476	0.749539	0.790209	0.787153
Weather (extended)	✓	✓	✓	✓	✓	✓
Municipality FE	✓	✓	✓	✓	✓	✓
Municipality-by-month FE		✓	✓		✓	✓
Month-by-year FE	✓	✓	✓	✓	✓	✓
DoW & Holiday FE		✓	✓		✓	✓
Standard errors	Rob	Rob	Clust	Rob	Rob	Clust

*Notes:* the table reports the estimates  $\eta_0$  from Equation 2 (Columns 1 to 3) and the estimates  $\eta_k$  coefficients from Equation 1, where pre-trend coefficients are set to zero. Weather controls include temperature, wind direction, wind speed, rainfall, radiance, humidity, and average planetary boundary layer height, interacted with each other up to three lags. Robust (Columns 1-2 and 4-5) and clustered at sensor level (Columns 3 and 6) standard errors, are reported in parentheses. \*\*\* p<0.01, \*\* p<0.05, \* p<0.1.

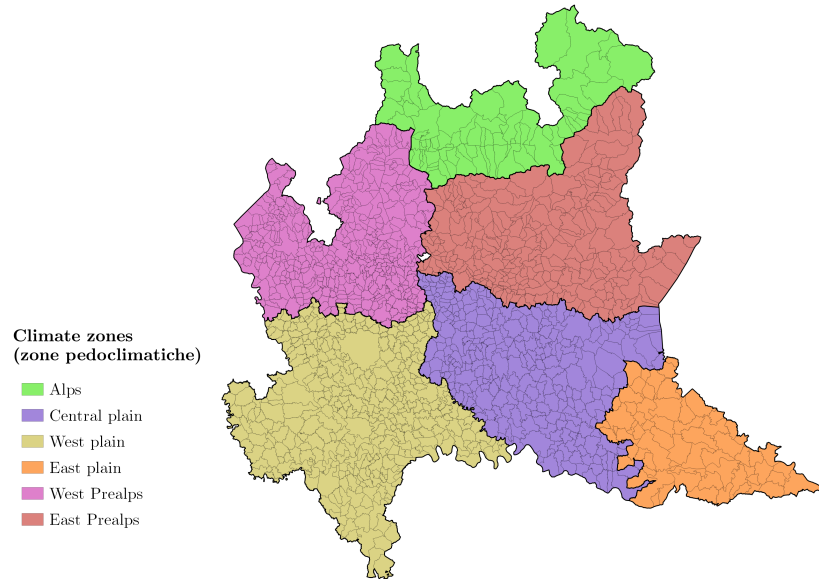
## E Supplementary Figures

Figure E.1: Spatial correlation between livestock presence and GHGs concentrations in Lombardy



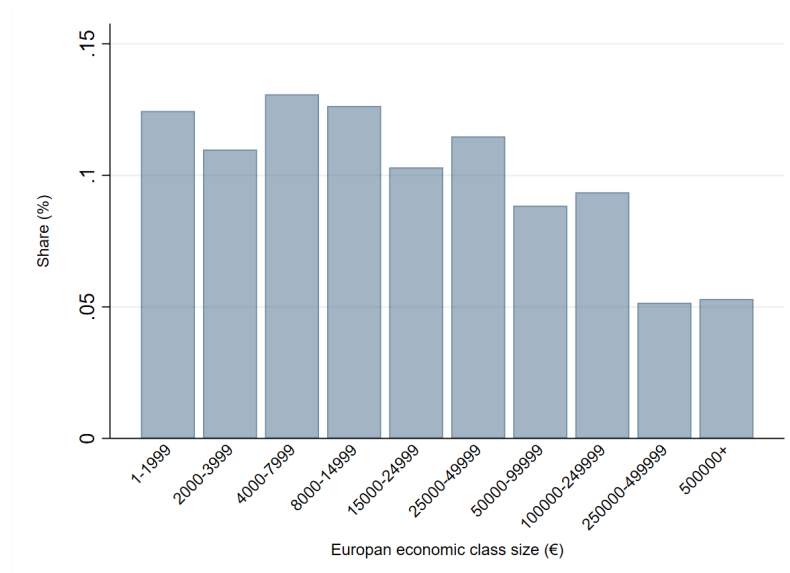
*Notes:* the figure shows high correlation between NO<sub>2</sub> and CH<sub>4</sub> concentrations and livestock presence in the region. Livestock units represent the weighted average number of units between 2016 and 2019; weighting follows the strategy explained in Section 4. Concentrations of pollutants are expressed as the yearly average (tons) in year 2017 (Source: INEMAR). Livestock units Spearman indices: 0.8541 (NO<sub>2</sub>); 0.5538 (CH<sub>4</sub>); 0.0261 (CO<sub>2</sub>).

Figure E.2: Lombardy region divided into manure application climate zones



*Notes:* the figure shows climate zones borders for the purpose of manure application prohibitions. Climate zone areas are: *Alps* (provinces: SO); *Central plain* (provinces: BG, BS, CR); *West plain* (provinces: LO, MI, PV); *East plain* (provinces: MN); *West Prealps* (provinces: BG, CO, LC, MB); *East Prealps* (provinces: BG, BS).

Figure E.3: European economic size class of farms in Lombardy



*Notes:* The figure plots the share of farms in Lombardy over economic size class. The measure of economic size is defined at European level (Commission Regulation (EC) No 1242/2008). Source: 2010 Agricultural Census, ISTAT.

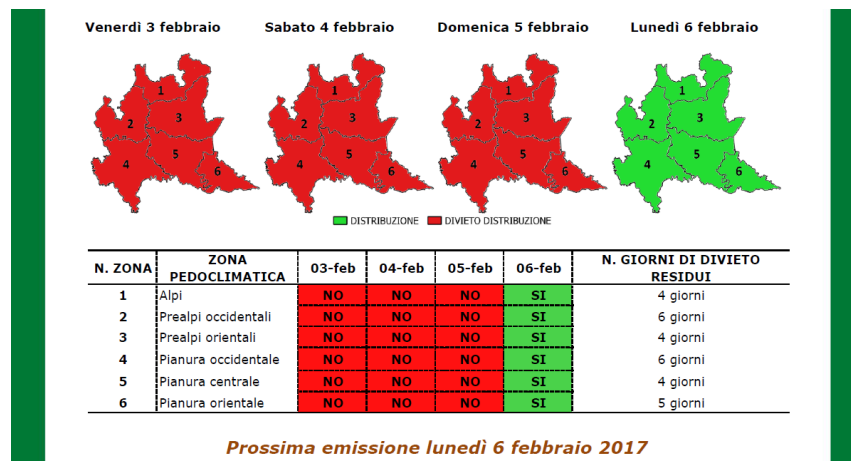


Figure E.4: Spreading bulletins layout

Panel [A] - App version



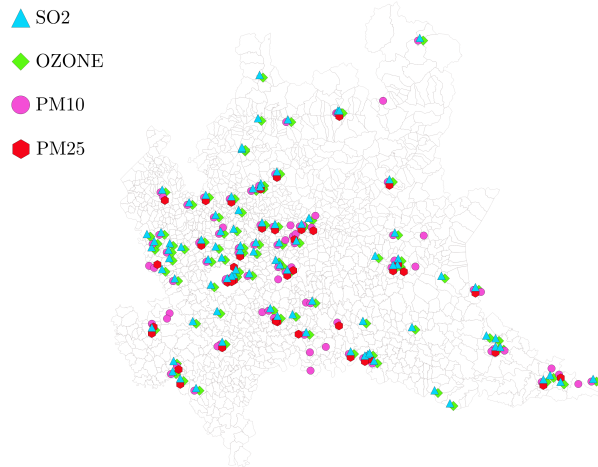
Panel [B] - PDF version



Notes: the figure shows the App and PDF document layout of the bulletins available to farmers to learn the status of prohibitions between November and March. Provider: ERSAF Lombardia. App: *Nitrati*.

Figure E.5: Stations Geolocations

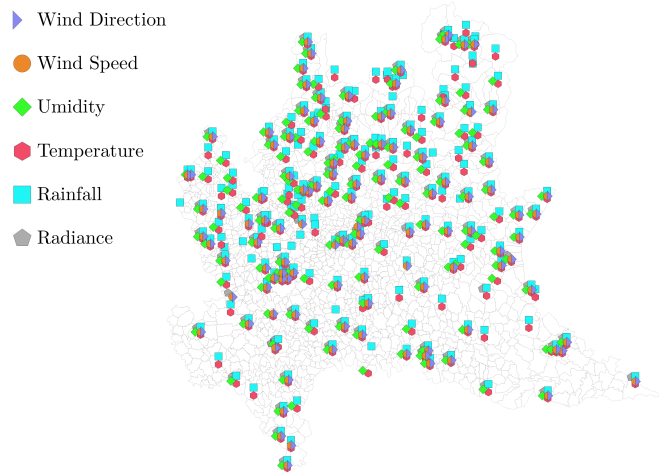
Panel [A]



Stations count

Ozone	25
PM <sub>10</sub>	39
PM <sub>2.5</sub>	41
SO <sub>2</sub>	36

Panel [B]

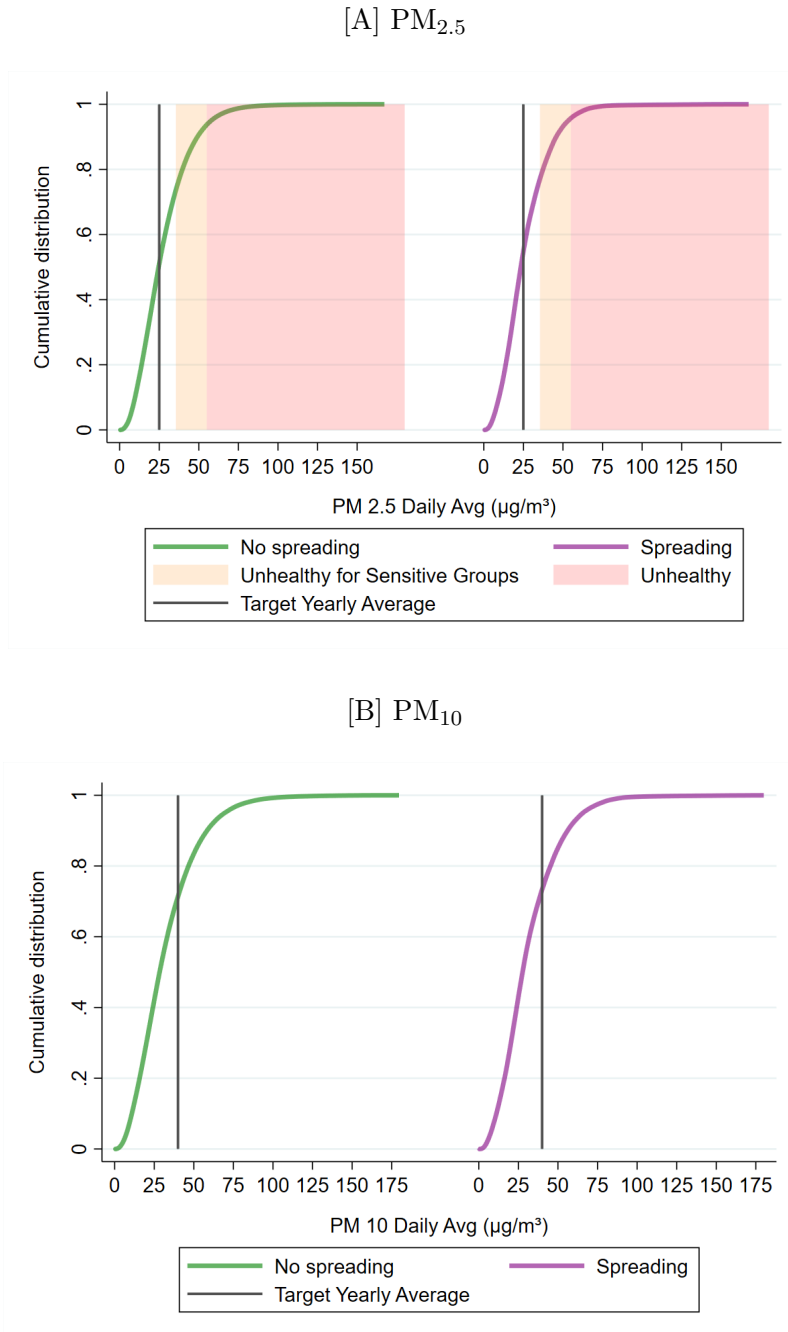


Stations count

Humidity	94
Radiance	82
Rainfall	154
Temperature	154
Wind Direction	112
Wind Speed	112

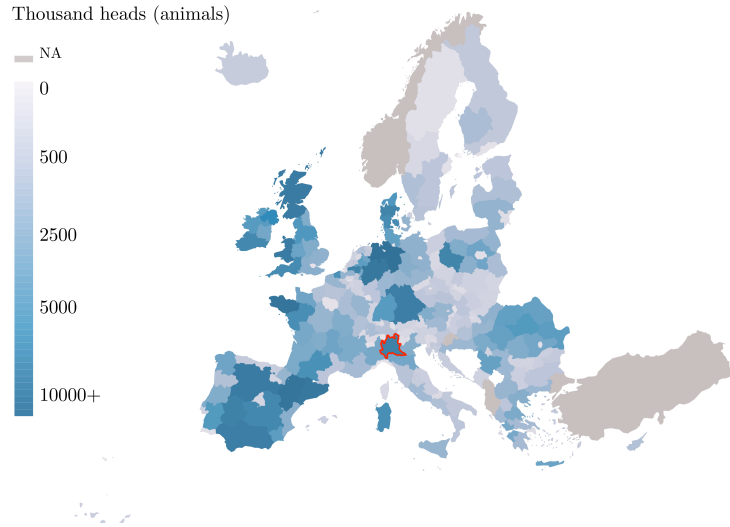
*Notes:* The figure reports geolocation and counting of stations for pollutants concentrations (Panel A) and weather factors (Panel B) in the Lombardy region. Only stations active continually between 2016 and 2019 are considered.

Figure E.6: Daily average distributions (November to February) - PM<sub>2.5</sub> and PM<sub>10</sub>



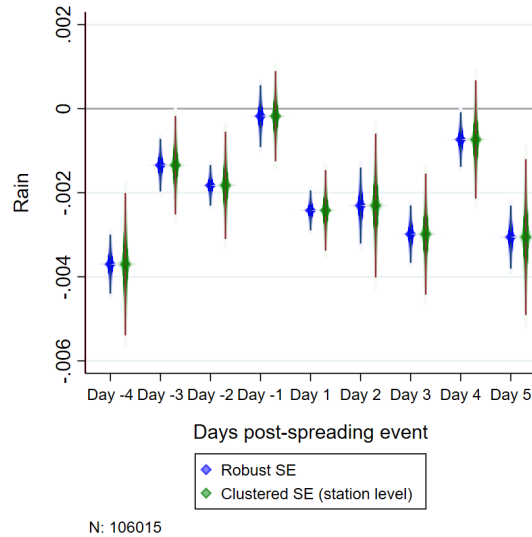
*Notes:* the figure plots the cumulative distribution of daily average concentrations of PM<sub>2.5</sub> (Panel [A]) and PM<sub>10</sub> (Panel [B]), when spreading prohibitions are enforced (left) and when they are lifted (right). Vertical lines mark Italy's target values for yearly average concentrations. For PM<sub>2.5</sub>, levels unhealthy for sensitive groups ( $35 \mu\text{g}/\text{m}^{-3}$ ) and generally unhealthy ( $55 \mu\text{g}/\text{m}^{-3}$ ) are reported. Reference values are defined according to the standards for the Air Quality Index (AQI) set by the US Environmental Protection Agency (EPA).

Figure E.7: Farming animals concentration - EU NUTS-2 level (2010-2021 average)



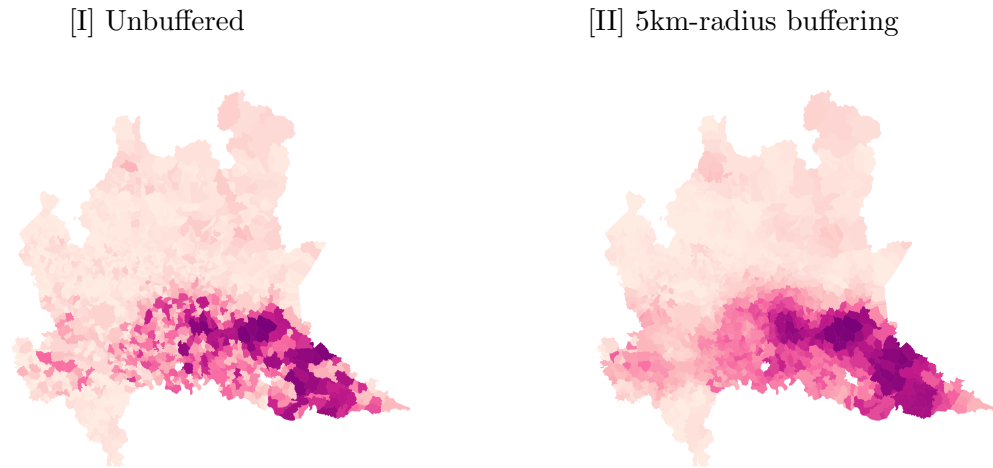
*Notes:* the figure shows the average total headcount of four livestock animals (bovine, sheep, goats, suine) between 2010 and 2021. Data is aggregated at NUTS-2 Eurostat classification level (Germany and UK data is only available at NUTS-1 level).  
 EU average (SD): 1300.8 (1817.715); EU max: 11267.27; Lombardy average: 5714.293.  
 Source: Eurostat: Animal Production Statistics.

Figure E.8: Rainfall and window days correlation



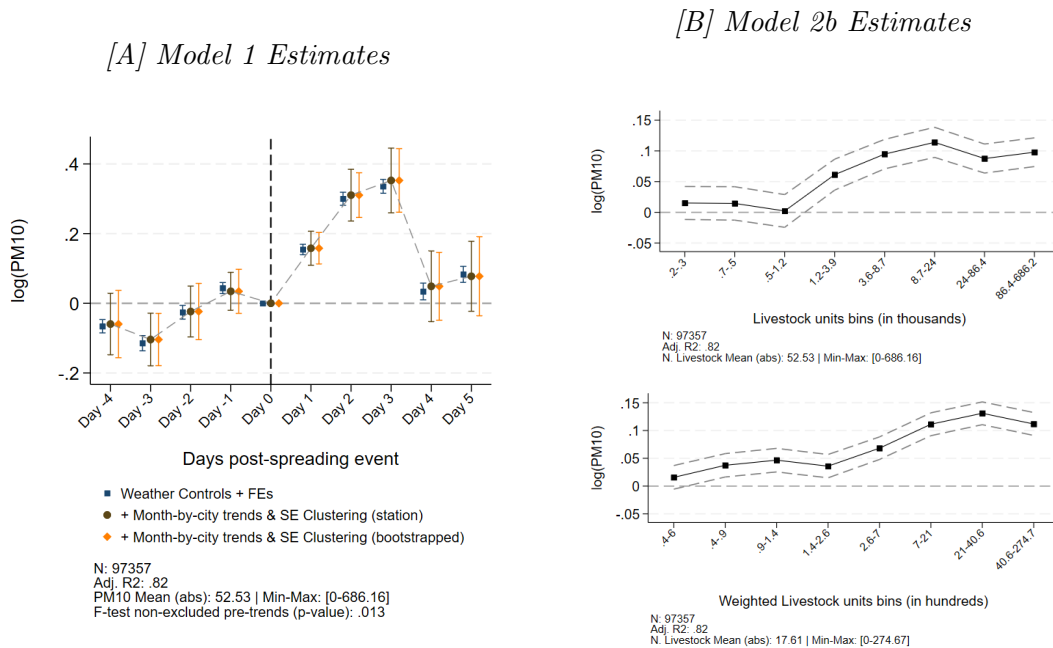
*Notes:* the figure plots the coefficient of a regression of rainfall levels on a set of indicators for relative time from the window opening, weather controls and FEs. Weather controls include temperature, humidity, radiance, wind speed and direction, average PBLH, up to a third lag and interacted within each other. FEs comprise day-of-the-week-by-year, holiday, municipality-by-month, month-by-year, and window. Clustering of standard errors happens at rainfall station level.

Figure E.9: Rainfall and window days correlation



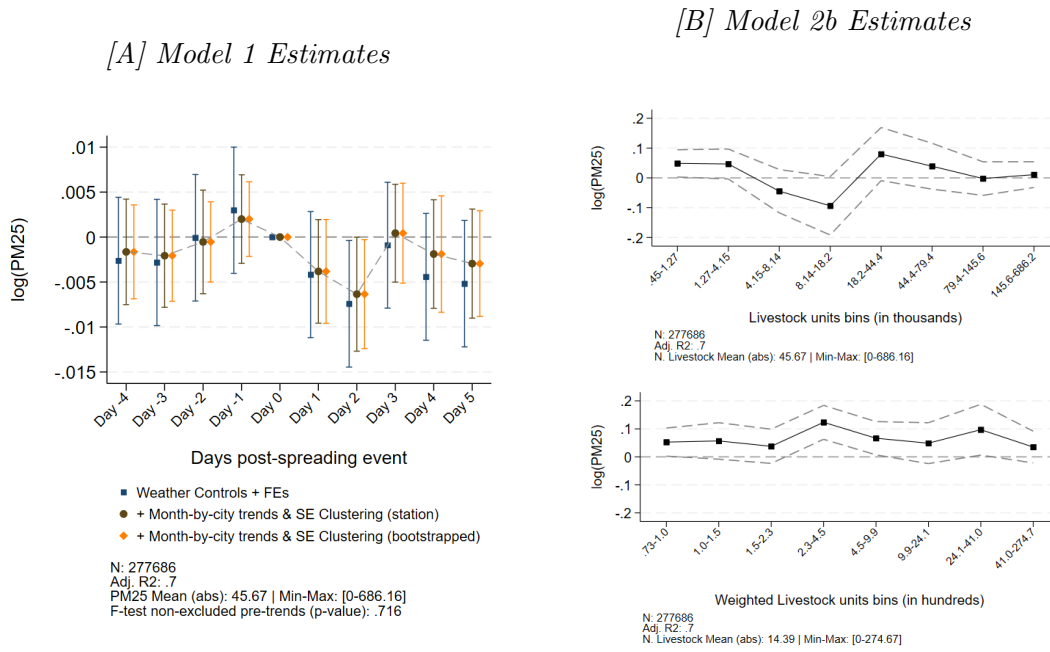
*Notes:* the figure exemplifies a visual representation of how livestock concentration is calculated using buffering. The stock of animals at municipal levels is recomputed as the average of animal stocks in neighbouring municipalities within a 5km radius. Using 2km and 10km radius leads to comparable results.

Figure E.10: Effect of manure spreading on PM<sub>10</sub> concentrations (baseline)



*Notes:* Panel [A] plots the effect of manure spreading windows opening on log PM<sub>10</sub> as in Figure 7. Controls include weather conditions up to the third lag and interacted in each period, and FEs include municipality, month-by-year, day of the week, holiday, window. Bootstrapped standard errors are sampled with 100 iterations. Coefficients on last prohibition day (day 0) are set to zero. Confidence level plotted at 95% level. Panel [B] provides the estimates of the  $\rho_b$  coefficients in the static model 2b.

Figure E.11: Placebo test - effect of rain windows on PM<sub>2.5</sub> concentrations

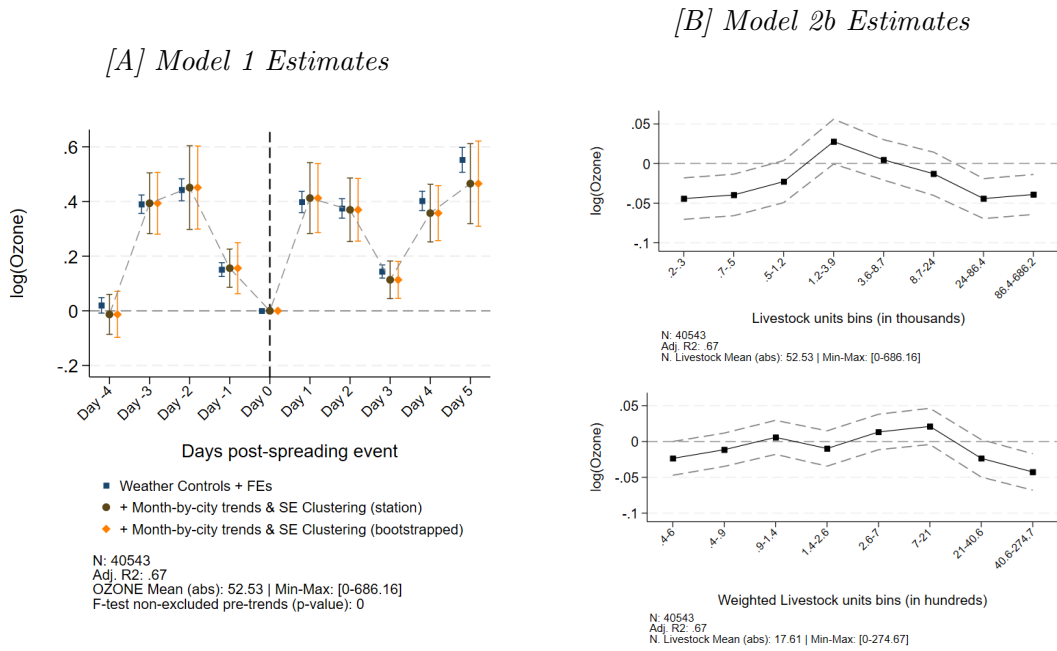


*Notes:* Panel [A] plots the effect of placebo rain windows opening on log PM<sub>2.5</sub> concentrations. Controls include weather conditions up to the third lag and interacted in each period, and FEs include municipality, month-by-year, day of the week, holiday, window. Bootstrapped standard errors are sampled with 100 iterations. Coefficients two days after the rainy event (day 0) are set to zero. Confidence level plotted at 95% level.

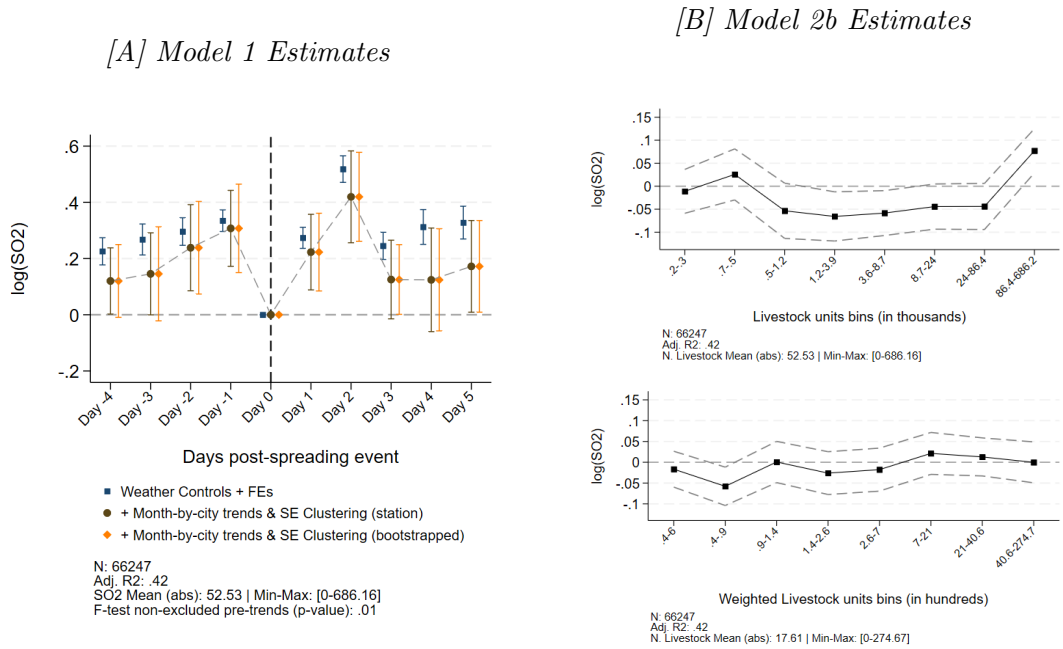
Panel [B] provides the estimates of the  $\rho_b$  coefficients in the static model 2b, with placebo rain window opening. Weighted livestock units at municipality level are computed using the weights in Table 2.

Figure E.12: Effect of manure spreading on O<sub>3</sub> and SO<sub>2</sub> concentrations

Panel [I - Ozone]



Panel [II - SO<sub>2</sub>]



*Notes:* the figure plots the effect of manure spreading windows opening on log concentrations of other pollutants, plotting the estimates for  $\eta_k$  [A] and  $\rho_b$  [B] coefficients from Equation 1 and 2 where the outcome variable is  $\log(\text{SO}_2)$  and  $\log(\text{O}_3)$  concentrations. Controls include weather conditions up to the third lag and interacted in each period, and FEs include municipality, month-by-year, day of the week, holiday, window. Bootstrapped standard errors are sampled with 100 iterations. Coefficients on last prohibition day (day 0) are set to zero. Confidence level plotted at 95% level. Weighted livestock units at municipality level are computed using the weights in Table 2. Panel [I] reports the coefficients for  $\text{O}_3$ , Panel [II] those for  $\text{SO}_2$ .